Universidade do Minho
Escola de Engenharia

Sofia Gabriel Meirinho

Development of a novel aptamer-based multi-sensor device for the detection of osteopontin

October 2015

Sofia Gabriel Meirinho **Development of a novel aptamer-based multi-sensor device for the detection of osteopontin**

UMinho | 2015

Universidade do Minho
Escola de Engenharia

Sofia Gabriel Meirinho

Development of a novel aptamer-based multi-sensor device for the detection of osteopontin

Doctoral Dissertation for PhD degree in Chemical and Biological Engineering

Supervisor:
Doutora Lígia Raquel Marona Rodrigues

Co-supervisor:
Doutor António Manuel Coelho Lino Peres

October 2015

DECLARAÇÃO

Nome: Sofia Gabriel Meirinho

E-mail: smeirinho@deb.uminho.pt

Número do Cartão de Cidadão: 11562397

Título da tese:

Development of a novel aptamer-based multi-sensor device for the detection of osteopontin.

Orientadores:

Doutora Lígia Raquel Marona Rodrigues

Doutor António Manuel Coelho Lino Peres

Ano de conclusão: 2015

Doutoramento em Engenharia Química e Biológica

Universidade do Minho, 26 de Outubro de 2015

_____

(Sofia Gabriel Meirinho)

I hereby declare having conducted my thesis with integrity. I confirm that I have not used plagiarism or any form of falsification of results in the process of the thesis elaboration.

I further declare that I have fully acknowledged the Code of Ethical Conduct of the University of Minho.

University of Minho, October 26nd 2015

_____

(Sofia Gabriel Meirinho)

AGRADECIMENTOS

Quero aqui expressar os meus sinceros agradecimentos a todos os que, direta ou indiretamente colaboraram para a concretização deste trabalho.

Em primeiro lugar, gostava de agradecer aos meus orientadores, Doutora Lígia Rodrigues e Doutor António Peres pela oportunidade que me deram ao orientarem o meu trabalho, pelo imenso apoio e dedicação, pelos conhecimentos transmitidos e pela sua paciência, confiança e otimismo.

Gostava também de agradecer ao Doutor Luís Dias pelo seu apoio, dicas para o trabalho experimental e pela grande ajuda na análise dos dados experimentais. Muito obrigada pela disponibilidade sempre demonstrada e pelo pensamento positivo mesmo nos momentos mais difíceis.

Aos colegas da Plataforma de Biologia Molecular e Sintética, principalmente aos "compinchas" de bancada, o meu muito obrigada pelo bom ambiente e por ouvirem os meus desabafos, pelas grandes discussões científicas e os momentos hilariantes.

Aos colegas do Laboratório de Bioprocessos e do LTEB por estarem sempre disponíveis a emprestar o medidor de pH.

Ao "Gang dos Magníficos" Ana Cristina Rodrigues, Patrícia Ferreira, Cláudia Fonseca, Joaquim Barbosa, António Machado, pela grande amizade, carinho, companheirismo, grandes aventuras e "Que a dança da vida nunca nos separe".

Gostava de agradecer aos meus companheiros de viagem por terras do Minho, Cláudia Araújo, Eva Pinho, Daniela Correia, Isabel Ferrari, Isabel Carvalho, Sara Gonçalves, Jorge Padrão pelo seu apoio, carinho, por ouvirem os meus desabafos e amizade.

Gostava de agradecer aos meus amigos de Bragança, pelo apoio e ajuda constante, estarem sempre disponíveis a ouvirem-me falar do trabalho, Ana Sofia Lima, Ana Paula Pereira, José Luís Martins, Filomena Pires.

Finalmente gostaria de dedicar esta tese a minha Mãe e irmãos pela paciência ou falta dela, um grande Obrigado.

A quem eu me esqueci de agradecer diretamente, um muito obrigada a todos!

Gostaria também de agradecer à Universidade do Minho (Centro de Engenharia Biológica) e ao Instituto Politécnico de Bragança (Escola Superior Agrária) por me acolherem.

SGM

Este trabalho apresentado nesta tese foi apoiada financeiramente por uma bolsa de doutoramento (Ref.ª SFRH / BD / 65021/2009) da Fundação para a Ciência e a Tecnologia (FCT) e do Fundo Social Europeu (POPHQREN), o Projeto FCT Estratégico UID/BIO/04469/2013 unidade, o projeto RECI/certificação-EBI/0179/2012 (FCOMP-01-0124-FEDER-027462) e do Projeto "BioInd – "Biotechnology and Bioengineering for improved Industrial and Agro-Food processes", REF. NORTE-07-0124-FEDER-000028, co-financiado pelo Programa Operacional Regional do Norte (ON.2 - O Novo Norte), QREN, FEDER.

"O único homem que está isento de erros,

é aquele que não arrisca acertar."

Albert Einstein

This page was intentionally left blank

ABSTRACT

Breast cancer is the most prevalent cancer in women worldwide and its mortality is closely associated with the development of metastasis of the primary tumor. It is currently the fifth cause of death from cancer (522,000 deaths), with 1.67 million new breast cancer cases estimated in 2012. An early diagnosis is crucial to improve patients survival and disease prognostic. Hence, sensitive and specific methods ought to be developed and improved towards this purpose. The use of aptamers as bioreceptors in the design of electrochemical aptasensors has offered new prospects in diagnostic assays in the areas of protein disease biomarkers detection.

In this thesis, the possibility of using an electrochemical aptamer-based biosensor for the detection of osteopontin (OPN) has been studied. Aptamers are artificial oligonucleotides (DNA or RNA) that bind their targets with high affinity and specificity. OPN is a glycoprotein present in many tissues and body fluids that is considered a potential biomarker for breast cancer. Initially, an RNA aptamer against OPN, previously reported, was used as the bioreceptor element in the design of an aptasensor. The OPN-binding RNA aptamer was immobilized onto a screen printed gold electrode through a biotin-streptavidin interaction. The electrochemical RNA aptasensor showed a good sensitivity to human OPN and for thrombin (a protein commonly found in human serum). Thus, other specific bioreceptors that could enable the selective detection of human OPN were selected. A DNA aptamer was isolated through the SELEX methodology. This aptamer was characterized by fluorescence assays and presented a good affinity to OPN, thus it was used as the bioreceptor in the design of a new electrochemical DNA aptasensor. This aptasensor exhibited a better performance regarding the sensitivity and selectivity for the detection of human OPN as compared to the above mentioned RNA aptasensor that used the same electrode surface, immobilization method and voltammetry techniques. Finally, these two aptamers (DNA and RNA) were used to develop a label-free aptasensor array that could simultaneously detect OPN using a dual-screen printed gold electrode. In conclusion, the electrochemical aptasensors herein developed can be an alternative to the standard methods currently used to detect/quantify protein disease biomarkers and could be a useful tool in the diagnosis of breast cancer disease.

This page was intentionally left blank

RESUMO

O cancro da mama é o mais frequente entre mulheres em todo o mundo, a sua mortalidade está associada ao desenvolvimento de metástases do tumor primário. Atualmente, é a quinta causa de morte por cancro (522.000 mortes), tendo sido diagnosticados cerca de 1,67 milhões de novos casos em 2012. O diagnóstico precoce é crucial para aumentar a taxa de sobrevivência e sucesso do prognóstico. Neste sentido, urge o desenvolvimento de métodos sensíveis e específicos para melhorar o diagnóstico precoce. O uso de aptâmeros, como elementos de reconhecimento biológico no desenho de biossensores eletroquímicos (*aptasensors*), tem oferecido novas perspetivas de diagnóstico em particular nas áreas de deteção de proteínas associadas ao cancro (biomarcadores).

Nesta tese, avaliou-se a possibilidade de usar um biossensor eletroquímico, baseado em aptâmeros, para a deteção da osteopontina humana (OPN). A OPN é uma glicoproteína presente em muitos tecidos e fluidos corporais, sendo considerada um potencial biomarcador do cancro da mama. Os aptâmeros são ácidos nucleicos artificiais de cadeia simples (ADN ou ARN) que reconhecem e se ligam com elevada afinidade e especificidade aos seus alvos. Inicialmente, um aptâmero de ARN específico para a OPN, descrito na literatura, foi utilizado como elemento de reconhecimento no desenvolvimento de um "*aptasensor*". O aptâmero foi imobilizado num elétrodo de ouro através de uma interação biotina-estreptavidina. O biossensor eletroquímico, baseado no aptâmero de ARN, apresentou boa sensibilidade para OPN humana e para trombina (proteína presente no soro humano). Nesse sentido, selecionou-se outro aptâmero de ADN com maior especificidade e seletividade para a OPN humana usando para o efeito a metodologia SELEX. Este aptâmero ADN foi então usado no desenvolvimento de um novo biossensor eletroquímico. Este novo biossensor apresentou melhor sensibilidade e seletividade para a OPN humana comparativamente com o anteriormente referido, utilizando a mesma superfície de elétrodo, método de imobilização e técnicas voltamétricas. Finalmente, um multi-biossensor foi desenvolvido usando os dois aptâmeros (ADN e ARN) para detetar simultaneamente a OPN humana. Em conclusão, os biossensores electroquímicos desenvolvidos podem ser uma alternativa aos métodos convencionais utilizados para detetar/quantificar biomarcadores, bem como uma ferramenta útil para o diagnóstico precoce do cancro da mama.

This page was intentionally left blank

TABLE OF CONTENTS

This page was intentionally left blank

LIST OF FIGURES

LIST OF TABLES

This page was intentionally left blank

LIST OF SYMBOLY AND ABBREVIATIONS

ΔEp - potential variation between cathodic and anodic peaks

ΔG - Gibbs free energy

ΔI - relative current change

ACV - alternating current voltammetry

AE - auxiliary electrode

AFP - α-fetoprotein

Ag - silver

Ag/AgCl - silver/silver chloride

AgNPs - silver nanoparticles

AMD - age-related macular degeneration

AP - alkaline phosphatase

AQ - anthraquinone

ASCO - American Society of Clinical Oncology

Au - gold

AuMNPs - gold magnetic nanoparticles

AuNPs - gold nanoparticles

AuNRs - gold nanorods

BRCA1 - breast cancer type 1 susceptibility protein

BRCA2 - breast cancer type 2 susceptibility protein

BSA - bovine serum albumin

CA - cancer antigen

CB[7] - Cucurbit[7]uril substract

CEA - carcinoembryonic antigen

CNTs - carbon nanotubes

CPE - carbon paste electrode

CRP - C-reactive protein

CT - computed tomography

CV - cyclic voltammetry

DEPC - diethypyrocarbonate

DNA - deoxyribonucleic acid

DPA - 3,3-dithiodipropionic acid

DPV - differential pulse voltammetry

dsDNA - double strand deoxyribonucleic acid

EDCA - N-(3-dimethylaminopropyl)-N-ethylcarbodiimide hydrochloride

EIS - electrochemical impedance spectroscopy

ELISA - enzyme-linked immunosorbent assays

ER - estrogen receptor

ETA - ethanolamine

FAM - 6-carboxyfluorescein

Fc - ferrocene

FDA - Food and Drug Administration

GCE - glassy carbon electrode

GNs - Graphene nanosheets

GOD - glucose oxidase

GSPEs - graphite screen-printed electrodes

HCC - hepatocellular carcinoma

HER2 - human epidermal growth factor receptor 2

HRP - horseradish peroxidase

IARC - International Agency of Research on Cancer

IFN-γ - interferon gamma

I_p - peak current intensity

I_{pa} - anodic peak current

I_{pc} - cathodic peak current

IUPAC - International Union of Pure and Applied Chemistry

$K_3Fe(CN)_6$ - potassium hexacyanoferrate (III)

$K_4Fe(CN)_6$.- potassium hexacyanoferrate (II)

KCl - potassium chloride

K_d - dissociation constants

KH_2PO_4 - potassium dihydrogen phosphate

LOD - detection limit

LOQ - quantification limit

LSV - linear sweep voltammetry

LYS - lysozyme

MB - methylene blue

MIR - magnetic resonance imaging

MNPs - magnetic nanoparticles

MRI - magnetic resonance imaging

MUC1 - mucin 1

MWCNTs - multi-walled carbon nanotubes

Na_2HPO_4 - sodium hydrogen phosphate

NaCl - sodium chloride

NHS - N-hydroxysuccinimide

NPs - nanoparticles

Nt - nucleotides

OPN - osteopontin

OPN-c - osteopontin isoform c

PAGE - polyacrylamide gel electrophoresis

PAMAM - Polyamidoamine

PBS - phosphate buffer saline

PCR - polymerase chain reaction

PDGF - platelet-derived growth factor

PDGF - platelet-derived growth factor B-chain

PEG - polyethylene glycol

PET - positron emission tomography

PR - progesterone receptor

Pt - platinum

PtNPs - platinum nanoparticles

QDs - quantum dots

rbOPN - recombinant bovine OPN

RE - reference electrode

rhOPN - recombinant human OPN

RNA - ribonucleic acid

RSD - relative standard deviation

RT-PCR - reverse transcriptase polymerase chain reaction

SAMs - self-assembled monolayers

SCE - saturated calomel electrode

SELEX - Systematic Evolution of Ligands by Exponential Enrichment

SPE - screen printed electrode

SPGEs - screen-printed gold electrodes

ssDNA - single strand DNA

SWCNTs - single-walled carbon nanotubes

SWV - square wave voltammetry

THR - thrombin

TNF-α - tumor necrosis factor alpha

VEGF - vascular endothelial growth factor

WE - working electrode

WHO - Word Health Organization

This page was intentionally left blank

CHAPTER 1

Context, Aims and Thesis Outline

This chapter introduces the context of the work, as well as its aims. The outline of the thesis and its output is also presented.

This page was intentionally left blank

1.1. Context and Motivation

Breast cancer is the most common cancer among women worldwide, with an estimated 1.67 million new cancer cases diagnosed in 2012 (corresponding to 25 % of all cancers) (Ferlay et al., 2013; Torre et al., 2015). The early detection of breast cancer through the use of sensitive and specific diagnostic methods can have a great impact on patients survival (Bohunicky and Mousa, 2011). Advances in breast cancer detection may involve the specific detection of proteins and the development of rapid diagnostic methods with improved performances, including high sensitivity and specificity, fast response time, continuous measurement, suitability for the prognosis and monitoring of the disease (Hong et al., 2012). The development of electrochemical aptasensors can constitue a good alternative for the early detection of protein biomarkers. Indeed, electrochemical aptasensors have been used in the clinics for the design of diagnostic methods for detecting protein disease biomarkers due to their high sensitivitv, low cost, fast detection, low sample volume, portability and operational stability (Kim et al., 2008; Mascini, 2009; Radi, 2011; Sassolas et al., 2009). The success of aptasensors is mainly due to the use of aptamers as the bioreceptor elements (Song et al., 2012). Aptamers are specific nucleic acid sequences (DNA or RNA) that can bind to a wide range of targets with high affinity and specificity and can discriminate between closely related targets (Cho et al., 2009; Famulok and Mayer, 2011; Meyer et al., 2011; Radom et al., 2013). Other advantagens of the aptamers for diagnostic methods include their chemical stability under a wide range of buffer conditions, resistance to harsh treatments without loss of bioactivity, reversible thermal denaturation, and versatility in labelling, immobilization, signaling and regeneration (Hianik and Wang, 2009; X. Li et al., 2010; Radi, 2011; Strehlitz et al., 2008). Aptamers have been isolated by selection evolution of ligands by exponential enrichment (SELEX) against a large variety of targets including proteins disease biomarkers (e.g. osteopontin) (Dua et al., 2011; Ozer et al., 2014; Santosh and Yadava, 2014). Osteopontin (OPN) is a phosphorylated glycoprotein found in almost all body fluids that has been detected in approximately 90 % of primary breast carcinomas (Rodrigues et al., 2009). Indeed, its overexpression may be indicative of tumor formation, cancer progression, metastasis and poor prognosis (Rodrigues et al., 2009; Shevde and Samant, 2014; Weber, 2011; Weber et al., 2011, 2010; Xu et al., 2015; S. Zhao et al., 2011). For this reason, OPN has been reported as a potential breast cancer biomarker (Nassar et al., 2015; Opstal-van Winden et al., 2011; Weber et al., 2011). Accordingly, the purpose of this thesis is to develop and characterize a novel electrochemical

aptamer-based mono/multi-sensor device capable of detecting and quantifying OPN in biological samples from breast cancer patients.

1.2. Research Aims

The overall purpose of this thesis was to develop a simple and sensitive diagnostic device for the detection of OPN (a potential breast cancer biomarker) for future application using biological samples. The specific objectives included:

1. Development of an electrochemical RNA aptasensor using a previsoulsy reported RNA aptamer specific for target OPN. Optimization of the conditions for the design of the RNA aptasensor.

2. Selection of a new bioreceptor with high affinity and specificity for human OPN protein and development of an electrochemical DNA aptasensor.

3. Immobilization of the bioreceptors (RNA and DNA aptamer) onto the screen-printed gold electrode (SPGE).

4. Characterization and optimization of the aptasensor devices by electrochemical transduction.

5. Evaluation and optimization of the electrochemical aptasensors for the most important detection parameters by cyclic voltammetry.

6. Assembly of the RNA and DNA aptamers onto a dual-electrode surface for the simultaneous detection of OPN.

1.3. Thesis outline

This thesis was structured in **seven chapters** that cover the research aims stated above:

- **Chapter 1**. Provides the context and motivation of this thesis, describes the research aims, the thesis outline and lists the publications and communications related with the developed work.

- **Chapter 2.** Presents the literature review that supports the work developed. It starts with a general overview about breast cancer, the role of the OPN protein in breast cancer, and the main components of biosensors such as bioreceptor elements and signal transducers, specifically emphasizing the aptamers as bioreceptor elements and electrochemical (voltammetric) transducers. The use and development of electrochemical aptasensors for the detection of protein disease biomarkers are described and discussed. Additionally, the type of electrode surfaces, different methods of immobilization of aptamers onto the electrodes surfaces and the different electrochemical strategies used for the design aptasensors are reviewed.

The experimental results are presented in several chapters, namely from **Chapter 3** to **Chapter 6**. In each chapter, a brief introduction, materials and methods, results and discussion, conclusions and references are provided.

- **Chapter 3.** Presents the preliminary results on the aptasensor performance regarding the detection of rhOPN in standard samples, as well as its selectivity towards other 'contaminant' proteins (bovine serum albumin, lysozyme, recombinant bovine OPN and thrombin).

- **Chapter 4.** Describes a simple and label-free electrochemical RNA aptasensor against human OPN. The RNA aptamer-binding OPN described in the literature was characterized through binding fluorescence assays to determine the dissociation constants and it was further used as the bioreceptor element. For the development of the aptasensor, the biotinalated RNA aptamer was immobilized onto the SPGE through the streptavidin-biotin interaction. The immobilization of the RNA aptamer was confirmed by cyclic voltammetry and square-wave voltammetry using a ferro/ferricyanide solution ($[Fe(CN)_6]^{3-/4-}$) as redox probe. The electrochemical RNA aptasensor was characterized and evalued by cyclic voltammetry.

- **Chapter 5.** Describes the identification of a specific DNA aptamer recognizing OPN that was selected by the SELEX methodology. The selected aptamer was analyzed using an alignment software to identify identical sequences and highly conserved regions, and the MFold software to predict its secondary structure. The affinity and selectivity of the DNA aptamer towards OPN was characterized using fluorescence assays. Also, its dissociation constant was determined. The DNA aptamer was modified in the 5'-end with biotin and immobilized onto the gold working electrode by streptavidin-biotin interaction. All steps of the DNA aptamer immobilization onto the electrode surface were characterized by cyclic voltammetry and square wave voltammetry using $[Fe(CN)_6]^{3-/4-}$ as the redox

probe. Sensitivity, specificity over interfering proteins, reproducibility, stability and reusability were evaluated by cyclic voltammetry.

- **Chapter 6**. Describes the development of an electrochemical aptasensor array for the simultaneous detection of human OPN using the RNA and DNA aptamers studied in the previous chapters. The electrochemical aptasensor array was fabricated using a dual-screen-printed gold electrode (dual-SPGE). The dual-SPGE consisted of a Ag/AgCl reference electrode, a gold counter electrode and two gold working electrodes (WE1 and WE2). The recognition of the binding of both aptamers to OPN was evaluated by cyclic voltammetry.

- **Chapter 7.** Contains the main concluding remarks and perspectives for further research on this topic.

1.4. Scientific output

The results presented in this thesis have been partially published elsewhere.

1.4.1. Papers published or accepted in peer reviewed journals

Meirinho, Sofia G., Dias, Luís G., Peres, António M., Rodrigues, Lígia R., (2015). Development of an Electrochemical RNA-Aptasensor to detect Human Osteopontin. Biosens. Bioelectron. 71, 332-341.

Meirinho, Sofia G., Dias, Luís G., Peres, António M., Rodrigues, Lígia R., (2014). Development of an electrochemical aptasensor for the detection of human osteopontin, Procedia Eng., 87, 316-319.

1.4.2. Papers submitted to peer reviewed journal

Meirinho, Sofia G., Dias, Luís G., Peres, António M., Rodrigues, Lígia R., (2015). Voltammetric aptasensors for protein disease biomarkers detection: a review. Angewandte Chemie International. (submitted in October 2015).

Meirinho, Sofia G., Dias, Luís G., Peres, António M., Rodrigues, Lígia R., (2015). Electrochemical Aptasensor for Human Osteopontin Detection using a DNA Aptamer Selected by SELEX. Biosens. Bioelectron. (submitted in September 2015).

1.4.3. Communications presented in conferences

Meirinho, Sofia G., Dias, Luís G., Peres, António M., Rodrigues, Lígia R. Development of an electrochemical aptasensor for the detection of human osteopontin protein. The 28th European Conference on solid-State Transducers, Eurosensors 2014, 2014, Brescia, Italy, (poster communication).

Meirinho, Sofia G., Dias, Luís G., Peres, António M., Rodrigues, Lígia R. Development of an electrochemical aptasensor for the detection of human osteopontin protein. World Academy of Science, Engineering and Technology, 2013, Paris, France, (poster communication and oral presentation).

Meirinho, Sofia G., Dias, Luís G., Peres, António M., Rodrigues, Lígia R. Development of an electrochemical aptasensor for protein detection. 3rd Forum on Electrochemistry and Innovation (3ª Jornadas de Electroquímica e Inovação 2013): Electrochemistry and Nanomaterials, 2013, Vila Real, Portugal (poster communication).

1.5. References

Bohunicky, B., Mousa, S.A., 2011. Nanotechnol. Sci. Appl. 4, 1–10.

Cho, E.J., Lee, J., Ellington, A.D., 2009. Annu. Rev. Anal. Chem. 2, 241–264.

Dua, P., Kim, S., Lee, D.-K., 2011. Methods 54(2), 215-225.

Famulok, M., Mayer, G., 2011. Acc. Chem. Res. 44(12), 1349–1358.

Ferlay, J., Soerjomataram, I., Ervik, M., Dikshit, R., Eser, S., Mathers, C., Rebelo, M., Parkin, D.M., Forman, D., Bray, F., 2013. GLOBOCAN 2012 v1.0, IARC Cancer Base. No. 11.

Hianik, T., Wang, J., 2009. Electroanal. 21, 1223 – 1235.

Hong, P., Li, W., Li, J., 2012. Sensors 12, 1181–1193.

Kim, Y.S., Lee, S.J., Gu, M.B., 2008. BioChip J. 2, 175–182.

Li, X., Liu, J., Zhang, S., 2010. Chem. Comm. 46, 595–597.

Mascini, M., 2009. Aptamers in Bioanalysis. A JOHN WILEY & SONS, INC.

Meyer, C., Hahn, U., Rentmeister, A., 2011. J. Nucleic Acids 2011, Article ID 904750, 1-18.

Nassar, H.R., Namour, A.E., Shafik, H.E., El Sayed, A.S., Kamel, S.M., Moneer, M.M., Zakhary, N.I., 2015. Forum of Clin. Oncol. 6, 27–32.

Opstal-van Winden, A.W.J., Krop, E.J.M., Kåredal, M.H., Gast, M.-C.W., Lindh, C.H., Jeppsson, M.C., Jönsson, B. a G., Grobbee, D.E., Peeters, P.H.M., Beijnen, J.H., van Gils, C.H., Vermeulen, R.C.H., 2011. BMC Cancer 11(1), 381-392.

Ozer, A., Pagano, J.M., Lis, J.T., 2014. Mol. Ther. Nucleic Acids 3, e183.

Radi, A.-E., 2011. Int. J. Electrochem. 2011, 1–17.

Radom, F., Jurek, P.M., Mazurek, M.P., Otlewski, J., Jeleń, F., 2013. Biotech. Adv. 31, 1260–1274.

Rodrigues, L.R., Lopes, N., Sousa, B., Vieira, D., Milanezi, F., 2009. Open Breast Cancer J. 1, 1–9.

Santosh, B., Yadava, P.K., 2014. Biomed Res. Int. 2014, Article ID 540451, 1-13.

Sassolas, A., Blum, L.J.J.J., Leca-Bouvier, B.D.D.D., Lyon, D., 2009. Electroanal. 21, 1237–1250.

Shevde, L. a, Samant, R.S., 2014. Matrix Biol. 37, 131–141.

Song, K.-M., Lee, S., Ban, C., 2012. Sensors 12, 612–631.

Strehlitz, B., Nikolaus, N., Stoltenburg, R., 2008. Sensors 8, 4296–4307.

Torre, L. a, Bray, F., Siegel, R.L., Ferlay, J., Lortet-Tieulent, J., Jemal, A., 2015. CA. Cancer J. Clin. 65, 87–108.

Weber, G.F., 2011. Cancer Genom. Proteom. 8, 263–288.

Weber, G.F., Lett, G.S., Haubein, N.C., 2010. Br. J. Cancer 103, 861–869.

Weber, G.F., Lett, G.S., Haubein, N.C., 2011. Oncol. Rep. 25, 433–441.

Xu, Y.-Y., Zhang, Y.-Y., Lu, W.-F., Mi, Y.-J., Chen, Y.-Q., 2015. Mol. Clin. Oncol. 3, 357–362.

Zhao, B., Sun, T., Meng, F., 2011. J. Cancer Res. Clin. Oncol. 137, 1061–1070.

This page was intentionally left blank

CHAPTER 2

Literature Review

Osteopontin (OPN) is a phosphorylated glycoprotein present in many tissues and body fluids that is considered by many researchers a potential biomarker for breast cancer. Traditionally, the detection of this protein is accomplished by immunohistochemistry. However, this technique is laborious, expensive and not always conclusive depending on the specificity of the antibodies used. Additionally, it requires the use of tissue samples which are not always readily available. Therefore, new techniques for the detection and monitoring of protein disease biomarkers present in body fluids ought to be further designed. The Systematic Evolution of Ligands by Enrichment (SELEX) methodology allows the selection of aptamers with high affinity and specificity for protein targets, thus its application as bioreceptor elements in the development of electrochemical aptasensors, appears to be a very promising tool. An electrochemical aptasensor is a compact analytical device where the bioreceptor (aptamer) is coupled to a transducer surface to convert a biological interaction into a measurable signal (current) that can be easily processed, recorded and displayed. Several advantages are recognized, compared to the conventional techniques, namely the fast, simple and low-cost detection. In this chapter, a special emphasis is given to the potential use of electrochemical aptasensors for the detection of proteins present in biological fluids using voltammetry techniques. Also, different methods of immobilization of aptamers onto electrodes surfaces are discussed, as well as different electrochemical strategies used for target detection by aptasensors.

The contents of this Chapter were submitted to Angewandte Chemie International:

Meirinho, Sofia G., Dias, Luís G., Peres, António M., Rodrigues, Lígia R. Voltammetric aptasensors for protein disease biomarkers detection: a review. Angew. Chem. Int. (submitted in October 2015).

2.1. Introduction

Breast cancer is the most prevalent cancer in women worldwide and the cancer-related mortality is closely associated with the development of metastatic potential of the primary tumor (Xu et al., 2015), accounting for 23 % of the total cancer cases (1.38 million) and 14 % of the cancer deaths (458,400) (Jemal et al., 2011; Porika and Tippani, 2011). According to new data of GLOBOCAN2012 these values increased, around 1.67 million new cancer cases were diagnosed (representing 12 % of all new cancers and 25 % of all cancers in women), being presently the fifth cause of death from cancer overall (522,000 deaths, 15 % of all cancer deaths among women). In the European Union, 362,000 new cases were diagnosed in 2012 and 92,000 women were expected to die from breast cancer (Ferlay et al., 2013; Torre et al., 2015). According to the Portuguese League against Cancer (*Liga Portuguesa Contra o Cancro* - LPCC), currently in Portugal for a 5 million female universe, there are 4,500 new cases of breast cancer per year, i.e. 11 new cases being diagnosed and 4 deaths per day due to this disease. In recent years, despite the efforts to reduce the number of cases, breast cancer metastasis and breast cancer–related mortality, the prognosis remains poor (Xu et al., 2015), thus reinforcing the relevance of developing new methods for early diagnosis that could result in more effective treatments (Mendes et al., 2015).

For an early detection of breast cancer, imaging (non-invasive means) and patient serum profiling (invasive means) are the most common techniques (Misek and Kim, 2011). Imaging technologies include mammography, ultrasonography, magnetic resonance imaging (MRI), positron emission tomography (PET) and computed tomography (CT) (Devi et al., 2015; Karellas and Vedantham, 2008). Mammography is currently the primary screening technique used worldwide, however in the next decade the primary imaging tool for breast cancer screening must provide a higher resolution and contrast (Karellas and Vedantham, 2008; Misek and Kim, 2011). This technique is able to detect 80 to 90 % of breast cancers and allows reducing the risk of death in 15 % in all women screened, but also generates a high rate of false positives and detects indolent localized cancers that may not require treatment. Other approaches based on cell morphology and microscopy (biopsies) are also not conclusive for an early diagnosis of cancer (Devi et al., 2015; Martin et al., 2010; Torre et al., 2015). These techniques are applied almost exclusively for screening, diagnosis and clinical management of cancer, as well as for assessing the integrity of breast implants. Nevertheless, these techniques are unsuitable for early detection of cancer biomarkers or their quantification (Devi et al.,

2015). Despite the existence of several sophisticated techniques for breast cancer imaging, there is still a huge need for a diagnosis system with greater specificity and sensitivity for tumors in an initial stage and that could also be comfortable for the patient. As an alternative to imaging techniques, the discovery of biomarkers and development of rapid diagnostic methods with improved features, namely high specificity and sensitivity, low cost, suitability for prognosis and disease monitoring, may represent the future for breast cancer diagnosis, and consequently for the decrease of its related mortality worldwide.

In biomedical applications, the development of methodologies to detect and quantify proteins, specifically protein biomarkers, has increasingly become essential for several areas of knowledge, such as in clinical analysis, for detection and treatment of certain diseases that can be correlated with changes in concentration of a protein biomarker in biological fluids. Determining the amounts of specific proteins in a given sample is particularly interesting and challenging. These proteins are effective diagnosis and prognosis tools for many diseases depending on the capability of easily quantifying low concentrations of proteins in biological samples (Csordas et al., 2010; Hanash, 2011). A biomarker is an indicator of the biological state of a certain disease and it can be a protein, a protein fragment, DNA, or RNA (Bohunicky and Mousa, 2011; Choi et al., 2010; Devi et al., 2015). The biomarker levels in body fluids such as blood, serum, plasma, saliva, urine, or cerebral spinal fluids, are extremely low. Biomarkers can potentially indicate the occurrence of a wide variety of primary tumors and metastasis located throughout the body (Bohunicky and Mousa, 2011; Martin et al., 2010). Moreover, biomarkers are used to evaluate treatment effects or to assess the potential for metastatic disease in patients with established disease (Rodrigues et al., 2007). The detection of protein biomarkers directly in blood samples is typically made using immunological assays like enzyme-linked immunosorbent assays (ELISA), which provide a good sensitivity and excellent specificity. Nevertheless, this standard assay has some drawbacks, such as the requirement of specific antibodies, the need of large amounts of samples, low stability, reduced dynamic concentration range, involvement of multiple steps and long response times (Csordas et al., 2010; Javaherian et al., 2009). Other techniques largely used in the detection and simultaneous profiling of multiple protein biomarkers are mass spectrometry, 2-D western blotting, and 2-D gel electrophoresis (Lee et al., 2008). However, the identification and quantification of biomarkers can be very complex, expensive and time consuming (Strehlitz et al., 2008). Also, these techniques require well-trained and skilled technicians, as well as additional steps of sample pre-treatment that

increase the time and cost of the analysis (Leca-Bouvier and Blum, 2005; Sassolas et al., 2009) and usually are not well-suited for comparative analysis of a large number of samples or the multiplexed detection of many targets within an individual sample. The use of microarray techniques can be a good alternative, but their application for protein biomarkers detection is still limited (Lee et al., 2008). Due to their rapidity, ease-of-use, relative low cost, simplicity, portability, inherent good selectivity and sensitivity, and possibility of continuous monitoring, biosensors represent a promising alternative to the conventional analytical methods (Leca-Bouvier and Blum, 2005; Sassolas et al., 2009).

Biomarkers that can be detected in the initial states of a disease are of utmost relevance since they allow cancer diagnosis at an early stage and, consequently may enhance the patients survival and enable a better control of the disease (Martin et al., 2010), thereby facilitating diagnosis and treatment of cancer in its pre-invasive state prior to metastasis (Misek and Kim, 2011). For example, the survival rate of patients with early diagnosed of localized breast cancer is 98 % as compared with a dismal of 27 % for those whose cancer, when diagnosed, already progressed and presents metastasis (Martin et al., 2010). For breast cancer detection, very few protein biomarkers are currently available and are used in clinical practice, which include cancer antigen 15.3 (CA15.3), cancer antigen (CA27.29) and carcinoembryonic antigen (CEA) (Gam, 2012; Porika and Tippani, 2011). These proteins were approved by the U.S. Food and Drug Administration (FDA) and their use was recommended by the American Society of Clinical Oncology (ASCO). Nevertheless, these proteins are useful only for monitoring the effect of therapy in advanced stages of breast cancer or to evaluate its recurrence (Gam, 2012; Mirza et al., 2008). Indeed, these biomarkers present low specificity (below 75 %) and sensitivity (below 25 %) for early stage breast cancer diagnosis (Mirza et al., 2008; Porika and Tippani, 2011). Other biomarkers that are related to breast cancer are the breast cancer type 1 susceptibility protein (BRCA1), breast cancer type 2 susceptibility protein (BRCA2), CA 125, NY-BR-I, ING-I, human epidermal growth factor receptor 2 (HER2), estrogen receptor (ER), progesterone receptor (PR) and Mucin (MUC-1) (Tothill et al., 2009; Bohunicky and Mousa, 2011). An important biomarker often evaluated in breast cancer patients is the CA15.3, being reported that its concentration increases by 10 % in stage I, 20 % in stage II, 40 % in stage III, and 75 % in stage IV breast cancers. ER and PR are poor prognosis markers; however, they may be used to select the most adequate cancer therapy. In turn, overexpression of HER2 is associated with poor prognosis and only occurs in about one third of patients with breast cancer (Bohunicky and

Mousa, 2011). Another protein that has been reported as a potential breast cancer biomarker is osteopontin (OPN) since its concentrations increase in plasma and serum of breast cancer patients, it is highly expressed in mammary tumor tissue and during the disease progression and metastasis (Bramwell et al., 2014, 2006; Nassar et al., 2015; Opstal-van Winden et al., 2011; Weber et al., 2011). In 2009, Macrì et al. studied the expression of OPN in breast cancer patients. The protein levels quantified in the serum suggested that OPN may play an important role in the development and progression of the neoplastic disease, thus constituting an adequate biomarker. Therefore, evaluating the OPN levels in breast cancer patients can be an alternative for the diagnosis, prognosis and monitoring of the disease.

2.2. Osteopontin: a potential breast cancer biomarker

OPN is a phosphorylated glycoprotein found in some body fluids that has been detected in approximately 90 % of primary breast carcinomas (Rodrigues et al., 2009). Several studies demonstrated that circulating levels of OPN may be indicative of cancer progression, metastasis, and poor prognosis (Ahmed and Kundu, 2010; Bache et al., 2010; Bramwell et al., 2014; Mirza et al., 2008; Rodríguez Portal et al., 2009; Shevde and Samant, 2014; Wai and Kuo, 2008; Weber, 2011; Weber et al., 2010; Xu et al., 2015; S. Zhao et al., 2011), as well as a possible therapeutic target for blocking tumor growth and subsequent metastasis (Bandopadhyay et al., 2014; Mi et al., 2009). Bache et al., (2010) also showed that increased serum and tumor OPN protein levels may be associated with several clinical parameters, such as tumor stage, grade, subtype, size and time of relapse. In breast cancer, a high OPN expression, measured both in plasma and in tumor tissue, has been related with a decreased survival rate. This protein has been clinically and functionally associated with cancer (Anborgh et al., 2011a; Beausoleil et al., 2011), modifying the behavior of cancer cells and promoting malignancy (Anborgh et al., 2011; Zhang et al., 2014) through its binding to several cell surface receptors, growth factor/receptor pathways and interaction with several integrins (Zhang et al., 2014). OPN was found to be overexpressed in tumors and serum in a variety of cancers types, including breast (Rodrigues et al., 2009; Tuck et al., 2007), lung (Blasberg et al., 2010; Zhao et al., 2011), cervical (Cho et al., 2008), colon (Agrawal et al., 2002; Li et al., 2012), gastric (Cao et al., 2012; Wu et al., 2007), ovary (Davidson et al., 2011; Kim et al., 2002; G. Song et al., 2008), prostate (Anborgh et al., 2009; Forootan et al., 2006), liver (Cao et al., 2012; Chen et

al., 2011) and pancreatic (Koopmann et al., 2004). Also, this protein is involved in signaling pathways related to adhesion and extracellular matrix interactions affecting multiple cellular functions, including inflammation and angiogenesis (Beausoleil et al., 2011; Davidson et al., 2011). For these reasons, OPN has been suggested as a potential diagnostic and prognostic cancer biomarker (Weber, 2011; Weber et al., 2011; Xu et al., 2015).

Several researchers studied the role of OPN isoforms in breast cancer. Mirza et al., (2008) described an OPN isoform (OPN-c) as a selective biomarker of breast cancer. The authors reported that OPN-c is expressed in 75 – 80 % of breast carcinomas, but not in normal tissues. In comparison with other breast cancer biomarkers, such as ER, PR or HER2, the OPN-c was detected in higher percentage, being its levels also correlated with tumor grade. This makes OPN-c, a very interesting candidate biomarker for the invasive potential of breast tumors, which could lead to novel diagnostic approaches. Patani et al., (2008) reported that high OPN-c levels are associated with tumor grade, poor prognosis, increased recurrence rates and poorer disease-free survival. Recently, Ortiz-Martínez et al., (2014) evaluated the role of OPN and OPN-c expression in HER2 and triple-negative/basal-like breast carcinomas subtypes, as well as their recurrences. This study highlighted the role of OPN-c as a prognostic biomarker in breast carcinomas subtypes. The total OPN mRNA was overexpressed in HER2-positive and triple negative/basal-like tumors, while OPN-c mRNA was specific for tripe-negative/basal-like tumors. Those results support the suggestion that OPN-c is a good biomarker of metastatic breast cancer.

2.3. Biosensors

According to the International Union of Pure and Applied Chemistry (IUPAC) “a biosensor is a self-contained integrated device which is capable of providing specific quantitative or semi-quantitative analytical information using a biological recognition element (biochemical receptor) which is in direct spatial contact with a transducer element” (Labuda et al., 2010; Thévenot et al., 1999, 2001). Another commonly used definition for biosensors is “analytical devices that are based on a bioreceptor and that are capable of sensing biologically-relevant analytes with either electrical or optical readout” (Cheng et al., 2009). As illustrated in **Fig. 2.1**, the main components of all biosensors are the bioreceptors or biorecognition elements; transducers or the detector devices; and displays or

electronic parts comprised by a signal amplifier and the data processor (Cheng et al., 2009; Strehlitz et al., 2008; Velusamy et al., 2010).

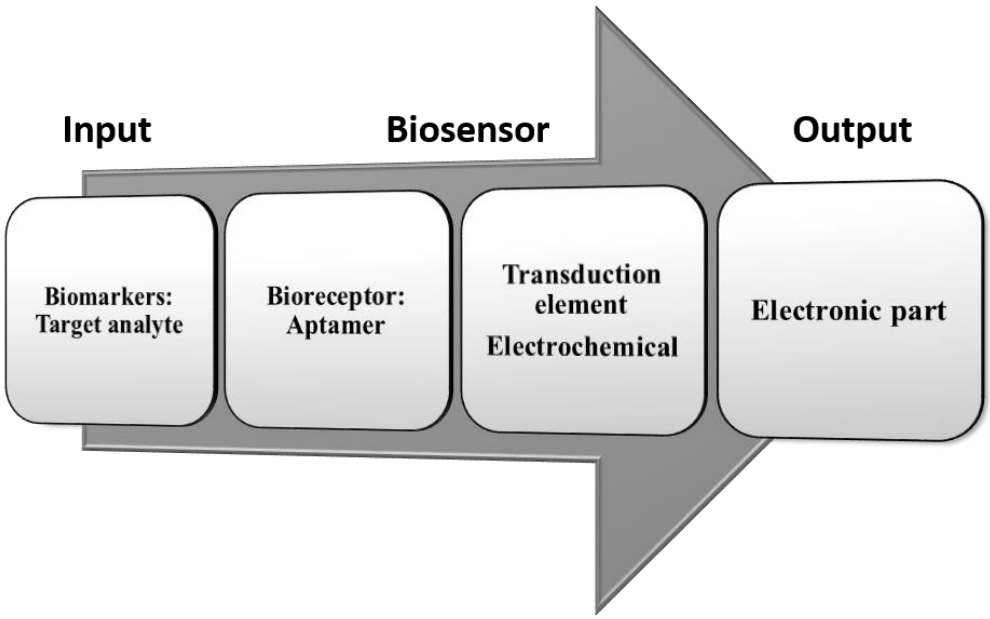

Fig. 2.1. Schematic illustration of a biosensor. The bioreceptors are immobilized on the surface of the transducer (signal converter). The binding event (i.e. binding of the bioreceptor to the target molecule) is then transformed into a measurable signal by the transducer, which leads to a measurement unit within the electronic device.

The basic principle of detection of the biosensor is the specific binding of the target of interest to the bioreceptor immobilized on a suitable support matrix, usually an electrode. The interaction between the target and the bioreceptor results in one or more physicochemical modifications (pH modification, electron transfer, mass variation, heat transfer and gases or ions release) that can be detected and measured by the transducer (Kumar and D'Souza, 2012). The typical purpose of a biosensor is to produce either discrete or continuous signals, which are proportional to a property of a single target or a related group of analytes. The signals are then transformed into a digital format that can be recognized by the end users (Strehlitz et al., 2008). The choice of the bioreceptor is crucial in the development of a biosensor, since it determines its selectivity/specificity. The bioreceptor will be responsible for the specific sensor response to a given target or group of targets of interest, thus minimizing the interference from other substances in complex mixtures (Viswanathan and Radecki, 2008). On the other hand, the transducer determines the sensitivity of the biosensor and is

responsible for converting the biological signal into a measurable signal (Monošík et al., 2012; Sassolas et al., 2009). The selectivity and sensitivity of the bioreceptor and transducer make the biosensors an attractive analytical tool in several areas and applicable to a large variety of samples including body fluids, food, cell cultures and environmental samples (Cheng et al., 2009; Grieshaber et al., 2008; Sassolas et al., 2009). Usually, the biosensors can be classified according to the bioreceptors type and signal transduction or transducer. Bioreceptors or biological recognition elements are commonly grouped in five classes, namely enzymes, antibodies/antigens, nucleic acids, cellular structures/cells and recently biomimetic materials or synthetic bioreceptors (e.g. aptamers) (Velusamy et al., 2010). Additionally, according to the method used for the signal transduction, the biosensor can be grouped in different classes, such as electrochemical, optical and mass sensitive. Each of these classes can be divided into many subclasses, creating a nearly infinite number of possible transduction or combined methods (Arshak et al., 2009; Monošík et al., 2012; Velusamy et al., 2010). The specific application of a biosensor determines the best method to use, since each detection method presents advantages and disadvantages. In this chapter, the electrochemical transduction will be detailed. The electrochemical transduction presents considerable advantages over optical, piezoelectric or thermal detection (Deng et al., 2013; Radi, 2011), such as high sensitivity and selectivity, the ability to work with turbid samples, compatibility with novel microfabrication technologies, inherent miniaturization, disposability and accuracy, simplicity, robustness, possibility of usage for on-line control, fast response, and relatively low manufacturing cost, thus making electrochemical aptasensors extremely attractive for diagnostic and use in point-of-care devices, as well as for simultaneous multi-analyte detection (Arshak et al., 2009; Radi, 2011; Saberian et al., 2011; Song et al., 2008; Velasco-Garcia and Missailidis, 2009; Velusamy et al., 2010; Xu et al., 2009).

2.4. Aptamers as bioreceptors

Aptamers are short nucleic acids (≈ 12-80 nucleotides long) of RNA or single-stranded DNA that possess unique binding characteristics to their targets, such as high sensitivity/affinity, specificity and ability to fold into numerous tertiary conformations (e.g. hairpin, G-quartet, stem-bulge, pseudoknot, T-junction) (Cho et al., 2009; de-los-Santos-Álvarez et al., 2008; Famulok and Mayer, 2011; Lakhin et al., 2013; Meyer et al., 2011; Radom et al., 2013). The aptamers have been

selected against a large variety of targets including proteins, ions, toxins, drug molecules, cells, and tissues (Lee et al., 2008; Shamah et al., 2008; Stoltenburg et al., 2007). Most of the aptamers reported have been selected using purified and soluble forms of a target protein (Shamah et al., 2008). The dissociation constants (*Kd*) of aptamers (DNA or RNA) and their proteins are in the low micromolar to high picomolar ranges, which allows discriminating between related proteins that share common sets of structural domains (Labuda et al., 2010; Jing et al., 2011; Kim et al., 2013). Typically, aptamers are isolated through an *in vitro* selection procedure known as SELEX (Systematic Evolution of Ligands by Exponential Enrichment) (**Fig. 2.2**). The generation of aptamers through SELEX must take into account a number of variables including the starting random oligonucleotides library; type of target molecule; type of aptamer (e.g. DNA, RNA, modified nucleic acid); any modifications included in the library (to make it compatible with T7 RNA polymerase, reverse transcriptase and/or DNA polymerase); buffers, pH and temperature; as well as the immobilization, or not, of the target; method used for partitioning the sequences bound to the target; time and cost to complete the whole process (Ozer et al., 2014). The SELEX methodology starts with a chemically synthesized random oligonucleotides library (up to 10^{15} different sequences). The selection process may be divided into 3 steps that are repeated in order to obtain nucleotides with improved binding ability towards the desired target (Dua et al., 2011; Santosh and Yadava, 2014; Vikesland and Wigginton, 2010). In the first step, so-called binding step, a random oligonucleotides library is incubated with the target molecule. The target can bind the oligonucleotides either in an immobilized form on a certain matrix (e.g. magnetic beads, affinity column, microtiter plates) or in the free form (Gopinath, 2007; Mairal et al., 2008). In this case, the target is exposed directly to millions of sequences present in the library using a specific incubation period. This procedure favors the separation process, but can import some non-specific adsorption and affect the targets' conformation to some degree; in the free form it can keep the conformation of the target but make it harder to separate (Wang and Jia, 2009). In the second step, so-called separation or partitioning step, the bound sequences with strong affinity to their targets are isolated from the unbound ones through a suitable partitioning method (e.g. filtration often using a filter membrane for the target protein, or using a column with the target covalently immobilized, or by affinity chromatography for small molecules targets). For large targets (e.g. cells), the separation can be achieved by centrifugation. However, the methods are often defined depending on the target, the aptamer purpose and the expected outcome of the SELEX (Du and Li, 2010; Zhou et al., 2014). After the bound aptamers sequences are eluted from the targets, which may be done using high temperature and/or high salt

concentration, they are enriched by precipitation and centrifugation for the next step (Du and Li, 2010). In the third step, so-called amplification step, the sequences that were bound to the target are amplified by polymerase chain reaction (PCR) when using a DNA library, or by reverse transcriptase (RT)-PCR when using a RNA library, to create a new pool of sequences for the following selection cycle that is enriched in oligonucleotides that specifically bind the target.

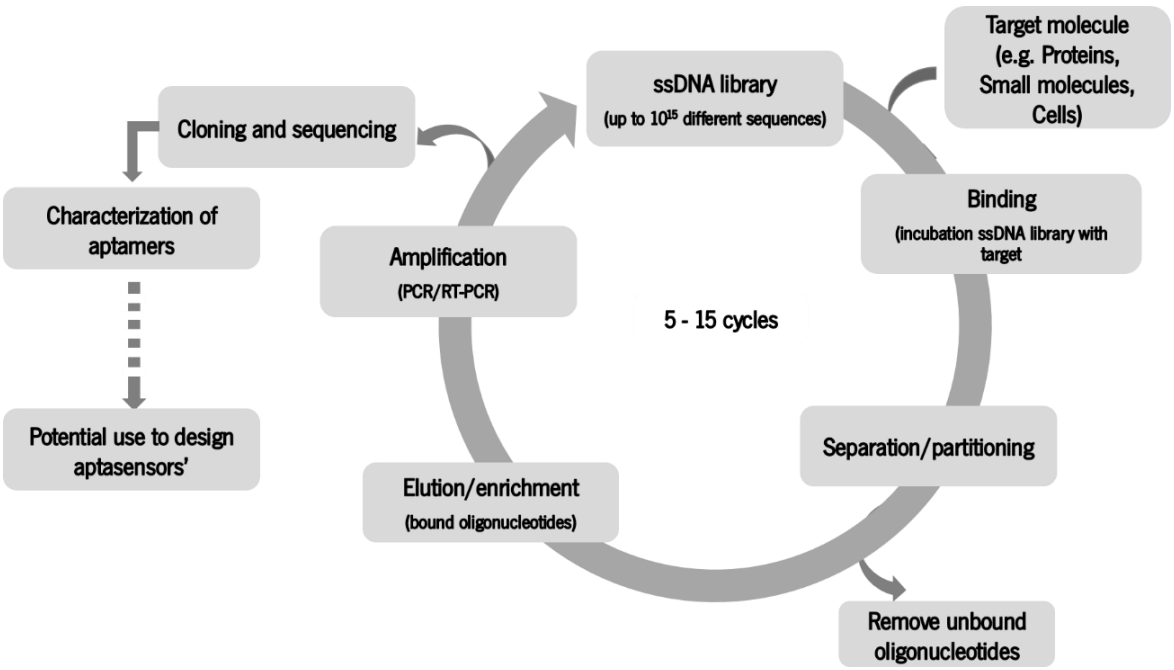

Fig. 2.2. Systematic Evolution of Ligands by Exponential Enrichment (SELEX) methodology.

After PCR amplification, the dsDNA is transcribed *in vitro* by T7 RNA polymerase resulting in a randomized RNA library, which is used for the next round of the RNA SELEX. In the case of DNA SELEX, the dsDNA has to be separated in ssDNA before the next round. Several methods have been described for this purpose, such as the streptavidin/biotin system, asymmetric PCR amplification, thermal denaturation, lambda exonuclease digestions and size separations on denaturing urea polyacrylamide gel electrophoresis (PAGE) (Kulbachinskiy, 2007; Marimuthu et al., 2012; Stoltenburg et al., 2007). After a number of cycles (generally 5-15 cycles), the sequences obtained are cloned, sequenced and characterized in order to select an aptamer with high affinity and specificity to the target molecule (Dua et al., 2011; Kim et al., 2008; Radom et al., 2013; Song et al., 2012; Stoltenburg et al., 2007; Syed and Pervaiz, 2010). Finally, the selected aptamers are

analyzed using alignments software to evaluate their complexity and to identify identical sequences and highly conserved regions that are often involved in the specific target binding of the aptamers (Stoltenburg et al., 2007), analysis of secondary structures by free energy minimization using the MFold program (Zuker, 2003). Then, the aptamer-protein binding is determined using several methods like ultrafiltration, gel and capillary electrophoresis, fluorescence assays, circular dichroism, surface plasmon resonance and isothermal titration calorimetry (Jing et al., 2011; Tang et al., 2007).

Since its discovery, continuous efforts have been conducted to improve the SELEX methodology towards a faster generation of aptamers, hence several SELEX variants have been developed, making the selection of aptamers more efficient, cost effective, faster and less laborious (Darmostuk et al., 2015; Radom et al., 2013). These are mainly related with the methods used for the separation/partitioning step (e.g. nitrocellulose filter binding-, beads based-, electrophoretic-, microfluidic-, microarray based- and microscopic-SELEX), with the type of target (e.g. cell-SELEX and small-molecule SELEX) and/or use of SELEX *in vivo* (Ozer et al., 2014; Radom et al., 2013). Other variants were also developed to reduce the number of selection cycles, such as MonoLEX, Nano Selection and Aptamer Selection Express (Axp) (Darmostuk et al., 2015). After running all the SELEX steps, some post-SELEX modifications can be included to avoid compromising the aptamer function (Bugaut et al., 2006; Mckeague and Derosa, 2014; Stoltenburg et al., 2007). However, the modified RNA/DNA aptamers generally exhibit lower affinities to the target compared to the original unmodified aptamers (Kuwahara and Sugimoto, 2010). The replacement of the DNA phosphate backbone by phosphorothioation is one of the post-SELEX modifications that stabilizes the structure of the DNA aptamers against nucleases (Kim et al., 2008; Mayer, 2009). Besides the phosphorothioation, the RNA aptamers can be modified by substitution of the 2'-OH groups of the riboses from pyrimidines (with 2'-fluoro or 2'-amino groups) which protect the aptamers from nucleases degradation. Moreover, these aptamers can be stabilized by the substitution of the 2'-OH groups of the riboses from purines (with O-methylation) (de-los-Santos-Álvarez et al., 2008; Kim et al., 2008; Kulbachinskiy, 2007). The use of mirror analogs of natural nucleotides (on the basis of L-ribose or L-deoxyribose) is another alternative to obtain nuclease-resistant aptamers and increase their half-life and stability. These aptamers were named as Spiegelmers (Kulbachinskiy, 2007). The fixation of the 3'-end with streptavidin-biotin that inverts the thymidine (3'-idT, creates a 3'-3' linkage) or several 5'-caps (amine, phosphate, polyethylene glycol (PEG), cholesterol, fatty acids, proteins, among others) protects the oligonucleotides from the action of the exonucleases (Guo et al., 2008;

Prieto-Simón et al., 2010; Sassolas et al., 2009; Stoltenburg et al., 2007; Vikesland and Wigginton, 2010; You et al., 2011). Another modification often used in aptamers is the locked nucleic acids (LNAs), enhancing its thermal stability, thus enabling an excellent mismatch discrimination when hybridized with RNA or DNA. All chemical modifications described above have been used to increase the half-life and nuclease resistance of aptamers, besides improving the *in vivo* stability of aptamers designed for clinical applications.

The SELEX methodology is a powerful and universal tool to identify aptamers with high affinity and specificity to a wide variety of targets. The selection conditions have to be adapted depending on the target, desired features of the aptamers and envisaged applications (Stoltenburg et al., 2007). The selection conditions (e.g. buffer composition, temperature, binding time), the design of the randomized oligonucleotide library, or additional selection steps can strongly affect the specific binding features (affinity, selectivity) of the aptamers. Frequently observed problems of the aptamers selection include the enrichment of non-specifically bound oligonucleotides or repeated selections of already known aptamer sequences (Mascini, 2009). The main disadvantage of the SELEX methodology is the uncertainty of a successful selection of the best aptamer, i.e. the methodology cannot guarantee that at the end the aptamer is the most adequate for the target molecule (Mayer, 2009). To date, several aptamers have been used in numerous studies concerning their use to diagnosis many diseases, as therapeutic tools and/or as bioreceptor elements in several biosensing detections, as well as in the development of new drugs and drug delivery processes (Khati, 2010; Song et al., 2012). The first aptamer approved by the FDA is a therapeutic RNA aptamer against the protein VEGF (known as Macugen, Pegaptanib) for age-related macular degeneration (AMD) treatment (Guo et al., 2008). Aptamers exhibit a number of advantages as compared to antibodies, such as high selectivity and affinity, easier artificial synthesis, chemical stability under a wide range of buffer conditions, resistance to harsh treatments without loss of bioactivity, reversible thermal denaturation, adaptability to various targets, ease of storage, and versatility in labeling, immobilization, signaling and regeneration (Feng et al., 2008; Hianik and Wang, 2009; Y. Li et al., 2010; Radi, 2011; Strehlitz et al., 2008). The small size of aptamers allows their efficient immobilization at high densities in the different surfaces. Thus, production, miniaturization, integration and automation of biosensors can be accomplished more easily with aptamers than with antibodies (Strehlitz et al., 2008). Altogether these properties make aptamers an appropriate tool in the development of aptasensors (de-los-Santos-Álvarez et al., 2008; Guo et al., 2008; Hianik and

Wang, 2009; Lee et al., 2008; Park et al., 2009; Song et al., 2012; S. Song et al., 2008; Tombelli et al., 2005; Velasco-Garcia and Missailidis, 2009; Zhang and Chen, 2010). In biosensing applications, DNA aptamers are suitable for designing reusable aptasensors, whereas RNA aptamers allow single shot measurements since they are more susceptible to nucleases attack (Sassolas et al., 2009; Strehlitz et al., 2008). As previously referred, some chemical modifications can enhance nuclease resistance (i.e. biostability in serum) and increase the half-life of aptamers. These chemical modifications can be introduced in the oligonucleotides libraries and either during or after the SELEX cycle (Kuwahara and Sugimoto, 2010; Stoltenburg et al., 2007).

In summary, the detection of a disease as cancer at an early stage allows a better diagnosis, together with the definition of more adequate treatments that ultimately will lead to an increased survival. The selection and design of aptamers that are specific to recognized cancer biomarkers (e.g. OPN) can represent a good alternative for diagnostic and treatment of the disease. An RNA aptamer binding to OPN was reported (Mi et al., 2009) to block the interaction with its cognate receptors (CD44 and integrin) significantly inhibiting migration and invasion *in vitro*, as well as local progression and distant metastasis formation (Hunter et al., 2012; Mi et al., 2009). Also, this aptamer was able to inhibit *in vivo* and *in vitro* the metastatic function of MDA-MB231 human breast cancer cells (Mi et al., 2009). This study suggested that the use of a specific aptamer against OPN could represent a viable therapeutic intervention for inhibiting the breast cancer cells growth and the development of metastasis.

2.5. Aptamer–based biosensors: Aptasensors

Biosensors that use DNA or RNA aptamers as bioreceptors have been named as “aptasensors” (Cheng et al., 2009; Hianik and Wang, 2009; Radi, 2011; Sassolas et al., 2009). The aptasensors emerged in the early 1990’s with the introduction of aptamers as sensing probes (Cheng et al., 2009) considered an important alternative to the classical analytical methods for protein detection. The specific properties of aptamers as bioreceptors offers some advantages over methods that are mainly based on standard affinity receptors (e.g. antibodies) in the development of aptasensors. These advantages include the possibility of performing several analyzes with mild alteration of specificity and selectivity of the binding; and of using different designs and detection strategies for

fast and easy detection of protein in real samples (Cheng et al., 2009; Hianik and Wang, 2009; Hianik et al., 2007; Kim et al., 2008; Nguyen et al., 2009; S. Song et al., 2008; Zhou et al., 2011).

The lack of specific aptamers for the majority of protein disease biomarkers, as well as the existence of few aptamers with two recognition sites for a single target, may constitute a limitation in the development of aptasensors. Nevertheless, over the years with the use of different SELEX methodologies, a large number of aptamers have been isolated and applied in aptasensors developed to detect small molecules and protein disease biomarkers. The production of aptasensors at a large scale is subject to some difficulties that must be overcome, such as the aptamer stability during immobilization and the signal registration in complex biological samples, mainly due to the interferences from other molecules also present in those samples (Hianik and Wang, 2009; Hianik et al., 2007). In this chapter some electrochemical transducers for the detection of proteins are discussed, as well as methods of immobilization of aptamers and the detection strategies used in the production of electrochemical (voltammetric) aptasensors.

2.6. Electrochemical aptasensors

Electrochemical aptasensors use an electrode surface for immobilization of the aptamer with an electrochemical transducer to monitor the aptamer-target interaction, by detecting current or potential changes that occur at the transducer/bioreceptor interface/surface (Hong et al., 2012; Monošík et al., 2012; Sadik et al., 2009; Thevenot et al., 1999; Thévenot et al., 2001). The first aptasensor for the detection of a target protein at nanomolar level was reported in 1998, using a DNA aptamer against thrombin (Zhou et al., 2011). Later, Hianik et al., (2005) described the first voltammetric aptasensor using DNA aptamers against thrombin immobilized onto a gold electrode surface. This biosensor detected the thrombin-aptamer interactions through the measurement of charge changes by differential pulse voltammetry (DPV) and using methylene blue (MB) as the electrochemical indicator (Hianik et al., 2005). The electrochemical transduction of biosensors using aptamers as bioreceptors can be divided in voltammetric, amperometric, potentiometric, impedimetric and conductometric, depending on the measurable parameters such as current and potential, current, potential, impedance, and conductance, respectively (Arshak et al., 2009; Velusamy et al., 2010). Among voltammetric biosensors, different voltammetry techniques can be

used such as cyclic voltammetry (CV), DPV, square wave voltammetry (SWV), and alternating current voltammetry (ACV). The voltammetric and/or amperometric biosensors are characterized by applying a potential to a working electrode *versus* a reference electrode. The corresponding current is a result of electrolysis by means of an electrochemical reduction or oxidation at the working electrode. Amperometric biosensors may be considered a subclass of voltammetric biosensors since they operate under an imposed constant potential (voltage) that is maintained at the working electrode with respect to a reference electrode, being the change in current monitored as a function of time. On the other hand, in the voltammetric biosensors the potential is scanned over a set potential range and both the current and potential are measured and recorded. For amperometric and voltammetric biosensors, the recorded current response is proportional to the concentration of the target molecule in the sample (Grieshaber et al., 2008; Kumar and D'Souza, 2012; Liu, 2000; Rahman et al., 2008; Ronkainen et al., 2010; Viswanathan and Radecki, 2008). A remarkable advantage of voltammetric biosensors is the low related noise observed, hence providing reliable and reproducible data for the quantification of a target molecule, which can endow the biosensor with higher sensitivity and specificity. In addition, voltammetry allows the detection of multiple compounds, which have different peak potentials, in a single electrochemical experiment (or scan), thus offering the possibility of simultaneously detecting multiple analytes. Among the voltammetric aptasensors, those based on CV, DPV and SWV are the most frequently used. However, the CV technique can be used to evaluate the electrode surface, namely its purity, stability, reproducibility and repeatability. CV may also be used for cleaning and for monitoring the immobilization of aptamers on the electrode surface since it allows a fast visualization of the redox behavior over a wide potential range (Ferreira et al., 2011). Moreover, it can also be used to study the performance of an electrochemical aptasensor during the detection of several molecules, such as proteins (Cheng et al., 2007; Meirinho et al., 2015; Wang et al., 2009; Yuan et al., 2011).

The electrochemical aptasensors can be applied in several areas such as health (specifically in clinical diagnostic and for therapeutic purposes), food industry and environmental monitoring (Hong et al., 2012; Palchetti and Mascini, 2012; Sett et al., 2012). In this chapter, the application of electrochemical aptasensors for clinical diagnosis, particularly for the detection of protein disease biomarkers, which is an emergent field of research, will be discussed.

The electrode/transducer surface (e.g. thickness and stability of the materials), the immobilization method and the detection technique are relevant factors that must be considered whenever

developing an electrochemical aptasensor (Zhang et al., 2000). Usually, a three-electrode configuration is included in the surface of a voltammetric aptasensor, namely the working, auxiliary or counter and the reference electrodes (Lim et al., 2010). The working electrode, also known as the sensing or redox electrode, corresponds to the electrode in which the current is measured and possesses a surface area of few square micrometers to square millimeters. The material used in the preparation of the working electrode surface determines the overall performance of the analytical electrochemical-based device, especially the immobilization efficiency of the bioreceptors. A potential is applied to this electrode and the potential difference between it and the reference electrode, which is also in contact with the test solution, is measured. The common material used as the working electrode surface is carbon and noble metals, for which different immobilization strategies and detection approaches can be applied. Metals such as gold, platinum, silver and stainless steel have long been used for electrochemical electrodes due to their excellent electrical and mechanical properties (Hayat and Marty, 2014; Ronkainen et al., 2010; Zhang et al., 2000). These materials are chemically inert and provide a wide range of anode working potentials with low electrical resistivity (Zhang et al., 2000). The reference electrode is usually of silver (Ag), silver/silver chloride (Ag/AgCl) or a saturated calomel electrode (SCE, Hg/Hg_2Cl_2). This electrode should be kept at a certain distance from the reaction site in order to maintain a known and stable potential. It is important to notice that this electrode contributes to the stability and reproducibility of the sensor (Liu, 2000). The counter electrode or auxiliary electrode is part of a feedback system that supplies current to the test solution whenever necessary, in order to maintain the correct potential at the working electrode-solution interface (Daniels and Pourmand, 2007). In summary, the working electrode serves as the transduction element in the biochemical reaction, while the counter electrode establishes a connection with the electrolytic solution so that a current can be applied to the working electrode (Grieshaber et al., 2008). Other electrode surfaces can be used in the development of electrochemical aptasensors, such as screen printed electrodes (SPE), glassy carbon electrodes (GCE), carbon paste electrodes (CPE), depending on the target molecule to be detected. SPEs, are mini-electrode systems that include a working, reference and counter electrode and can be easily fabricated using screen-printing technology or via the use of semiconductor chips with macro/micro-array patterns allowing the development of rapid, inexpensive and disposable biosensors (Tothill, 2009). The thick-film technology is commonly used for the fabrication of disposable electrodes in large scale with high reproducibility and low-cost. These SPEs can be produced with different materials and modified with the same methods used for the solid supports (Wei et al., 2009). This

technology led to the miniaturization of the electrodes and it has opened the horizon for *in vivo* and *in vitro* applications of electrochemical sensors systems, thus allowing the reduction of volume samples and reagents up to few microliters. In addition, these sensors avoid the contamination between samples and exhibit a reproducible sensitivity (Ronkainen et al., 2010; Tothill, 2009; Wei et al., 2009).

Other essential step in the development of electrochemical aptasensors is the immobilization of the aptamer, which plays a major impact in the overall biosensor performance. The stability, affinity and sepecificiy of the aptamer towards the target molecule depend on the technique used to immobilize it onto the electrode/transducer surface. Thus, it is crucial to treat and control the surface to assure high reactivity, orientation/accessibility and stability of the surface-bound aptamer, as well as to minimize non-specific binding/adsorption phenomena (Hianik and Wang, 2009; Lim et al., 2010). The choice of the immobilization method depends on several factors, such as the nature of the bioreceptor and electrode/transducer surface, the physicochemical properties of the target molecule and the operating conditions of the biosensor. Therefore, the selected method should ensure that the binding affinity and selectivity of the aptamers in solution are kept in order to obtain the maximum activity whenever they are immobilized as the bioreceptor (Balamurugan et al., 2008; Velasco-Garcia and Missailidis, 2009). The immobilization methods usually applied are physisorption (physical adsorption), chemisorption (chemical adsorption), streptavidin/avidin/neutravidin-biotin interaction and covalent attachment via functional groups (Balamurugan et al., 2008; de-los-Santos-Álvarez et al., 2008; Sassolas et al., 2009; Zhou et al., 2011) (**Fig. 2.3**). In the first method, no aptamer modification is required and the aptamer is immobilized on the electrode surface by means of electrostatic forces. This method is simple but, in general, it is not suitable for the development of reusable aptasensors due to the low stability resulting from the aptamers' desorption from the surface (Hianik and Wang, 2009; Paniel et al., 2013; Radi, 2011; Sassolas et al., 2009). In the other three methods, the aptamers are modified with a thiol group (-SH), a biotin protein and a chemical functional group (e.g. amino groups ($-NH_2$)), respectively (de-los-Santos-Álvarez et al., 2008; Zhou et al., 2011).

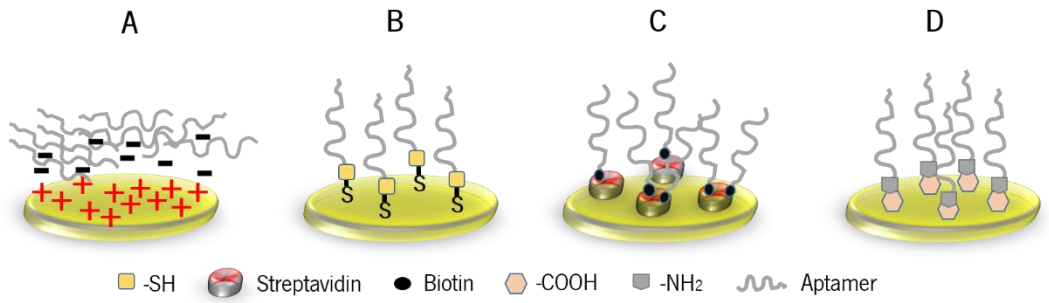

Fig. 2.3. Immobilization methods of aptamers into gold electrodes surfaces for the development of electrochemical aptasensors. A) Physical adsorption; B) Chemisorption; C) Streptavidin-biotin interaction; D) Covalent attachment.

Aptamers can be modified and attached to the electrode surface either by the 5'-end or the 3'-end. Both positions have been used to develop aptasensors, although very few works evaluated the effect of the type of the aptamer's end position, used for the attachment to the surface, on the immobilization and aptasensor performances. However, some studies suggest that it depends on the particular aptamer, although the 3'-end could be more suitable for biological targeting since it is the primary target for exonucleases and its binding to the solid support would simultaneously confer resistance to nucleases (Hayat and Marty, 2014; Hianik and Wang, 2009; Velasco-Garcia and Missailidis, 2009). These immobilization methods allow obtaining a stable, flexible and repeatable aptamer layer on the surface (Radi, 2011; Xu et al., 2009; Zhou et al., 2011). The chemisorption method consists in the direct immobilization of the thiolated aptamer onto the electrode surface. It is a simple and effective method based on the strong affinity of thiol groups (-SH) for gold electrode surface that enables the formation of covalent bonds between the sulfur and gold atoms forming a stable and flexible self-assembled monolayer (SAM) with repeatable aptamer surface layers (Paniel et al., 2013; Sassolas et al., 2009). The immobilization of aptamers based on the streptavidin/avidin/neutravidin-biotin interaction has been exploited due to the specific and strong affinity between the streptavidin (or derivatives) and the biotin. The streptavidin and avidin proteins have four identical binding sites for biotin (Chung et al., 2011; Hayat and Marty, 2014). However, the streptavidin is preferably used over avidin, leading to fewer non-specific interactions associated to the low isoelectric point (pI) as compared to avidin (Lim et al., 2010; Sassolas et al., 2009, 2008). The streptavidin (or derivatives) can easily be linked on the electrode surface through physical adsorption or non-covalent bonding (Hianik et al., 2007, 2005; Nimse et al., 2014; Zhou et al., 2011). Other advantages can be pointed out, namely the need of very low amounts of biotinylated

aptamer (Chung et al., 2011); the fact that it is less affected by changes of buffer concentration, pH, denaturants and high temperatures; as well as the decrease of non-specific adsorption and improvement of the signal-noise ratio (Paniel et al., 2013; Zhou et al., 2011). In the covalent attachment method, the electrodes surfaces are modified with chemical groups (e. g. amine: -NH_2; hydroxyl: -OH; carboxylic acid: -COOH; aldehyde: -CHO) that interact with the modified aptamer exhibiting the corresponding chemical functional group to form an ordered aptamers layer on the electrode surface. Commonly, the amino (-NH2)-modified aptamer were covalently attached onto electrode surface functionalized with thiolic acids and then the terminal carboxylic group (-COOH) is activated with 1-ethyl-3-[3-dimethylaminopropyl]-carbodiimide hydrochloride (EDC)/N-hydroxysulfosuccinimide (sulfo-NHS) (Balamurugan et al., 2008; Zhou et al., 2011). This method can be performed on different surfaces such as gold or platinum electrodes, glassy carbon, carbon pasta, silicate and polymer surfaces and, more recently, gold nanoparticles (AuNPs) and gold nanorods (AuNRs) (Zhou et al., 2011). However, the choice of the surface functionalization strategy to be implemented depends on the type of terminal functional groups linked to the aptamer (Balamurugan et al., 2008). This method allows increasing the specificity of the aptasensors and decreasing the non-specific adsorption (Paniel et al., 2013). Another method that can be used is the application of the partially complementary sequences that are immobilized on the electrodes surfaces using one of the methods described above. In this case, the aptamers are immobilized by hybridization. However, in this method the experimental conditions are difficult to control since it involves annealing and hybridization steps (Han et al., 2009; Hianik and Wang, 2009). Whenever manufacturing aptasensors, it is important to evaluate how the immobilization methods can affect their performance regarding the detection of the target molecule. Hianik et al., (2007) evaluated the sensitivity of aptasensors using three aptamer immobilization methods, namely the bonding through affinity (avidin-biotin interaction), direct chemisorption of aptamers modified with -SH groups and polyamidoamine (PAMAM) dendrimers layers. The best results were obtained for the aptamer immobilization by means of avidin-biotin interaction, followed by the dendrimer layer and lastly the aptamer chemisorbed directly onto the gold surface. Similarly, Ostatná et al., (2008) demonstrated that the immobilization of the aptamers by means of the streptavidin-biotin interaction showed the best results regarding the sensor specificity and sensitivity.

Different design strategies may be adopted in the fabrication of electrochemical aptasensors depending on the envisaged use. These strategies (reviewed by Cheng et al., (2009) and Han et al.,

(2010)) can be divided into three or four types based on the differences in the design of the DNA/RNA-modified electrodes. Cheng et al., (2009) classified electrochemical aptasensors in three categories in which the analyte/target molecule detection relies on a configuration change (i.e. target binding induces either an assembly or dissociation of the aptamer); conformation change (i.e. target binding induces a modification in the conformation of the aptamer immobilized onto the surface); and conductivity change (i.e. target binding "switches on" the conductivity of the surface-bound aptamer–DNA). On the other hand, Han et al., (2010) suggested four possible design strategies, viz. target-induced structure switching mode; sandwich or sandwich-like mode; target-induced dissociation or displacement mode; and competitive replacement mode. **Fig. 2.4** illustrates the main strategies/designs used in the development of electrochemical aptasensors.

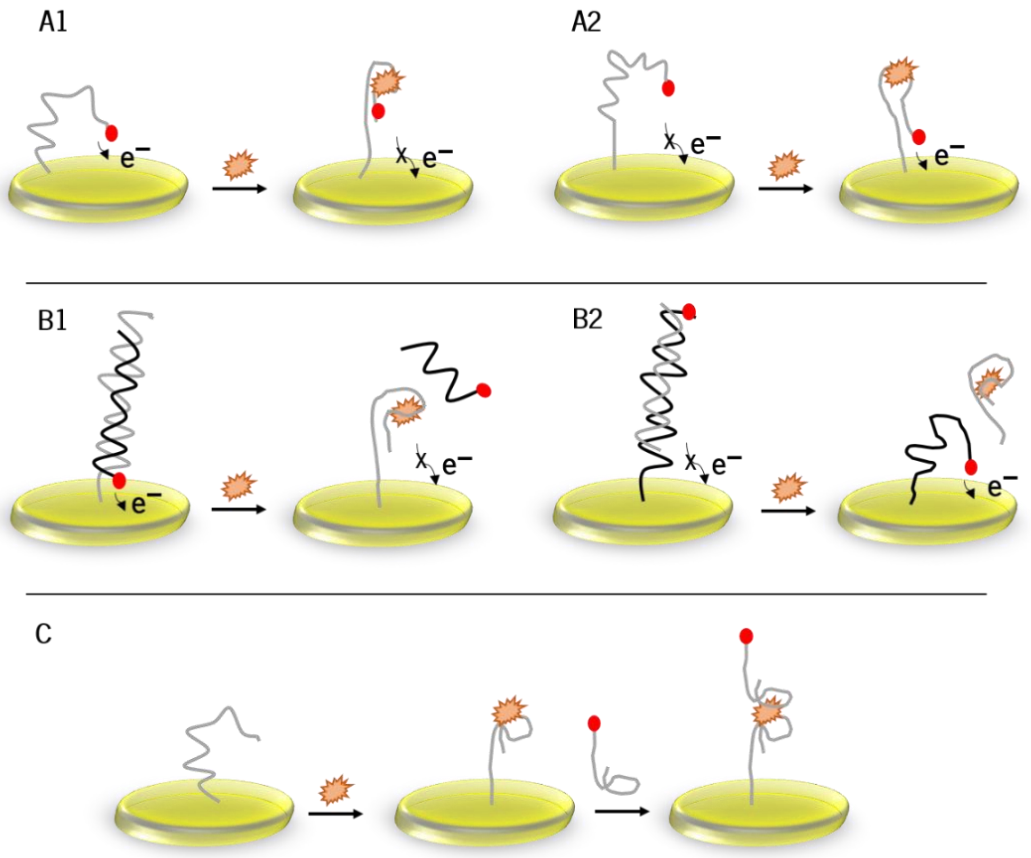

Fig. 2.4. Strategies/designs to develop electrochemical aptasensors. A) Target binding-induced aptamer conformation change: A1) "signal-off" and A2) "signal-on". B) Target binding-induced aptamer-complementary sequence dissociation/displacement: B1) "signal-off" and B2) "signal-on". C) Sandwich assays.

Regarding the electrochemical aptasensors detection, two main approaches have been used, namely the label (using labelled aptamers) and label-free (using non-labelled aptamers) approaches. The measurement of changes in the electrode surface of electrochemical aptasensors can be either "signal-on" (positive readout signal) or "signal-off" (negative readout signal), i.e. an increase or a decrease of the response following upon aptamer-target interaction, depending on the format of the assay used in the aptasensor fabrication (Hayat and Marty, 2014; Radi, 2011; Sassolas et al., 2009; Song et al., 2008; Strehlitz et al., 2008). However, the aptasensor based in "signal-off" are usually less sensitive, more susceptible to background variation and small signal changes (Zhou et al., 2014). In the literature, the detection "signal-on" or "signal-off" is usually associated with target binding-induced aptamer conformational change (Baldrich et al., 2006; Lai et al., 2007; Liu et al., 2010; Ma et al., 2013; Sánchez et al., 2006; Xiao et al., 2005a) and target binding-induced aptamer-complementary sequence dissociation/displacement (Lu et al., 2008; Xiao et al., 2005b) strategies. This is due to the fact that aptamer-label or aptamer-complementary sequence-label after binding to its target, promotes the approximation of the label on the electrode surface, thus increasing the current ("signal-on") or a distancing of the label from the electrode surface, thus decreasing the current ("signal-off") (Sassolas et al., 2009). However, this classification signal-on and signal-off, is also often employed in the sandwich assays (Centi et al., 2009, 2007; Zhang et al., 2007, 2009) or label-free aptasensors, when an increase or decrease of the signal is observed after the formation of the aptamer-target complex (Cheng et al., 2007; Degefa and Kwak, 2008; Meirinho et al., 2015; Rodríguez and Rivas, 2009).

Thrombin has been the most used protein to study electrochemical aptasensors. Its detection is crucial in many areas of biomedical research and diagnostic (Wang et al., 2011), as it is a multifunctional serine protease, whose concentration level in blood has high relevance in some pathologies (Wang et al., 2011). Therefore, the strategies used for the detection of thrombin can be a point of start for many other cancer-related proteins such as platelet-derived growth factor (PDGF), OPN, VEGF and mucin 1 (MUC1).

2.6.1. Label electrochemical aptasensors

In the label approaches, the bioreceptor can be labelled with a great variety of different redox compounds. These redox compounds can be covalently bound to the aptamer and modulate the electrochemical signal upon formation of the aptamer–target complex (Hayat and Marty, 2014;

Palchetti and Mascini, 2012; Prieto-Simón et al., 2010; Sassolas et al., 2009). The aptamers can be labelled at both 3'- and 5'- ends. At one end, for immobilization at the electrode surface and at the other end, the redox compounds for signal amplification (Strehlitz et al., 2008). The horseradish peroxidase (HRP), glucose oxidase (GOD) and alkaline phosphatase (AP) enzymes can also be used as redox compounds (Prieto-Simón et al., 2010). However, the most commonly used are ferrocene (Fc), MB and recently nanomaterials such as quantum dots (QDs) and nanoparticles (NPs), which present some advantages over the enzymes for biosensing assays (Hayat and Marty, 2014). **Table 2.1** compiles some of the most relevant works that report the development of label electrochemical aptasensors using voltammetric techniques for the detection of specific proteins. The electrochemical cell, aptamer immobilization technique, redox compounds, design and detection assay type, detection limit, working range and applications are described for each example.

Xiao et al., (2005a) developed a label "signal-off" electrochemical aptasensor for detection of thrombin in blood serum. Before binding the protein, 3'-end MB-label aptamer is close to the electrode surface, thus allowing the transfer of electrons with the electrode surface due to the flexible structure of the aptamer. After thrombin binding, the aptamer forms a stable and rigid structure (G-quadruplex structure) and the MB-label is kept away from the electrode surface, the electron transfer is inhibited, resulting in a current decrease. The electrochemical measurements were performed by ACV and a detection limit of 6.4 nM was reported. The same strategy was used by Liu et al., (2010) for the detection of interferon gamma (IFN-γ). The aptamer against IFN-γ was 5'-end thiolated, conjugated with 3'-MB-label and immobilized on a gold electrode surface. The IFN-γ binding induced an aptamer conformation change, increased the distance of MB-label from the electrode surface and led to a decrease of the electron transfer and consequently of the current. The SWV was used to quantify the current decrease and a detection limit of 0.06 nM was achieved. This label "signal-off" electrochemical aptasensor proved to be sensitive and specific to IFN-γ in the presence of overabundant serum protein. The sensor was found to be reusable multiple times after treatment with a 7 M urea buffer during 1 min. Ma et al., (2013) developed a label "signal-off" electrochemical aptasensor towards MUC1, a glycoprotein implicated in some cancers including breast cancer. The thiolated DNA aptamer was immobilized onto a gold electrode surface and the other aptamer end was labelled with MB to enable the electrochemical measurements. In the absence of MUC1, one hairpin structure was formed and the electrode transfer between MB-label and the gold electrode was facilitated. Upon MUC1 binding, a conformational change of the aptamer was induced, the MB-

label was removed from the electrode surface and a decrease in the current was observed. The electrochemical measurements were performed by SWV and a detection limit of 50 nM and a large dynamic response range (up to 1.5 μM) were reported. This electrochemical aptasensor showed good specificity in the presence of other proteins and could be seen as a promising tool in clinical applications. Lai et al., (2007) reported a label "signal-on" electrochemical aptasensor for the detection of platelet-derived growth factor B-chain (PDGF-BB) in clinical samples. The aptasensor was constructed by immobilizing a MB-label aptamer onto a gold electrode surface through a thiol group. In the absence of PDGF-BB, the MB-label is far away from the electrode surface. Upon PDGF-BB binding, the aptamer forms a stable structure holding the MB-label close to the electrode surface, improving the electron transfer. The ACV was employed to monitor the changes at the electrode surface and a detection limit of 1 nM was obtained in blood serum and of 50 pM in serum 2-fold diluted with buffer. This aptasensor showed excellent stability in real samples and could be regenerated by disrupting aptamer-PDGF-BB complex with a 10 % (w/v) sodium dodecyl sulphate solution followed by a deep rinsing with deionized water during 4 min. In 2011, Zhao et al. reported a label "signal-on" aptasensor for the detection VEGF in human whole blood, a cancer-related protein. The aptasensor was fabricated through self-assembly monolayer at the electrode surface, using a polycrystalline gold disk electrode as working electrode (geometric area of 0.0314 cm^2) and thiol- and MB-modified DNA aptamer. Upon VEGF binding the partially unfolded aptamer formed a conformational restrict stem-loop structure. This conformational change forces the MB label to be in the close proximity of the electrode, thus resulting in a significant increase of the electron transfer and current signal. A detection limit of 5 pM (190 pg/mL) was achieved in 50 % of blood serum. In the same work, a gold-plated screen-printed carbon electrode was tested showing a similar performance.

Table 2.1. Label electrochemical aptasensors using voltammetric techniques for the detection of protein disease biomarkers.

Aptamers	Electrochemical Cells	Aptamer immobilization	Redox compounds	Electrochemical technique	Assay Type	Detection limit (LOD)	Working/linear range	Application	Reference
Thrombin (DNA)	WE: Au RE: Ag/AgCl AE: Pt wire	5'-end thiolated; Chemisorption	3'-end MB label aptamer	ACV	Signal-off; Target binding-induced aptamer conformational change	6.4 nM	50 - 768 nM	Thrombin detection in blood serum	(Xiao et al., 2005a)
Thrombin (DNA)	WE: Au RE: Ag/AgCl AE: Pt	3'-end thiolated; Chemisorption	5'-end Fc label aptamer	DPV	Signal-on; Target binding-induced aptamer conformational change	0.5 nM	5 - 35 nM	Thrombin detection	(Radi et al., 2006)
Thrombin (DNA)	WE: Au RE: Ag/AgCl AE: Pt wire	3'-end thiolated; Chemisorption	5'-end Fc label aptamer	SWV	Signal-on; Target binding-induced aptamer conformational change	1 nM	1 - 35nM	Thrombin detection	(Sánchez et al., 2006)
PDGF-BB	WE: Au RE: Ag/AgCl AE: Pt wire	5'-end thiolated; Chemisorption	3'-end MB label aptamer	ACV	Signal-on; Target binding-induced aptamer conformational change	1 nM (blood serum); 50 pM (diluted serum)	ND	PDGF detection in blood serum	(Lai et al., 2007)
C-reactive protein (CRP) (RNA)	WE: carbon RE: Ag AE: carbon	5'-end biotinylated; Streptavidin-biotin interaction	AP conjugated biotinylated antibody	DPV	Signal-on Sandwich (APT/CRP/antibody)	2 nM (free serum)	1 nM – 0.5 μM	CRP detection in free serum and serum samples	(Centi et al., 2009)
IFN-γ (DNA)	WE: Au; RE: Ag/AgCl AR: Pt wire	5'-thiolated; Chemisorption	3'-end MB label aptamer	SWV	Signal-off; Target binding-induced aptamer conformational change	0.06 nM	Up to 10 nM	IFN-γ detection	(Liu et al., 2010)

Table 2.1. Label electrochemical aptasensors using voltammetric techniques for the detection of protein disease biomarkers (Continued).

Aptamers	Electrochemical cells	Aptamers immobilization	Redox compounds	Electrochemical technique	Assay Type	Detection limit (LOD)	Working/linear range	Application	Reference
MUC 1 (DNA)	WE: Au RE: Ag/AgCl AE: Pt	5'-thiolated; Chemisorption	3'-end MB label aptamer	SWV	Signal-off; Target binding-induced aptamer conformational change	50 nM	Up to 1.5 μM	MUC1detection	(Ma et al., 2013)
VEGF	WE: Au disk RE: Ag/AgCl AE: Pt	5'-thiolated; Chemisorption	3'-end MB label aptamer	ACV	Signal-on Target binding-induced aptamer conformational change	5 pM (190pg/mL)	50 pM to 0.15 nM	VEGF detection in human whole blood	(Zhao et al., 2011)
PDGF-BB (DNA)	WE: Au RE: SCE AE: Pt	5'-end thiolated; Chemisorption	3'-end Fc label attached secondary aptamer	DPV	Signal-on; Sandwich (APT1/THR/APT2)	1 pg/mL	1.0 pg/mL -1.0 ng/ mL	PDGF-BB detection	(Zhang et al., 2007)
Thrombin (DNA)	WE: carbon RE: Ag AE: carbon	Two 5'-end biotinylated; Streptavidin-biotin interaction.	AP conjugated secondary aptamer	DPV	Signal-on; Sandwich (APT1/THR/APT2)	0.5 nM	ND	Thrombin detection in serum	(Centi et al., 2007)
TNF-α (RNA)	WE: Au RE: Ag/AgCl AE: Pt wire	5'-thiolated; Chemisorption	5'-end MB label aptamer	SWV	Signal-off; Target binding-induced aptamer conformational change	50 pM	Up to 6 nM	TNF-α detection in blood	(Liu et al., 2013)

Note: ACV (alternating-current voltammetry); AE (auxiliary electrode); Ag (silver); Ag/AgCl (silver/silver chloride); AP (alkaline phosphatase); APT 1 (aptamer 1); APT 2 (aptamer 2); Au (gold); CRP (C-reactive protein); DPV (differential pulse voltammetry); Fc (ferrocene); IFN-γ (Interferon gamma); MB (methylene blue); MUC1 (Mucin 1); ND (not defined); PDGF (platelet-derived growth factor); Pt (platinum); RE (reference electrode); SCE (saturated calomel electrode); SWV (square wave voltammetry); THR (thrombin); TNF-α (tumor necrose factor alpha); VEGF (vascular endothelial growth factor); WE (working electrode).

Apart from the target binding-induced aptamer conformational change, other designs have been explored to develop electrochemical aptasensors. The sandwich format presents an increased sensitivity and selectivity concerning the detection of the target molecule. However, two conditions are required for this sensor arrangement, namely (a) the target must have two independent binding sites (epitopes) to which two different ligands (aptamers) may bind the target molecule without affecting the binding of other targets; and (b) two or more aptamers are selected against the target (Han et al., 2010; Palchetti and Mascini, 2012). In this type of arrangement, generally, one aptamer is used for immobilization onto the electrode surface, while the other is used as a label for signal amplification. Very few target molecules (PDGF and thrombin) have two binding sites and two or more isolated aptamers, which limits the use of this type of sensor format. However, this limitation can be circumvented through the use of the two following formats for the design of an aptasensor, namely the aptamer-protein-aptamer (using the same aptamer) and aptamer-protein-antibody (Han et al., 2010; Palchetti and Mascini, 2012). Commonly, the secondary ligands can be labelled with different redox labels such as MB, Fc, nanomaterials (e.g. NPs) or enzymes (e.g. HRP or AP). Another disadvantage of this format is the time consuming steps of incubation (Palchetti and Mascini, 2012). Some works have reported the use of the sandwich-format aptasensor for the detection of different proteins, namely thrombin (Centi et al., 2007; Ding et al., 2010; Kang et al., 2008; Zhao et al., 2011), C-reactive protein (CRP) (Centi et al., 2009) and PDGF (Wang et al., 2009; Zhang et al., 2007, 2009).

Centi et al., (2007) developed a label "signal-on" electrochemical aptasensor for the detection of thrombin in complex matrices using the sandwich assay with magnetic particles as solid supports. Two biotinylated aptamers against thrombin were used for the aptasensor design. A biotinylated aptamer was captured onto streptavidin-coated magnetic beads and the resulting aptamer-modified magnetic beads were incubated with thrombin. Upon binding with thrombin, a biotinylated secondary aptamer was added, ready to bind in a further step to a streptavidin–AP conjugate. The changes in the electrode surface were detected by DPV and a low detection limit (0.50 nM) was achieved in complex matrices (serum and plasma). These authors used the same strategy for detecting the CRP protein. However, in this example a biotinylated aptamer with affinity for CRP immobilized onto streptavidin magnetic beads (capture probe) and a biotinylated monoclonal antibody anti-CRP conjugated with alkaline phosphatase (AP) (detection probe) were used. The electrochemical detection through DPV allowed a detection limit of 2 nM in serum samples (Centi et al., 2009). A

similar sandwich strategy was design by Zhang et al., (2007 and 2009) to detect proteins PDGF-BB and PDGF, respectively. In these works, the detection of the protein targets was based on the proximity-dependent surface hybridization assay. Two aptamers that recognize different sites of the protein target were used. The 5'-end of both aptamers was coupled to a short complementary sequence. The recognition of the protein by the pair of aptamers enabled the hybridization between the complementary sequences of both aptamer probes, which promotes the proximity of the two tail sequence of both aptamers and the cooperative annealing of the aptamer-protein-aptamer complex on capture probes immobilized on the electrode. As a result, an increase of the redox signal by proximity of ferrocene label attached to the secondary aptamer with the gold electrode was promoted. Detection limits of 1 pg/mL for PDGF-BB and 0.1 ng/mL for PDGF were obtained by DPV, respectively.

2.6.2. Label-free electrochemical aptasensors

In the label-free approaches, the bioreceptor is not labelled with redox compounds (Prieto-Simón et al., 2010; Sassolas et al., 2009; Strehlitz et al., 2008). The aptamers are immobilized on the electrode surface and the target-aptamer interaction is detected by electrochemical techniques (such as voltammetry and electrochemical impedance spectroscopy (EIS)) through electroactive molecules such as ferricyanide and ruthenium complexes ($[Fe(CN)_6]^{3-/4-}$and $[Ru(NH_3)_6]^{3+}$, respectively) that can be electrostatically associated or can diffusively interact (attraction/repulsion) with the aptamers (Prieto-Simón et al., 2010). However, in some cases labelled aptamer-complementary sequences or MB-intercalate can be used in these approaches (Prieto-Simón et al., 2010; Sassolas et al., 2009; Strehlitz et al., 2008) and the changes into the electrode surface can result in target binding-induced aptamer-complementary sequence dissociation/displacement or target binding-induced aptamer conformational change, respectively. **Table 2.2** summarizes some reports on electrochemical aptasensors using voltammetric techniques that have been developed for specific protein detection using label-free detection.

Degefa and Kwak (2008) reported a label-free approach for detecting the PDGF cancer-related protein using $[Fe(CN)_6]^{3-/4-}$ as a redox probe. The DNA aptamer against PDGF was self-assembled in a monolayer onto the gold surface which, in the absence of the PDGF, showed a dynamic state and efficient electron transfer between the redox probe and the electrode surface. After PDGF binding-induced aptamer conformation change, the electron transfer was significantly affected and a linear

decrease of the peak current with the protein concentration (1 - 40 nM) was observed. A similar strategy was used for the OPN protein, a potential biomarker for breast cancer (Meirinho et al., 2015). An RNA aptamer was immobilized on a streptavidin-modified gold surface through the streptavidin-biotin interaction. After binding the OPN, the current decrease was measured by CV in the presence of $[Fe(CN)6]^{3-/4-}$ that is the redox probe. The "signal-off" electrochemical aptasensor showed sensitivity and selectivity towards OPN (detection limit of 3.7 nM) and was able to detect OPN in the presence of other interfering proteins, with the exception of thrombin.

Another strategy for the design of electrochemical aptasensors is based on the target-induced aptamer dissociation/displacement. This strategy is grounded mainly in the strong affinity of the label-free aptamer to its specific target with a labelled aptamer-complementary sequence (Han et al., 2010). Upon binding of the target-aptamer, the dissociation/displacement of the complementary sequences of the aptamer occurs, which leads to the change of detectable signals. This strategy was used to detect thrombin (Lu et al., 2008; Xiao et al., 2005b). Xiao et al., (2005b) developed a "signal-on" aptasensor using an aptamer immobilized onto a gold electrode and then hybridized with a partially complementary DNA sequence labelled with MB. Upon thrombin binding, the aptamer adopted a G-quadruplex conformation and labelled aptamer-cDNA sequence pushed MB closer to the gold electrode surface, thus giving rise to a detectable current that could be measured by ACV. This aptasensor allowed the detection of thrombin in a linear concentration range up to 80 nM with a detection limit of 3 nM. Lu et al., (2008) developed a "signal-off" aptasensor for the same protein, using a Fc-labelled short aptamer-complementary DNA sequence to form dsDNA duplex with the aptamer immobilized on a gold electrode. The target binding led to the dissociation of the label-sequence that was followed by a decrease in the DPV current signal due to the distance between the Fc-label and the gold electrode. The aptasensor was found to be reusable and highly specific with a detection limit of 2 nM.

Table 2.2. Label-free electrochemical aptasensors using voltammetric techniques for the detection of protein disease biomarkers.

Aptamer	Electrochemical cells	Aptamers immobilization	Redox compounds	Electrochemical technique	Assay Type	Detection limit (LOD)	Working/linear range	Application	Reference
Thrombin (DNA)	WE: Au	5'-end thiolated; Chemisorption	MB-attached partially cDNA sequence	ACV	Signal-on; Target binding-induced aptamer-cDNA sequence displacement	3 nM	Up to 80 nM	Thrombin detection	(Xiao et al., 2005b)
Thrombin (DNA)	WE: Au RE: Ag/AgCl AE: Pt wire	3'-end biotinylated; Streptavidin-biotin interaction	MB-intercalated label	DPV	Signal-on; Target binding-induced aptamer conformational change	10 nM	ND	Thrombin detection	(Hianik et al., 2005)
Thrombin (DNA)	WE: Au RE: Ag/AgCl AE: Pt wire	5'-end amine; Covalent attachment	MB-intercalated label	DPV	Signal-off; Target binding-induced aptamer conformational change	11 nM	Up to 50.8 nM	Thrombin detection	(Bang et al., 2005)
Thrombin (DNA)	WE: Au RE: Ag/AgCl AE: Pt wire	5'- end thiolated; Chemisorption	Fc-short labelled cDNA sequence	DPV	Signal-off; Target binding-induced aptamer-cDNA sequence dissociation	2 nM	Up to 10 nM	Thrombin detection	(Lu et al., 2008)
Lysozyme (DNA)	WE: Au RE: Ag/AgCl AE: Pt wire	5'-end Thiolated Chemisorption	$[Ru(NH_3)_6]^{3+}$	CV	Signal-off; Target binding-induced aptamer conformational change	0.5 µg/mL	ND	Lysozyme detection	(Cheng et al., 2007)
PDGF	WE: Au RE: MSE AE: Pt wire	5'-thiolated; Chemisorption	$(Fe(CN)_6)^{3-/4-}$	DPV	Signal-off; Target binding-induced aptamer conformational change	ND	1-40 nM	PDGF detection	(Degefa and Kwak, 2008)
$VEGF_{165}$ and MUC1 (DNA/DNA)	WE: Au RE: SCE AE: Pt wire	5'-Thiolated cDNA sequence Chemisorption	Fc-labelled cDNA sequence	SWV	Signal-on Hybridization reaction between cDNA sequence and two aptamers	MUC1: 0.33 nM $VEGF_{165}$: ND	1 to 20 nM	$VEGF_{165}$ and MUC1 detection	(Zhao et al., 2012)
Osteopontin (RNA)	WE: Au; RE: Ag AE: Au	5'-end-biotinylated; Streptavidin-biotin interaction	$[Fe(CN)_6]^{3-/4-}$	CV	Signal-off; Target binding-induced aptamer conformational change	3.7 nM	25-2402 nM	Osteopontin detection	(Meirinho et al., 2015)

Note: ACV (alternating-current voltammetry); AE (auxiliary electrode); Ag (silver); Ag/AgCl (silver/silver chloride); Au (gold); CV (cyclic voltammetry); DPV (differential pulse voltammetry); Fc (ferrocene); MB (methylene blue); MSE (Hg|HgSO4|K2SO4 (sat) electrode); MUC1 (Mucin 1); ND (not defined); PDGF (platelet-derived growth factor); Pt (platinum); RE (reference electrode); SCE (saturated calomel electrode); SWV (square wave voltammetry); VEGF (vascular endothelial growth factor); WE (working electrode.

Recently, Zhao et al., (2012) reported a label-free electrochemical aptasensor for simultaneous determination of two tumor markers, MUC1 and $VEGF_{165}$ that are associated with a poor prognosis and poor survival of the breast cancer patients. In this aptasensor the Fc-labelled aptamer-complementary DNA sequence was immobilized onto gold disk electrode that hybridize with both MUC1 and VEGF165 aptamers to form a long double strand blocking the electrochemical signal. In the presence of the two tumor markers, the hybridization reaction between the cDNA with the aptamers was inhibited and, Fc-cDNA was close of electrode surface and increase in the current was detected by SWV. This simple "signal-on" electrochemical aptasensor allowed detect the two markers and discriminate their co-existence.

2.7. Application of nanomaterials in electrochemical aptasensors

In order to achieve highly sensitive electrochemical aptasensors, several nanomaterials have been explored for the immobilization of aptamers onto electrodes surfaces and for signal transduction. Metal nanoparticles (e.g. AuPNs, AgNPs, or PtNPs), QDs, magnetic nanoparticles (MNPs), carbon nanotubes (CNTs), graphene (GNs) and their nanocomposite have been used for the development of electrochemical biosensors (Citartan et al., 2012; Erdem et al., 2009; Palchetti and Mascini, 2012). These nanomaterials have unique physical and chemical properties and can be used in several electrode surfaces such as GCE (Ding et al., 2010; Y. Li et al., 2011) and SPE (Suprun et al., 2008) in a variety of applications. For electrochemical applications, these nanomaterials allowed an easy functionalization of the electrodes surfaces, namely an increase of the surface area for the aptamers attachment onto the electrodes surfaces, therefore facilitating the access of the target molecule to these aptamers, and acting as electrochemical labels by increasing the signal amplification or electron-transfer mediators (Citartan et al., 2012; Hernandez and Ozalp, 2012; Palchetti and Mascini, 2012; Vidotti et al., 2011; Vikesland and Wigginton, 2010). Taking into account these advantages, the application of nanomaterials in the development of aptasensors will lead to an increase in the sensitivity, i.e. in the detection of low levels of protein biomarkers. However, this strategy can also enclose some disadvantages, such as complicated procedures, increased expenses, decreased reproducibility and quantification, especially when the use of complex samples is envisaged (Palchetti and Mascini, 2012). **Table 2.3** summarizes some studies that used nanomaterials to develop electrochemical aptasensors using voltammetric techniques for specific

protein detection and disease diagnosis. Wang et al., (2011) reported an electrochemical aptasensor for the detection of thrombin using nanoparticles to increase the surface area (capture probe) and signal amplification (detection probe). The authors described a sandwich assay using GCE modified with chitosan-hollow CoPt alloy nanoparticle (Cs-HcoPt) film activated with glutaraldehyde (GA) for the immobilization of aptamer-1. For the signal amplification, the aptamer-2 was conjugated with high-quality hollow CoPt bimetal alloy nanoparticles (HcoPt) onto reduced graphene oxide sheet (HcoPt-RGs) with a redox probe thionine (Thi) and enzyme HRD. This aptasensor using CV and DPV techniques presented a low detection limit (0.34 pM) and a good specificity for thrombin. Another example for thrombin detection was reported by Zhao et al., (2011). The aptamer-1 was immobilized into core/shell Fe_3O_4/gold magnetic nanoparticles (AuMNPs), and the aptamer-2 was coupled with AuNPs and HRP for signal amplification. This electrochemical aptasensor using DPV and containing two different aptamers for the sandwich detection, allowed a detection limit of 30 fM for thrombin (Zhao et al., 2011). The recent use of nanomaterials has also enabled the development of some aptasensors for electrochemical detection of proteins associated with breast cancer. Cao et al., (2014) reported an electrochemical aptasensor for the detection of OPN using SVW. In this work, the RNA aptamer (R3-OPN) (Mi et al., 2009) was immobilized onto a functionalized electrode with cucurbit[7]uril support and AuNPs. This aptasensor presented a high specificity, good reproducibility and a detection limit of 10.7 ng/L. These results are of utmost relevance to support the development of new biosensors able to detect and quantify OPN in biological samples. Hu et al., (2014) developed an ultrasensitive electrochemical aptasensor for the detection of MUC1, an useful marker for breast cancer. AuNPs were used to manufacture this aptasensor, as well as the enzyme HRP and a GCE electrode modified with multi-walled carbon nanotubes and streptavidin. The aptamer was modified with thiol at the 5´-end and biotin at the 3'-end. The aptamer and HRP were immobilized on the AuNPs (APT-AuNPs-HRP), being the AuNPs used as label and bridges between the aptamer and the second label (HRP). After the aptamer-MUC1 interaction, the aptamer was disrupted and the biotin exposed was captured by the streptavidin-modified electrode. This "signal-on" aptasensor exhibited good linear correlation dynamic ranges from 8.8 nM to 353.3 nM and a low detection limit (2.2 nM) for MUC1. Ravalli et al., (2015) reported an electrochemical single-use aptasensor for the detection and analysis of VEGF a potential biomarker associated with diagnosis and prognosis of different types of cancer, included breast cancer. The proposed aptasensor based a sandwich assay using two different aptamers, AuNPs and an enzyme-amplified detection. The graphite screen-printed electrodes (GSPEs) were modified by electrodeposition of AuNPs for thiolated aptamer-1

immobilization. After aptamer-1-VEGF recognition, the biotinylated aptamer 2 was added and resulting complex was coupled with streptavidin-alkaline phosphatase for amplified detection. The electroactive product of the enzymatic reaction was detected by means of differential pulse voltammetry (DPV). The "signal-on" aptasensor response was found to be linearly related to the target concentration between 0 and 250 nM; the detection limit was 30 nM. Based in a dual signal amplification strategy, Bai et al., (2012) reported a sandwich assay for simultaneous detection of PDGF and thrombin. The aptasensor was fabricated using AuNPs functionalized single-walled carbon nanotubes (AuNPs@SWCNTs) as biosensor platform to capture a large amount of primary aptamers and amplify the detection response. The redox probes toluidine blue (Tb) and Fc were attached into the reduced graphene oxide sheets (rGS) coated with PtNPs (PtNPs-redox probes-rGS nanocomposites). The synthesized PtNPs-Tb/Fc-rGS nanocomposites were then used as carriers for glucose oxidase (GOD) and horseradish peroxidase (HRP) and the aptamer-2 (PDGF- and thrombin-binding), respectively. The linear range of PDGF was found to be 0.01 to 35 nM with a detection limit of 8 pM, while the linear range was 0.02 to 45 nM with a detection limit of 11 pM for thrombin are obtained by DPV. Recently using a similar strategy, Chen et al., (2015) reported a signal-on electrochemical aptasensors for detection MUC1. The poly(o-phenylenediamine)-AuNPs (PoPD-AuNPs) film was used as capture probe for the immobilization of aptamer-1. On the other hand, the AuNPs functionalized silica/multi-walled carbon nanotubes core-shell nanocomposites (AuNPs/SiO2@MWCNTs) were used to enhance the surface area for immobilizing the secondary aptamer, as well as to load large amounts of electrochemical probe thionine (Thi). The presence of MUC1 induced the formation of one complex between the PoPD-AuNPs-APT1 and the Thi-AuNPs/SiO2@MWCNTs-APT2. The current changes that resulted from the formation of such complex were registered by DPV and a detection limit of 1 pM was obtained.

The use of nanomaterials in the development of these aptasensors allowed an improvement of the sensibility in the detection of specific proteins (e.g. OPN, MUC1, PDGF and VEGF) and can hold a great promise for point-of-care diagnosis of genetic diseases and for the detection of cancer.

Table 2.3. Electrochemical aptasensors using voltammetric techniques for the detection of protein disease biomarkers with application the nanomaterials.

Aptamers	Nanomaterials	ElectrochemicalTechnique	Detection limit (LOD)	Working range	Application	Reference
Thrombin (DNA)	NPs	DPV	0.55 fM	1.0 – 10 fM	Thrombin detection in real samples	(Ding et al., 2010)
PDGF (DNA)	AuNPs	CV	$1x10^{-14}$ M (diluted) $1x10^{-12}$ M (undiluted)	n.d.	PDGF detection in purified samples and undiluted blood serum	(Wang et al., 2009)
Lysozyme (DNA)	AuNPs	SWV	0.1 pM	$1x10^{-13}$ to $1x10^{-9}$ M	Lysozyme detection	(L.-D. Li et al., 2010)
Thrombin (DNA)	AuMNPs and AuNPs	DPV	30 fM	0.1 – 60 pM	Thrombin detection	(Zhao et al., 2011)
Thrombin/Lysozyme (DNA/DNA)	MP	DPV	54.5 nM (thrombin) 769 nM (lysozyme)	0.3 - 3 μM (thrombin) 7 - 70 μM (lysozyme)	Thrombin and lysozyme detection	(Erdem et al., 2009)
Thrombin/Lysozyme (DNA/DNA)	CNTs	DPV	4 pM (thrombin) 12 pM (lysozyme)	8 pM-4.5 nM (thrombin) 14 pM-0.1 μM (lysozyme)	Thrombin and lysozyme detection	(Du et al., 2010)
Thrombin (DNA)	CdSe - QDs	DPV	0.08 μg/mL at 3σ	3 to 13 μg/mL and 14 to 31 μg/mL	Thrombin detection	(Li et al., 2011)
Thrombin (DNA)	GNs-CS	DPV	0.45x10-3 pM	1x10-6 to 1x10-4 nM	Thrombin detection	(Wang et al., 2012)
Thrombin (DNA)	GNs and AuNPs	DPV	0.2 pM	1x10-3 to 40 nM	Thrombin detection	(Yuan et al., 2011)
Thrombin (DNA)	GNs and NPs	DPV	3.4×10−13 M	1.0×10−12 to 5.0×10−8 M	Thrombin detection	(Wang et al., 2011)
PDGF	GNs and AuNPs	CV	1.7 pM	5x10-3 to 60 nM	PDGF detection	(Deng et al., 2013)
Osteopontin (RNA)	CB[7] and AuNPs	SWV	10.7 ng/mL	50 to 500 ng/mL	Osteopontin detection	(Cao et al., 2014)

Note: GNs (Graphene); CB[7] (Cucurbit[7]uril substract); QDs (quantum dots); PTCA (3,4,9,10-perylene tetracarboxylic acid); GOD (glucose oxidase); CNTs (Carbon nanotubes); MP (magnetic particles); AuMNPs (Gold magnetic nanoparticles); AuNPs (gold nanoparticles); NPs (nanoparticles); PDDA (poly(diallyldimethylammonium chloride); SWV (square wave voltammetry); CV (cyclic voltammetry); DPV (differential pulse voltammetry); MUC1 (Mucin 1); MWCNTs (multi-walled carbon nanotubes); VEGF (vascular endothelial growth factor), PoPD (poly(o-phenylenediamine) functional polymer); SWCNTs (single-walled carbon nanotubes); PtNPs (platinum nanoparticles)

2.7. Conclusions

In the recent years, there has been an increasing interest in the use of aptasensors for the detection of protein disease biomarkers employing different immobilization techniques, design strategies and modes of detection. However, most of these aptasensors have been developed for *in vitro* detection of biomarkers, therefore the design of *in vivo* detection solutions should be a priority in the future. The majority of cancer diseases are associated with the presence of more than one protein biomarker. Hence, further developments on the aptasensors field must involve the design of multiple detection sensors for different or even the same biomarkers, as these substances can be found in very low amounts in biological fluids. Multiple detection sensors would increase sensitivity and consequently provide more accurate information on biomarkers levels, thus improving the prognosis and treatment of diseases. The aptasensors arrays can be a good alternative offering the possibility of simultaneous measurements of a variety of targets, and thus shorten the time required for the analysis and decrease the detection costs. Another alternative is the use of microchips and nanochips to allow miniaturization and integration of nanomaterials that enhance the surface area, as well as for signal amplification in the development of electrochemical aptasensors. However, the simultaneous detection of multiple targets (e.g. protein biomarkers) using voltammetric aptasensors arrays has seldom been reported. The future of aptamer-based biosensors looks increasingly bright, yet many hurdles, such as lack of specific aptamers against protein biomarkers, lack of experience in multi-analyte detection and the complexity of clinical samples, remain to be solved especially in the field of biomedicine and point-of-care diagnostics.

2.8. References

Agrawal, D., Chen, T., Irby, R., Quackenbush, J., Chambers, A.F., Szabo, M., Cantor, A., Coppola, D., Yeatman, T.J., 2002. J. Nat. Cancer Inst. 94, 513–521.

Ahmed, M., Kundu, G.C., 2010. Mol. Cancer 9, 101–114.

Anborgh, P.H., Mutrie, J.C., Tuck, A.B., Chambers, A.F., 2011. J. Cell Commun. Signal. 5, 111–122.

Anborgh, P.H., Wilson, S.M., Tuck, A.B., Winquist, E., Schmidt, N., Hart, R., Kon, S., Maeda, M., Uede, T., Stitt, L.W., Chambers, A.F., 2009. Clin. Chem. 55, 895–903.

Arshak, K., Velusamy, V., Korostynska, O., Oliwa-Stasiak, K., Adley, C., 2009. Conducting Polymers and Their IEEE Sens. J. 9, 1942–1951.

Bache, M., Kappler, M., Wichmann, H., Rot, S., Hahnel, A., Greither, T., Said, H.M., Kotzsch, M., Würl, P., Taubert, H., Vordermark, D., 2010. BMC Cancer 10, 132-148.

Bai, L., Yuan, R., Chai, Y., Zhuo, Y., Yuan, Y., Wang, Y., 2012. Biomaterials 33, 1090–1096.

Balamurugan, S., Obubuafo, A., Soper, S. a, Spivak, D.A., 2008. Anal. Bioanal. Chem. 390, 1009–1021.

Baldrich, E., Radi, A.E., Dondapati, S., Sa, L., Katakis, I., Sullivan, C.K.O., Sanchez, J.L.A., Sanchez, L., 2006 Electroanal. 18, 1957–1962.

Bandopadhyay, M., Bulbule, A., Butti, R., Chakraborty, G., Ghorpade, P., Ghosh, P., Gorain, M., Kale, S., Kumar, D., Kumar, S., Totakura, K.V.S., Roy, G., Sharma, P., Shetti, D., Soundararajan, G., Thorat, D., Tomar, D., Nalukurthi, R., Raja, R., Mishra, R., Yadav, A.S., Kundu, G.C., 2014. Expert Opin. Ther. Targets 18, 883–95.

Bang, G.S., Cho, S., Kim, B., 2005. Biosens. Bioelectron. 21, 863–870.

Beausoleil, M.S., Schulze, E.B., Goodale, D., Postenka, C.O., Allan, A.L., 2011. BMC Cancer 11, 25-37.

Blasberg, J.D., Pass, H.I., Goparaju, C.M., Flores, R.M., Lee, S., Donington, J.S., 2010. J. Clin. Oncol. 28, 936–941.

Bohunicky, B., Mousa, S.A., 2011. Nanotechnol. Sci. Appl. 4, 1–10.

Bramwell, V.H.C., Doig, G.S., Tuck, A.B., Wilson, S.M., Tonkin, K.S., Perera, F., Vandenberg, T.A., Chambers, A.F., 2006. Clin. Cancer Res. 12, 3337–3343.

Bramwell, V.H.C., Tuck, A.B., Chapman, J.-A.W., Anborgh, P.H., Postenka, C.O., Al-Katib, W., Shepherd, L.E., Han, L., Wilson, C.F., Pritchard, K.I., Pollak, M.N., Chambers, A.F., 2014. Breast Cancer Res. 16, R8.

Bugaut, A., Toulmé, J.-J., Rayner, B., Toulm?, J.-J., 2006. Org. Biomol. Chem. 4, 4082–4088.

Cao, D.-X., Li, Z.-J., Jiang, X.-O., Lum, Y.L., Khin, E., Lee, N.P., Wu, G.-H., Luk, J.M., 2012. World J. Gastroenterol. 18, 3923–30.

Cao, Y., Chen, D., Chen, W., Yu, J., Chen, Z., Li, G., 2014. Anal. Chim. Acta 812, 45–54.

Centi, S., Sanmartin, B., Tombelli, S., Palchetti, I., 2009. Electroanal. 21, 1309–1315.

Centi, S., Tombelli, S., Minunni, M., Mascini, M., 2007. Anal. Chem. 79, 1466–1473.

Chen, R.-X., Xia, Y.-H., Xue, T.-C., Zhang, H., Ye, S.-L., 2011. Oncol. Rep. 25, 803–808.

Chen, X., Zhang, Q., Qian, C., Hao, N., Xu, L., Yao, C., 2015. Biosens. Bioelectron. 64, 485–492.

Cheng, A.K.H., Ge, B., Yu, H.-Z., 2007. Anal. Chem. 79, 5158–5164.

Cheng, A.K.H., Sen, D., Yu, H., 2009. Bioelectrochem. 77, 1–12.

Cho, E.J., Lee, J., Ellington, A.D., 2009. Annu. Rev. Anal. Chem. 2, 241–264.

Cho, H., Hong, S.W., Oh, Y.J., Kim, M. a, Kang, E.S., Lee, J.M., Kim, S.W., Kim, S.H., Kim, J.H., Kim, Y.T., Lee, K., 2008. J. Cancer Res. Clin. Oncol. 134, 909–917.

Choi, Y.-E., Kwak, J.-W., Park, J.W., 2010. Sensors 10, 428–455.

Chung, D.-J., Kim, K.-C., Choi, S.-H., 2011. Appl. Surf. Sci. 257, 9390–9396.

Citartan, M., Gopinath, S.C.B., Tominaga, J., Tan, S.-C., Tang, T.-H., 2012. Biosens. Bioelectron. 34, 1–11.

Csordas, A., Gerdon, A.E., Adams, J.D., Qian, J., Oh, S.S., Xiao, Y., Soh, H.T., 2010. Angew. Chem. 49, 355–358.

Daniels, J., Pourmand, N., 2007. Electroanal. 19, 1239–1257.

Darmostuk, M., Rimpelová, S., Gbelcová, H., Ruml, T., 2015. Biotechnol. Adv. 33, 1141–1161.

Davidson, B., Holth, A., Moripen, L., Trope', C.G., Shih, I.-M., 2011. Human Pathology 42, 991–997.

Degefa, T.H., Kwak, J., 2008. Anal. Chim. Acta 613, 163–168.

de-los-Santos-Álvarez, N., Lobo-Castañón, M.J., Miranda-Ordieres, A.J., Tuñón-Blanco, P., 2008. TrAC Trends Anal. Chem. 27, 437–446.

Deng, K., Xiang, Y., Zhang, L., Chen, Q., Fu, W., 2013. Anal. Chim. Acta 759, 61–65.

Devi, R.V., Doble, M., Verma, R.S., 2015. Biosens. Bioelectron. 68, 688–698.

Ding, C., Ge, Y., Lin, J.-M., 2010. Biosens. Bioelectron. 25, 1290–1294.

Du, Y., Li, B., 2010b. Bioanal. Rev. 1, 187–208.

Dua, P., Kim, S., Lee, D.-K., 2011. Methods 54(2), 215-225.

Erdem, A., Karadeniz, H., Mayer, G., Famulok, M., Caliskan, A., 2009. Electroanal. 21, 1278–1284.

Famulok, M., Mayer, G., 2011. Acc. Chem. Res. 44, 1349–1358.

Feng, K., Sun, C., Kang, Y., Chen, J., Jiang, J.-H., Shen, G.-L., Yu, R.-Q., 2008. Electrochem. commun. 10, 531–535.

Ferlay, J., Soerjomataram, I., Ervik, M., Dikshit, R., Eser, S., Mathers, C., Rebelo, M., Parkin, D.M., Forman, D., Bray, F., 2013. GLOBOCAN 2012 v1.0, IARC Cancer Base. No. 11.

Ferreira, A., Fugivara, C., Yamanaka, H., Benedetti, A., 2011. Biosens. Health, Environ. Biosec. 540.

Forootan, S.S., Foster, C.S., Aachi, V.R., Adamson, J., Smith, P.H., Lin, K., Ke, Y., 2006. J. Int. Cancer 118, 2255–2261.

Gam, L.-H., 2012. World J Exp Med. 2, 86–91.

Gopinath, S.C.B., 2007. Methods developed for SELEX. Anal. Bioanal. Chem. 387, 171–182.

Grieshaber, D., MacKenzie, R., Voeroes, J., Reimhult, E., 2008. Sensors 8, 1400–1458.

Guo, K.-T., Paul, A., Schichor, C., Ziemer, G., Wendel, H.P., 2008. Int. J. M. Sci. 9, 668–678.

Han, K., Chen, L., Lin, Z., Li, G., 2009. Electrochem. Commun. 11, 157–160.

Han, K., Liang, Z., Zhou, N., 2010. Sensors 10, 4541–57.

Hanash, S.M., 2011. Genome Med. 3, 66.

Hayat, A., Marty, J.L., 2014. Front. Chem. 2, 41.

Hernandez, F.J., Ozalp, V.C., 2012. Biosens. 2, 1–14.

Hianik, T., Ostatná, V., Sonlajtnerova, M., Grman, I., 2007. Bioelectrochem. 70, 127–133.

Hianik, T., Ostatná, V., Zajacová, Z., Stoikova, E., Evtugyn, G., Zajacova, Z., Ostatna, V., 2005. Bioorg. Med. Chem. 15, 291–295.

Hianik, T., Wang, J., 2009. Electroanal. 21, 1223 – 1235.

Hong, P., Li, W., Li, J., 2012. Sensors 12, 1181–1193.

Hu, R., Wen, W., Wang, Q., Xiong, H., Zhang, X., Gu, H., Wang, S., 2014. Biosens. Bioelectron. 53, 384–389.

Hunter, C., Bond, J., Kuo, P.C., Selim, M.A., Levinson, H., 2012. J. Surg. Res. 176, 348–358.

Javaherian, S., Musheev, M.U., Kanoatov, M., Berezovski, M.V., Krylov, S.N., 2009. Nucleic Acids Res. 37, 1–10.

Jemal, A., Bray, F., Center, M.M., Ferlay, J., Ward, E., Forman, D., 2011. CA. Cancer J. Clin. 61, 69–90.

Jing, M., Brwser, M.T., Bowser, M.T., 2011. Anal. Chim. Acta 686, 9–18.

Kang, Y., Feng, K.-J., Chen, J., Jiang, J., Shen, G., Yu, R., 2008. Bioelectrochem. 73, 76–81.

Karellas, A., Vedantham, S., 2008. Med. Phys. 35, 4878-4897.

Karley, D., Grupta, D., Tiwari, A., 2011. J. Mol. Biomark. Diagn. 2, 2–5.

Khati, M., 2010. British Med. J. 63, 480–487.

Kim, J.-H., Skates, S.J., Uede, T., Wong, K., Schorge, J.O., Feltmate, C.M., Berkowitz, R.S., Cramer, D.W., Mok, S.C., 2002. JAMAl 287, 1671–1679.

Kim, Y.S., Lee, S.J., Gu, M.B., 2008. BioChip J. 2, 175–182.

Koopmann, J., Fedarko, N.S., Jain, A., Maitra, A., Iacobuzio-Donahue, C., Rahman, A., Hruban, R.H., Yeo, C.J., Goggins, M., 2004. Cancer Epidemiol. Biomarkers Prev. 13, 487–491.

Kulbachinskiy, A. V, 2007. Biochem. 72, 1505–1518.

Kumar, J., D'Souza, S., 2012. Barc Newsletter 34–38.

Kuwahara, M., Sugimoto, N., 2010. Molecules 15, 5423–5444.

Labuda, J., Brett, A.M.O., Evtugyn, G., Fojta, M., Mascini, M., Ozsoz, M., Palchetti, I., Paleček, E., Wang, J., 2010. Pure Appl. Chem. 82, 1161–1187.

Lai, R.Y.R.Y., Plaxco, K.W.K.W., Heeger, A.J.A.J., 2007. Anal. Chem. 79, 229–233.

Lakhin, A. V, Tarantul, V.Z., Gening, L. V, 2013. Acta Naturae 5, 34–43.

Leca-Bouvier, B., Blum, L., 2005. Anal. Lett. 38, 1491–1517.

Lee, H.J., Wark, A.W., Corn, R.M., 2008. Analyst 133, 975- 983.

Li, J., Yang, G.-Z., Zhu, Z.-M., Zhou, Z.-Y., Li, L., 2012. Exp. Ther. Med. 3, 621–624.

Li, L.-D., Chen, Z.-B., Zhao, H.-T., Guo, L., Mu, X., 2010. Sensors Actuat. B. Chem. 149, 110–115.

Li, X., Liu, J., Zhang, S. , 2010. Chem. Commun. 46, 595–597.

Li, Y., Han, M., Bai, H., Wu, Y., Dai, Z., Bao, J., 2011. Electrochim. Acta 56, 7058–7063.

Lim, Y.C., Kouzani, A.Z., Duan, W., 2010. J. Biomed. Nanotechnol. 6, 93–105.

Liu, C.-C., 2000. Electrochemical Sensors, in: Bronzino, J.D. (Ed.), The Biomedical Engineering Handbook. CRC Press LLC.

Liu, Y., Tuleouva, N., Ramanculov, E., Revzin, A., 2010. Anal. Chem. 82, 8131–8136.

Liu, Y., Zhou, Q., Revzin, A., 2013. Analyst, 138, 4321-4326.

Lu, Y., Zhu, N., Yu, P., Mao, L., 2008. Analyst 133, 1256–1260.

Ma, F., Ho, C., Cheng, A.K.H., Yu, H.Z., 2013. Electrochim. Acta 110, 139–145.

Macrì, A., Versaci, A., Lupo, G., Trimarchi, G., Tomasello, C., Loddo, S., Sfuncia, G., Caminiti, R., Teti, D., Famulari, C., 2009. Tumori 95, 48–52.

Mairal, T., Özalp, V.C., Sánchez, P.L., Mir, M., Katakis, I., Sullivan, C.K.O., 2008. Anal. Bioanal. Chem. 390, 989–1007.

Marimuthu, C., Tang, T.-H., Tominaga, J., Tan, S.S.-C., Gopinath, S.C.B., 2012. Analyst 137, 1307–1315.

Martin, K.J., Fournier, M. V, Reddy, G.P.V., Pardee, A.B., 2010. Cancer Res. 70, 5203–5206.

Mascini, M., 2009. A JOHN WILEY & SONS, INC.

Mayer, G., 2009. Angew. Chem. 48, 2672–2689.

Mckeague, M., Derosa, M.C., 2014. Smith & Franklin 1, 1–16.

Meirinho, S.G., Dias, L.G., Peres, A.M., Rodrigues, L.R., 2015. Biosens. Bioelectron. 71, 332–341.

Mendes, T.F.S., Kluskens, L.D., Rodrigues, L.R., 2015. Adv. Sci. n/a–n/a.

Meyer, C., Hahn, U., Rentmeister, A., 2011. J. Nucleic Acids 2011, Article ID 904750, 1-18.

Mi, Z., Guo, H., Russell, M.B., Liu, Y., Sullenger, B. a, Kuo, P.C., 2009. Mol. Ther. 17, 153–161.

Mirza, M., Shaughnessy, E., Hurley, J.K., Vanpatten, K.A., Pestano, G. a, He, B., Weber, G.F., 2008. Int. J. Cancer 122, 889–897.

Misek, D.E., Kim, E.H., 2011. Int. J. Proteomics Volume 2011, Article ID 343582, 1-9.

Monošík, R., Streďanský, M., Šturdík, E., 2012. Acta Chim. Slovaca 5, 109–120.

Nassar, H.R., Namour, A.E., Shafik, H.E., El Sayed, A.S., Kamel, S.M., Moneer, M.M., Zakhary, N.I., 2015. Forum Clin. Oncol. 6, 27–32.

Nguyen, T.H., Hilton, J.P., Lin, Q., 2009. Microfluid. Nanofluidics 6, 347–362.

Nimse, S., Song, K., Sonawane, M., Sayyed, D., Kim, T., 2014. Sensors 14, 22208–22229.

Opstal-van Winden, A.W.J., Krop, E.J.M., Kåredal, M.H., Gast, M.-C.W., Lindh, C.H., Jeppsson, M.C., Jönsson, B. a G., Grobbee, D.E., Peeters, P.H.M., Beijnen, J.H., van Gils, C.H., Vermeulen, R.C.H., 2011. BMC Cancer 11(1), 381-392.

Ortiz-Martínez, F., Perez-Balaguer, A., Ciprián, D., Andrés, L., Ponce, J., Adrover, E., Sánchez-Payá, J., Aranda, F.I., Lerma, E., Peiró, G., 2014. Human Pathology 45, 504–512.

Ostatná, V., Vaisocherová, H., Homola, J., Hianik, T., 2008. Anal. Bioanal. Chem. 391, 1861–1869.

Ozer, A., Pagano, J.M., Lis, J.T., 2014.. Mol. Ther. Nucleic Acids 3, e183.

Palchetti, I., Mascini, M., 2012. Anal. Bioanal. Chem. 402, 3103–3114.

Paniel, N., Baudart, J., Hayat, A., Barthelmebs, L., 2013. Methods 3, 229-240.

Park, S., Ahn, J.Y., Jo, M., Lee, D., Lis, J.T., Craighead, H.G., Kim, S., 2009. Lab Chip 9, 1206–1212.

Patani, N., Jouhra, F., Jiang, W., Mokbel, K., 2008. Anticancer Res. 28, 4105–4110.

Porika, M., Tippani, R., 2011. Int. J. Clin. Onco. 6, 617-622.

Prieto-Simón, B., Campàs, M., Marty, J.-L., 2010. Bioanal. Rev. 1, 141–157.

Radi, A., Lluis, J., Sa, A., Baldrich, E., Sullivan, C.K.O., 2006. J. Am. Chem. Soc. 128, 117–124.

Radi, A.-E., 2011. Int. J. Electrochem. 2011, 1–17.

Radom, F., Jurek, P.M., Mazurek, M.P., Otlewski, J., Jeleń, F., 2013. Biotech. Adv. 31, 1260–1274.

Rahman, M.A., Kumar, P., Park, D.S., Shim, Y.B., 2008. Sensors 8, 118–141.

Ravalli, a., Rivas, L., De La Escosura-Muñiz, A., Pons, J., Merkoçi, a., Marrazza, G., 2015. JNN 15, 3411–3416.

Rodrigues, L.R., Lopes, N., Sousa, B., Vieira, D., Milanezi, F., 2009. TOBCANJ 1, 1–9.

Rodrigues, L.R., Teixeira, J.A., Schmitt, F.L., Paulsson, M., Lindmark-Mansson, H., 2007. Cancer Epidemiol. Biomark. Prev. 16, 1087–1097.

Rodríguez, M.C., Rivas, G.A., 2009. Talanta 78, 212–216.

Ronkainen, N.J., Halsall, H.B., Heineman, W.R., 2010. Chem. Soc. Rev. 39, 1747–1763.

Saberian, M., Hamzeiy, H., Aghanejad, A., Asgari, D., 2011. Bioimpacts 1, 31–37.

Sadik, O.A., Aluoch, A.O., Zhou, A., 2009. Biosens. Bioelectron. 24, 2749–2765.

Sánchez, J.L., Baldrich, E., Radi, A.E., Dondapati, S., Sa, L., Katakis, I., Sullivan, C.K.O., Sanchez, J.L.A., Sanchez, L., 2006. Electroanal. 18, 1957–1962.

Santosh, B., Yadava, P.K., 2014. Biomed Res. Int. 2014, Article ID 540451, 1-13.

Sassolas, A., Blum, L.J.J.J., Leca-Bouvier, B.D.D.D., Lyon, D., 2009. Electroanal. 21, 1237–1250.

Sassolas, A., Leca-Bouvier, B.D., Blum, L.J., 2008. Chem. Rev. 108, 109–139.

Sett, A., Das, S., Sharma, P., Bora, U., 2012. Open J. Appl.Biosens. 01, 9–19.

Shamah, S.M., Healy, J.M., Cload, S.T., 2008. Acc. Chem. Res. 41, 130–138.

Shevde, L. a, Samant, R.S., 2014. Matrix Biol. 37, 131–141.

Sivakumar, S., Niranjali Devaraj, S., 2014. J. Diabetes Metab. Disord. 13, 13-27.

Song, G., Cai, Q.-F., Mao, Y.-B., Ming, Y.-L., Bao, S.-D., Ouyang, G.-L., 2008. Cancer Sci. 99, 1901–1907.

Song, S., Wang, L., Li, J., Zhao, J., Fan, C., 2008. Anal. Chem. 27, 108–117.

Song, K.-M., Lee, S., Ban, C., 2012. Sensors. 12, 612–631.

Stoltenburg, R., Reinemann, C., Strehlitz, B., 2007. Biomol. Eng. 24, 381–403.

Strehlitz, B., Nikolaus, N., Stoltenburg, R., 2008. Sensors 8, 4296–4307.

Suprun, E., Shumyantseva, V., Bulko, T., Rachmetova, S., Rad'ko, S., Bodoev, N., Archakov, A., 2008. Biosens. Bioelectron. 24, 831–836.

Syed, M.A., Pervaiz, S., 2010. Oligonucleotides 20, 215–224.

Tang, Z., Shangguan, D., Wang, K., Shi, H., Sefah, K., Mallikratchy, P., Chen, H.W., Li, Y., Tan, W., 2007. Anal. Chem. 79, 4900–4907.

Thevenot, D.R., Toth, K., Durst, R.A., Wilson, G.S., Thévenot, D.R., 1999. Pure Appl. Chem. 71, 2333–2348.

Thévenot, D.R.D.R., Toth, K., Durst, R.A.R.A., Wilson, G.S.G., 2001. Biosens. Bioelectron. 16, 121–131.

Tombelli, S., Minunni, M., Mascini, M., 2005. Analytical applications of aptamers. Biosens. Bioelectron. 20, 2424–2434.

Torre, L. a, Bray, F., Siegel, R.L., Ferlay, J., Lortet-Tieulent, J., Jemal, A., 2015. CA. Cancer J. Clin. 65, 87–108.

Tothill, I.E., 2009. Semin. Cell Dev. Biol. 20, 55–62.

Tuck, A.B., Chambers, A.F., Allan, A.L., 2007. J. Cell. Biochem. 868, 859–868.

Velasco-Garcia, M.N., Missailidis, S., 2009. Gene Ther. Mol. Biol. 13, 1–9.

Velusamy, V., Arshak, K., Korostynska, O., Oliwa, K., Adley, C., 2010. Biotechnol. Adv. 28, 232–254.

Vidotti, M., Carvalhal, R.F., Mendes, R.K., Ferreira, D.C.M., Kubota, L.T., 2011. J. Braz. Chem. Soc. 22, 3–20.

Vikesland, P.J., Wigginton, K.R., 2010. Environ. Sci. Technol. 44, 3656–3669.

Viswanathan, S., Radecki, J., 2008. Pol. J. Food Nutr. 58(2), 157–164.

Wai, P., Kuo, P., 2008. Osteopontin : regulation in tumor metastasis. Cancer Metastasis 27, 103–118.

Wang, J., Meng, W., Zheng, X., Liu, S., Li, G., 2009. Biosen. Bioelectron. 24, 1598–1602.

Wang, W., Jia, L.-Y., 2009. Chinese J. Anal. Chem. 37, 454–460.

Wang, Y., Xiao, Y., Ma, X., Li, N., Yang, X., 2012. Chem. Commun. 48, 738-740.

Wang, Y., Yuan, R., Chai, Y., Yuan, Y., 2011. Biosens. Bioelectron. 30, 61–66.

Weber, G.F., 2011. Cancer Genom. Proteom. 8, 263–288.

Weber, G.F., Lett, G.S., Haubein, N.C., 2010. Br. J. Cancer 103, 861–869.

Weber, G.F., Lett, G.S., Haubein, N.C., 2011. Oncol. Rep. 25, 433–441.

Wei, F., Patel, P., Liao, W., Chaudhry, K., Zhang, L., Arellano-Garcia, M., Hu, S., Elashoff, D., Zhou, H., Shukla, S., Shah, F., Ho, C.-M., Wong, D.T., 2009. Clin. Cancer Res. 15, 4446–4452.

Wu, C.-Y., Wu, M.-S., Chiang, E.-P., Wu, C.-C., Chen, Y.-J., Chen, C.-J., Chi, N.-H., Chen, G.-H., Lin, J.-T., 2007. Gastric Cancer 56, 782–789.

Xiao, Y., Lubin, A.A., Heeger, A.J., Plaxco, K.W., 2005a. Angew. Chem. 44, 5456–5459.

Xiao, Y., Piorek, B.D., Plaxco, K.W., Heeger, A.J., 2005b. J. Am. Chem. Soc. 127, 17990–1.

Xie, S., Yuan, R., Chai, Y., Bai, L., Yuan, Y., Wang, Y., 2012. Talanta 98, 7–13.

Xu, Y., Cheng, G., He, P., Fang, Y., 2009. Electroanal. 21, 1251–1259.

Xu, Y.-Y., Zhang, Y.-Y., Lu, W.-F., Mi, Y.-J., Chen, Y.-Q., 2015. Mol. Clin. Oncol. 3, 357–362.

You, M., Chen, Y., Peng, L., Han, D., Yin, B., Tan, W., Ye, B., 2011. Chem. Sci. 2, 1003–1010.

Yuan, Y., Gou, X., Yuan, R., Chai, Y., Zhuo, Y., Ye, X., Gan, X., 2011. Biosens. Bioelectron. 30, 123–127.

Zhang, F., Chen, J., 2010. BMC Genomics 11, S12.

Zhang, H., Guo, M., Chen, J.-H., Wang, Z., Du, X.-F., Liu, P.-X., Li, W.-H., 2014. Cell Physiol Biochem 33, 991–1002.

Zhang, S., Wright, G., Yang, Y., 2000. Biosens. Bioelectron. 15, 273 – 282.

Zhang, S., Zhou, G., Xu, X., Cao, L., Liang, G., Chen, H., Liu, B., Kong, J., 2011. Electrochem. commun. 13, 928–931.

Zhang, Y., Huang, Y., Jiang, J., 2007. J. Am. Chem. Soc. 129, 15448–15449.

Zhang, Y.L., Pang-P.-F.-Peng-Fei, Jiang, J.H., Shen, G.L., Yu, R.Q., 2009. Electroanal. 21, 1327–1333.

Zhao, B., Sun, T., Meng, F., 2011. J. Cancer Res. Clin. Oncol. 137, 1061–1070.

Zhao, J., Zhang, Y., Li, H., Wen, Y., Fan, X., 2011. Biosens. Bioelectron. 26, 2297–2303.

Zhao, S., Yang, W., Lai, R.Y., 2011. Biosens. Bioelectron. 26, 2442–2447.

Zhao, J., He, X., Bo, B., Liu, X., Yin, Y., Li, G., 2012. Biosens. Bioelectron. 34, 249–252.

Zhou, L., Wang, M.-H., Wang, J.-P., Ye, Z.-Z., 2011. Chinese J. Anal. Chem. 39, 432–438.

Zhou, W., Huang, P.-J.J., Ding, J., Liu, J., 2014. Analyst 139, 2627–2640.

Zuker, M., 2003. Nucleic Acids Res. 31, 3406–3415.

This page was intentionally left blank

CHAPTER 3

Development of an Electrochemical Aptasensor for the Detection of Human Osteopontin

Electrochemical aptasensors, an emerging technology, enable the detection of protein biomarkers, which may be indicative of tumor activity. Osteopontin (OPN) is a protein present in body fluids, being a possible biomarker since its overexpression has been related with breast cancer progression. An RNA aptamer, previously described in the literature, with affinity for human OPN, was synthesized, immobilized onto a working gold electrode surface and used for the development of an electrochemical aptasensor for human OPN detection in standard solutions. The preliminary results using only cyclic voltammetry showed that this aptasensor allowed detecting human OPN with a detection limit of 8 nM, showing a satisfactory selectivity towards the target in the presence of others proteins, except for thrombin.

This chapter presents the preliminary results on the development of an electrochemical RNA aptasensor for human OPN detection.

The information presented in this Chapter was published in the Procedia Engineering, EUROSENSORS 2014, the XXVIII edition of the conference series:

Meirinho, Sofia G., Dias, Luís G., Peres, António M., Rodrigues, Lígia R., (2014). Development of an Electrochemical Aptasensor for the Detection of Human Osteopontin. Procedia Eng. 87, 316 – 319.

3.1. Introduction

The development of electrochemical aptasensors, as an emerging technology, has made possible the detection of protein biomarkers in standard and real samples. Biomarkers are produced by normal and tumor cells and can be indicative of tumor activity when detected in high amounts in the blood or other body fluids (Karley et al., 2011; Rodrigues et al., 2009). Osteopontin (OPN) is a possible protein biomarker because it is found in all body fluids and its overexpression has been related with breast cancer evolution and metastasis (Ahmed and Kundu, 2010; Macrì et al., 2009). A simple and sensitive electrochemical RNA aptasensor with high affinity for human OPN was developed to enable the detection of this non-invasive protein biomarker in real samples and ultimately to be used for cancer prognosis.

This chapter presents preliminary results concerning the aptasensor's performance for rhOPN detection in standard samples, as well as its selectivity towards others proteins (bovine serum albumin, lysozyme, recombinant bovine OPN and thrombin).

3.2. Materials and Methods

3.2.1. Material and reagents

Recombinant human OPN (rhOPN), recombinant bovine OPN (rbOPN) and thrombin (THR) were purchased from R&D Systems. Bovine serum albumin (BSA), lysozyme, diethypyrocarbonate (DEPC), 3,3-dithiodipropionic acid (DPA), N-(3-dimethylaminopropyl)-N-ethylcarbodiimide hydrochloride (EDC), N-hydroxysuccinimide (NHS), ethanolamine (ETA), sulfuric acid 99.999 % and streptavidin were obtained from Sigma-Aldrich. Potassium hexacyanoferrate (III) [$K_3Fe(CN)_6$] and potassium hexacyanoferrate (II) [$K_4Fe(CN)_6$] were obtained from Acros Organics and potassium dihydrogen phosphate (KH_2PO_4) from Merck. Sodium chloride (NaCl), potassium chloride (KCl) and sodium hydrogen phosphate (Na_2HPO_4) were acquired from Panreac. All chemicals were of analytical grade and used as received.

3.2.1.1. Solutions

Phosphate buffer saline (PBS) was prepared to contain 137 mM NaCl, 2.7 mM KCl, 8.1 mM Na_2HPO_4 and 1.47 mM KH_2PO_4, with adjusted pH 7.4. The redox probe was always freshly prepared in order to obtain a solution with concentration of 5 mM of $K_3Fe(CN)_6$ and $K_4Fe(CN)_6$ (1:1) and 10 mM of KCl in 100 mL of PBS, at pH 7.4. Stock solutions of 200 mM of EDC, 100 mM of NHS, as well as the stock solution of 1 mg/ml septravidin in PBS (pH 7.4) were prepared and stored -20 °C before use. Stock solutions of 200 nM of DPA and 100 mM of ETA were prepared and stored at 4 °C. Stock solutions of protein were prepared according to manufacturer specifications and stored at -20 °C. The protein working solutions were prepared and diluted to desired concentrations with PBS buffer and stored at 4 °C before use. Deionized water (18.2 MΩ) purified by a milli-QTM system (Millipore) was used throughout the experiment for aqueous solutions preparation.

3.2.1.2. RNA aptamer

A RNA aptamer against human OPN has been isolated through the SELEX process as described by Mi et al., (2009). The sequence of the biotinylated RNA aptamer that was synthesized by Integrated DNA Technologies (Belgium) is as follows: 5'- Biotin- CGG CCA CAG AAU GAA AAA CCU CAU CGA UGU UGC AUA GUU G-3'. Stock solutions of the synthetic oligonucleotides were prepared with deionized water containing 1 % of DEPC (v/v) to remove the interference of RNase. The working RNA aptamer solution was prepared every day by dilution to the desired concentration (4 nM) using fresh PBS.

3.2.2. Immobilization of the RNA aptamer on a gold surface

To construct an electrochemical-based aptamer biosensor with high affinity for rhOPN, the use of a specific aptamer and an efficient immobilization method are required. The biotinylated RNA aptamer was immobilized onto the screen-printed gold electrode (SPGE) by a streptavidin-biotin interaction (**Fig. 3.1**). The detailed procedure used was as follows: firstly, the working electrode surface was cleaned successively with three solutions (0.5 M H_2SO_4, 0.01 M KCl/0.1 M H_2SO_4 and 0.05 M H_2SO_4) under electric potential in the range of -0.3 to 1.5 V, and with a scan rate of 100 mV/s. Etching with $[Fe(CN)_6]^{-3/-4}$ solution was carried out to enhance the uniformity of the working electrode surface. Next, the self-assembled monolayer (SAM) was spontaneously formed through an

incubation of 200 mM of DPA for 30 min. After washing with deionized water, the working electrode was treated, during 1 hour, with the same volumes of 100 mM of EDC and 1 mM of NHS to activate the carboxyl groups, so that they can bind with the amino terminal of streptavidin. Afterwards, the working electrode was incubated overnight with streptavidin solution at 4 °C. The working electrode was then exposed to ETA(100 mM, pH 8.5) for 20 min to block any remaining activated -COOH groups. Finally, the biotinylated RNA aptamer in PBS buffer (pH 7.4) was attached to the modified gold surface using the streptavidin–biotin interaction for 40 min. All reactions were carried out at room temperature.

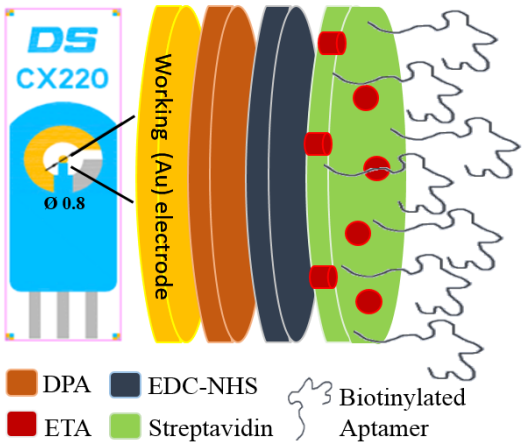

Fig. 3.1. Schematic illustration of a RNA aptamer immobilized onto a SPGE through streptavidin-biotin interaction.

3.2.3. Cyclic voltammetry analysis

Electrochemical analysis was performed at room temperature using a Potentiostat-Galvanostat device (PG580, Uniscan Instruments). The screen-printed gold electrodes chip (DropSens, S.L., Spain) used had a gold working electrode with a diameter of 0.8 mm, as well as a silver pseudo-reference electrode and gold counter electrode.

Standard solutions of rhOPN in PBS buffer (between 25 nM and 1601.6 nM) were dropped on the working electrode and incubated for 1 hour. After washing the electrode with distilled water, 60µL of $[Fe(CN)_6]^{-3/-4}$ solution (redox probe) was dropped on the electrodes chip until all three electrodes were immersed. Then, cyclic voltammetry (CV) was performed and a electrochemical signal was generated due to the aptamer–target molecule interaction in the presence of $[Fe(CN)_6]^{-3/-4}$, under

potential range of -0.5 to 0.6 V and with a scan rate of 50 mV/s. Specificity of the RNA aptasensor to other proteins was also assessed by means of the electrochemical signal generated from the interaction between the RNA aptamer and a solution of each protein (BSA, LYS, rbOPN and THR; 200 nM), under similar experimental conditions. The current decrease was calculated through relative current change, (ΔI %), the difference between the current values of the voltammogram oxidation peak recorded after analyzing the protein solution and that recorded after aptamer immobilization divided by this last one, using the equation (3.1):

$$\Delta I\,\% = (I_0 - I_1)/I_0 \times 100 \qquad (3.1)$$

where ΔI is relative current change; I_0 and I_1 represents the current before and after the sample treatment, respectively.

3.3. Results and Discussion

The electrochemical signal generated, during the CV assays, for the aptamer–rhOPN interaction, recorded at different rhOPN concentrations, was monitored in the presence of $[Fe(CN)_6]^{-3/-4}$ as a redox probe. The cyclic voltammograms show a current decrease as a consequence of the increase of rhOPN concentration, thus indicating a "signal-off" sensing mechanism. **Fig. 3.2** shows the performance of the RNA aptasensor for different rhOPN concentrations. Preliminary results suggest a linear relationship at low concentration levels of rhOPN (<100 nM) with detection and quantification limits of 7.9 and 23.9 nM, respectively.

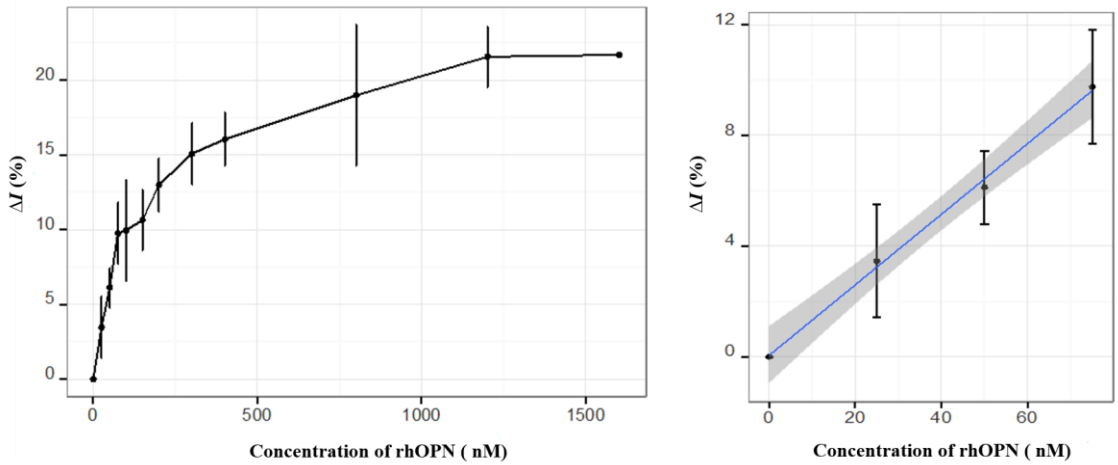

Fig. 3.2. Electrochemical aptasensor sensitivity analysis of rhOPN using an aptamer-immobilized SPGE. The increase of the relative current change (ΔI %) is proportional to the increase of rhOPN concentration in the: A) dynamic interval ranging from 0 nM to 1601.6 nM; B) interval ranging from 0 nM to 100 nM. Error bars indicate the relative standard deviation of three independent experiments.

Furthermore, and contrary to what was reported Mi et al., (2009), the RNA aptamer was found to be non specific for rhOPN (**Fig.3.3**), since the current changes observed in the experiments conducted with other proteins (BSA, LYS, rbOPN and TRH) could not be neglected as compared to the target (rhOPN), especially in the case of THR.

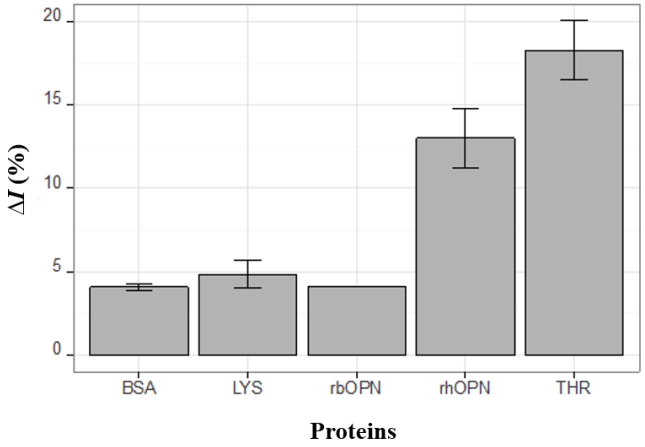

Fig. 3.3. Electrochemical aptasensor specificity response to different proteins at the same concentration (200 nM): BSA – bovine serum albumin, LYS – lysozyme, rbOPN – bovine osteopontin, rhOPN – human osteopontin and THR – thrombin. Error bars indicate the relative standard deviation of three independent experiments.

3.4. Conclusion

This preliminary work suggests that the proposed electrochemical RNA aptasensor is a simple and sensitive tool with satisfactory performance for the detection of rhOPN although it is not totally specific for this target protein. So, further studies are needed, namely involving the selection of new aptamers against human OPN, in order to improve its detection performance and selectivity.

3.5. References

Ahmed, M., Kundu, G.C., 2010. Mol. Cancer 9, 101-114.

Karley, D., Grupta, D., Tiwari, A., 2011. J. Mol. Biomark. Diagn. 2, 2–5.

Mi, Z., Guo, H., Russell, M.B., Liu, Y., Sullenger, B. a, Kuo, P.C., 2009. Mol. Ther. 17, 153–161.

Macrì, A., Versaci, A., Lupo, G., Trimarchi, G., Tomasello, C., Loddo, S., Sfuncia, G., Caminiti, R., Teti, D., Famulari, C., 2009. Tumori 95, 48–52.

Rodrigues, L.R., Lopes, N., Sousa, B., Vieira, D., Milanezi, F., 2009. TOBCANJ 1, 1–9.

CHAPTER 4

Development of an electrochemical RNA-aptasensor to detect human osteopontin

Electrochemical aptasensors may be used to detect protein biomarkers related to tumor activity. Osteopontin (OPN), a protein present in several body fluids, has been suggested as a potential biomarker since its overexpression seems to be associated with breast cancer progression and metastasis. In this chapter, a simple and label-free voltammetric aptasensor for the detection of human OPN, using an RNA aptamer previously reported to have affinity for human OPN as biorecognition element (bioreceptor), and the ferro/ferricyanide solution as a redox probe, was developed. The RNA aptamer was synthesized and immobilized in a working microelectrode gold surface (diameter of 0.8 mm) of a screen-printed strip with a silver pseudo-reference electrode and a gold counter electrode. The electrochemical behavior of the electrode surface after each preparation step of the aptasensor was studied using cyclic voltammetry and square wave voltammetry. The resulting voltammetric aptasensor was used to detect OPN in standard solutions. Cyclic voltammetry results showed that the aptasensor has reasonable detection and quantification limits (3.7 ± 0.6 nM and 11 ± 2 nM, respectively). Indeed, the detection limit falls within the OPN levels reported in the literature for patients with metastatic breast cancer. Moreover, the aptasensor was able to selectively detect the target protein in the presence of other interfering proteins, except for thrombin. Considering the overall results, a possible application of the aptasensor for cancer prognosis may be foreseen in a near future.

The information presented in this Chapter was published in Biosensors and Bioelectronics:

Meirinho, Sofia G., Dias, Luís G., Peres, António M., Rodrigues, Lígia R., (2015). Development of an Electrochemical RNA-Aptasensor to detect Human Osteopontin. Biosens. Bioelectron. 71, 332-341.

4.1. Introduction

Breast cancer is a major cause of mortality among women worldwide. According to the International Agency of Research on Cancer (IARC) and World Health Organization (WHO), in 2012, 1.67 million women were diagnosed with breast cancer, the second most common cancer in women and the fifth leading cause of death (522,000 deaths) (Ferlay et al., 2013). Breast cancer is a complex disease with a very heterogeneous clinical nature, for which it is crucial to identify new biomarkers associated with tumor growth, angiogenesis and metastasis (Thorat et al., 2013). Osteopontin (OPN) is a multifunctional phosphorylated glycoprotein, expressed as a 41-75 kDa protein due to varied post-translational modifications (Anborgh et al., 2011; Tuck et al., 2007; Wai and Kuo, 2008). OPN can be found in all body fluids and is considered as a potential serum tumor marker (Macrì et al., 2009; Rodrigues et al., 2007; Tuck et al., 2007; Weber et al., 2011, 2010), a possible therapeutic target for blocking tumor growth and subsequent metastasis, as well as a cancer regulator (Mi et al., 2009; Rodrigues et al., 2009). Recent studies demonstrated that circulating levels of OPN contribute to the tumor formation and aggressiveness, progression and metastasis (Ahmed and Kundu, 2010; Bache et al., 2010; Bramwell et al., 2014; Mirza et al., 2008; Rodrigues et al., 2007). Increased OPN protein levels in serum or tumor have been associated with several clinical parameters, such as tumor stage, tumor grade, tumor subtype, tumor size and the time of relapse (Bache et al., 2010). In breast cancer, a high OPN expression, measured both in plasma and tumor tissue, has been associated with a decreased survival (Bramwell et al., 2006), as well as poor prognosis and disease progression (Rudland et al., 2002; Weber et al., 2010). In 2014, Bramwell et al. were able to measure, using enzyme-linked immunosorbent assay (ELISA) the OPN levels in plasma samples of patients with metastatic breast cancer. The results showed that plasma OPN concentrations in patients with metastatic breast cancer were on average 46 ng/ml (ranging from 22.6 to 290 ng/ml).

Nowadays, traditional methodologies, such as mammography and ELISA, are used for early detection of breast cancer and detection of OPN in plasma, respectively. However, these techniques present some limitations, thus it is of utmost relevance to develop new non-invasive methods for the detection of tumor markers detection, as for example the detection of OPN in body fluids. These non-invasive methods would allow following the patients' treatment or facilitate the detection of breast cancer in an early stage of the disease, thus enabling an increased success of cancer treatments. Electrochemical aptasensors may be a suitable alternative to the abovementioned diagnosis

methods. Technically, aptasensors can be fabricated to respond to any target molecule for which an aptamer can be generated. Several electrochemical aptasensors have been reported for the specific detection of biomarker proteins in body fluids, such as thrombin (Xiao et al., 2005a, 2005b), C-reactive protein (Centi et al., 2009) and platelet-derived growth factor (PDGF) (Lai et al., 2007). Electrochemical detection has attracted considerable attention in the development of aptasensors since it exhibits high sensitivity, simple instrumentation, low production cost, fast response, and portability (Arshak et al., 2009; Radi, 2011; Saberian et al., 2011; S. Song et al., 2008; Velasco-Garcia and Missailidis, 2009; Velusamy et al., 2010; Xu et al., 2009). On the other hand, aptamers are short single-stranded DNA or RNA oligonucleotides with high affinity and specificity for a specific protein, which can be obtained using a selection process, namely the systematic evolution of ligands by exponential enrichment (SELEX). The dissociation constants of aptamer and their proteins are in the low micromolar to high picomolar ranges (Labuda et al., 2010; Jing et al., 2011; Kim et al., 2013). The potential use of aptamers in clinical applications implies understanding the aptamer-protein interactions. In the literature, several methods for dissociation constants determination have been described including dialysis, ultrafiltration, electrophoretic mobility shift gel, affinity capillary electrophoresis, fluorescence intensity and anisotropy, UV-vis absorption and circular dichroism, surface plasmon resonance and isothermal titration calorimetry (Jing et al., 2011; Tran et al., 2010). Aptamers are easy to synthesize and chemically modify, possessing high sensitivity and selectivity towards the target, good stability in complex environments and resistance to denaturation and degradation. Therefore, aptamers are ideal biological recognition elements for the development of biosensors, especially if compared with antibody-based strategies (Hianik and Wang, 2009; Radi, 2011; Song et al., 2012; Strehlitz et al., 2008). Recently, Mi et al., (2009b) isolated an RNA aptamer against human OPN (dissociation constant (*Kd*) of 18 nM) using SELEX, which could be further explored in the development of an electrochemical biosensor to detect OPN. Indeed, more recently, Cao et al., (2014), proposed an electrochemical aptasensor method for the detection of human OPN using the square wave voltammetry (SWV) technique with a pyrolytic graphite disk electrode (3.0 mm diameter), functionalized with gold nanoparticles in synthetic host macromolecule substrate, and the same RNA-aptamer (Mi et al., 2009). This electrochemical method allowed detecting human OPN with a detection limit of 10.7 ng/mL (Cao et al., 2014). However, the application of nanomaterials increase the cost of the biosensor and, in complex samples, its reproducibility and quantification may be affected (Yu et al., 2012). On the other hand, Chen et al., (2014), developed an electrochemical immunosensor for human OPN detection through the impedance spectroscopy

technique, which had a detection limit of 0.17 nM. Though, as mentioned above, aptamers present some advantages over immunological compounds, and the number of applications involving their use greatly increased in the recent years.

In this chapter, a simple electrochemical aptasensor for the detection of human OPN was developed based in a preliminary study of our research group (Meirinho et al., 2014) (Chapter 3). For that purpose, the RNA aptamer previously described by Mi et al., (2009) was studied regarding its aptamer-rhOPN binding affinity using fluorescence assays and as an aptasensor through its immobilization in a screen printed gold electrode (SPGE) by biotin-streptavidin interaction. Cyclic voltammetry (CV), with a $[Fe(CN)_6]^{3-/4-}$ redox probe, was used to evaluate the biosensor performance towards human OPN detection, as well as the influence of other interfering proteins. As a complementary technique, square wave voltammetry (SWV) was also applied to follow the steps of the aptasensor construction, enabling a comparison between the observed electrochemical behaviors after each step.

4.2. Materials and Methods

4.2.1. Material and reagents

Recombinant human osteopontin (rhOPN, 65 kDa) and recombinant bovine osteopontin (rbOPN, 60 kDa) were purchased from R&D Systems. Thrombin from human plasma (THR, 37.4 kDa), Bovine serum albumin (BSA, 66 kDa), lysozyme from chicken egg white (LYS, 14.3 kDa) and streptavidin were obtained from Sigma-Aldrich. All proteins were acquired lyophilized and manipulated according to the manufacturers' specifications. Diethypyrocarbonate (DEPC), 3,3-dithiodipropionic acid (DPA), N-(3-dimethylaminopropyl)-N-ethylcarbodiimide hydrochloride (EDC), N-hydroxysuccinimide (NHS), ethanolamine (ETA) and sulfuric acid (purity of 99.999 %) were obtained from Sigma-Aldrich. Potassium hexacyanoferrate (III) ($K_3Fe(CN)_6$) and potassium hexacyanoferrate (II) ($K_4Fe(CN)_6$) were obtained from Acros Organics and potassium dihydrogen phosphate (KH_2PO_4) from Merck. Sodium chloride (NaCl), potassium chloride (KCl) and sodium hydrogen phosphate (Na_2HPO_4) were acquired from Panreac. All chemicals were of analytical grade and used as received.

4.2.1.1. Solutions

Phosphate buffer saline (PBS) solution (137 mM NaCl, 2.7 mM KCl, 8.1 mM Na_2HPO_4 and 1.47 mM KH_2PO_4) with an adjusted pH of 7.4 was used. The ferro/ferricyanide redox probe (5 mM $K_3Fe(CN)_6$ and $K_4Fe(CN)_6$ (1:1) and 10 mM KCl in 100 mL of PBS), with an adjusted pH of 7.4, was daily prepared. Stock solutions of 200 mM EDC, 100 mM NHS, as well as the stock solution 1 mg/ml of septravidin in PBS (pH 7.4) were stored at -20 °C before use. Stock solutions of 200 nM DPA and 100 mM of ETA were stored at 4 °C. Stock solutions of each protein were prepared according to the manufacturer specifications and stored at -20 °C. The protein working solutions were obtained by dilution with PBS buffer (pH 7.4) and stored at 4 °C until use. Deionized water (18.2 MΩ) purified by a milli-QTM system (Millipore) was used throughout the experiment for aqueous solutions preparation.

4.2.1.2. RNA aptamer

The RNA aptamer herein used was reported by Mi et al., (2009). The sequence of the biotinylated RNA aptamer (5'-Biotin- CGG CCA CAG AAU GAA AAA CCU CAU CGA UGU UGC AUA GUU G-3') was synthesized by Integrated DNA Technologies (Belgium). Stock solutions (100 μM) of the synthetic oligonucleotides were prepared with ultra-pure water containing 1 % DEPC (v/v) to avoid the RNase interference. The working RNA aptamer solution was prepared by dilution using fresh PBS. Before the RNA aptamer immobilization on the gold working electrode, the biotinylated RNA aptamer prepared in PBS buffer (pH 7.4) was subjected to a temperature treatment (95 °C during 5 min, 4 °C for 5 min and 10 min at room temperature) in order to obtain an adequate structure flexibility of the aptamer.

4.2.1.3. Apparatus

Electrochemical analyzes were performed at room temperature using a Potentiostat-Galvanostat device (PG580, Uniscan Instruments). The screen-printed gold electrodes (SPGEs) (DropSens, S.L., Spain) has a gold working electrode with a diameter of 0.8 mm, as well as a silver pseudo-reference electrode and a gold counter electrode. The pH was measured using a pH meter (iHANNA instruments pH 211). The fluorescence measurements were performed in 96-dark-well plates using an ELISA reader (Synergy HT, BIO-TEK, IZASA) equipped with thermostat holding a temperature control accuracy of 0.1 °C and configured with 492 nm excitation and 518 nm emission filters. The

Gen5™ data analysis software was used for collecting microplate data and conducting the analysis after settle a range of excitation and emission wavelengths.

4.2.2. Fluorescence aptamer-protein binding affinity assays

Fluorescence assays were performed to evaluate the binding affinity of the RNA aptamer towards rhOPN. For that purpose, a fluorophore 6-carboxyfluorescein (FAM) was attached to the 5'-end of the RNA aptamer sequence (i.e., 5'-FAM-CGG CCA CAG AAU GAA AAA CCU CAU CGA UGU UGC AUA GUU G-3'), which was supplied by Alfagene (Portugal). Before each fluorescence assay, the FAM-RNA aptamer was heated at 95 °C during 5 min, then cooled at 4 °C for 5 min and finally 10 min at room temperature to facilitate the folding of the aptamer.

First, the fluorescence of the FAM-RNA aptamer was studied. FAM-RNA aptamer solutions with concentrations varying from 2.5 to 100 nM were prepared and the related fluorescence intensity of the free aptamer (non-bound to any protein) was measured. The different solutions of FAM-RNA aptamer were incubated for 30 min and 4 hours at room temperature. After this, the solutions were excited at 492 nm and fluorescence was measured at 518 nm. Based on these assays, calibration curves relating the fluorescence intensity and FAM-RNA aptamer concentrations were established for both incubation times (30 min and 4 hours), enabling the evaluation of the fluorescence contribution of the free aptamer and, if necessary, the estimation of the free aptamer concentration for the binding aptamer-protein studies.

Regarding the aptamer-protein complex formation, a 20 nM FAM-RNA aptamer solution was prepared in PBS buffer at pH 7.6. For each fluorescence assay, 60 µL of a 20 nM solution of RNA aptamer modified with FAM-RNA-aptamer, were incubated with the same volume of different concentrations of rhOPN (0, 3, 10, 100, 300, 370 nM) prepared in the same buffer (Potty et al., 2009; Tran et al., 2010), in 96-dark-well plates. The mixtures were incubated at room temperature for two different periods, i.e. 30 min and 4 hours. The mixture was excited at 492 nm and fluorescence was measured at 518 nm.

Since THR is a protein present in the human blood and could act as an interferent during the electrochemical analysis of blood samples, these same experiments were also conducted for THR. Indeed, rhOPN contains a THR cleavage domain, thus the RNA aptamer could hold a site that may also recognize THR.

4.2.3. Aptamer-protein binding affinity parameter

Fluorescence data were further used to determine the dissociation constant (*Kd*), which is the reciprocal of the binding pseudo-equilibrium constant of the aptamer-protein complex formation. A one-to-one binding aptamer-protein stoichiometry was assumed (i.e. identical and equivalent binding sites for protein and aptamer), thus it was supposed that one mole of protein could only bind to one mole of aptamer.

Briefly, the aptamer-protein complex (*P-APT*) formation may be represented by the equation proposed by Jing et al., (2011):

$$P + APT \leftrightarrow P - APT \tag{4.1}$$

being *P* and *APT* the protein and aptamer, respectively.

In this case, the dissociation constant could be calculated by:

$$K_d = \frac{[P][APT]}{[P - APT]} \tag{4.2}$$

where [*P*] and [*APT*] are the concentrations of free protein and free aptamer, i.e. non-bound, respectively.

Including the fraction of bound aptamer (f_{APT}), as the ratio between the concentrations of bound aptamer and the total aptamer (for assays with constant initial aptamer concentration and increasing protein concentrations, i.e. when RNA aptamer is titrated with a broad concentration range of protein), the following equation can be established:

$$f_{APT} = \frac{[APT]_{bound}}{[APT]_{initial}} = \frac{[P-APT]}{[P-APT]+[APT]} \tag{4.3}$$

Considering one-to-one equilibrium, $[APT]_{bound} = [\mathrm{P} - \mathrm{APT}]$ and $[APT]_{initial} = [APT]_{bound} + [APT]$ can be assumed.

Afterwards, replacing $[P - APT]$ in equation (4.3) with the result of the equation (4.2) the following relation can be derived:

$$f_{APT} = \frac{[P]}{K_d+[P]} \tag{4.4}$$

and after rearranging:

$$\frac{f_{APT}}{[P]} = \frac{1}{K_d} - \frac{f_{APT}}{K_d} \quad (4.5)$$

Equation (4.5) is often known as the Scatchard equation and a straight line with a slope equal to $-\frac{1}{K_d}$ will be obtained by plotting $\frac{f_{APT}}{[P]}$ *versus* f_{APT}. This procedure allows a straightforward calculation of the K_d value and to infer about the binding affinity between the aptamer and the protein. Alternatively, K_d can be calculated using non-linear optimization algorithms using equation (4.4). In both cases, it is necessary to estimate f_{APT} experimentally and the concentration of free protein ($[P]$) after each protein addition, assuming that the pseudo-equilibrium described by equation (4.1) is attained.

Some points must be considered, namely if the initial aptamer concentration is significantly smaller than K_d (i.e., $[APT]_{initial} \ll K_d$), the free protein concentration $[P]$ at equilibrium does not change significantly from the total protein concentration added, $[P]_t$ upon binding (i.e. $[P] \approx [P]_t$) and so equation (4.8) could be simplified to the one proposed by Jing et al., (2011):

$$\frac{f_{APT}}{[P]_t} = \frac{1}{K_d} - \frac{f_{APT}}{K_d} \quad (4.6)$$

(i) It is recommended to use data across the binding fraction range (i.e. f_{APT}values) of 0.2–0.8 (Jing et al., 2011).

(ii) The values of f_{APT} must be calculated using equation (4.3) based on the concentration of bound aptamer ($[APT]_{bound}$) estimated using the experimental fluorescence data.

Hence, to estimate $[APT]_{bound}$ the following procedure could be implemented. If both the aptamer non-bound and the aptamer-protein complex formed (F_{APT} and F_{P-APT}, respectively) exhibit fluorescence, then the total fluorescence measured (F_t) would result from:

$$F_t = F_{APT} + F_{P-APT} \quad (4.7)$$

where, F_{APT} could be calculated using the regression parameter (intercept *a* and slope *b*) of the calibration curve obtained by measuring the fluorescence of increasing aptamer concentration solutions without the presence of the protein,

$$F_{APT} = a + b[APT] \tag{4.8}$$

and F_{P-APT} may be estimated assuming a proportionality coefficient between fluorescence intensity and the complex concentration, $[P - APT]$, like:

$$F_{P-APT} = c[P - APT] \tag{4.9}$$

being the coefficient *c* estimated based on the constant maximum fluorescence intensity observed in the titration curve (increasing protein concentrations added to a fixed initial aptamer concentration), a situation where all the initial *APT* is bound to *P* (no free *APT* is available in the solution), thus all measured fluorescence would be due to the $P - APT$ complex, which concentration, for a one-to-one binding stoichiometry, could be assumed as:

$$[P - APT] = [APT]_{initial} \tag{4.10}$$

and so,

$$c = \frac{F_{t,maximum}}{[APT]_{initial}} \tag{4.11}$$

Replacing equations (4.8) to (4.11) into the equation (4.7), and by using the relations between the concentrations of protein and aptamer, bound or free, it is possible to obtain an explicit equation for $[APT]_{bound}$:

$$F_t = a + b[APT] + \frac{F_{t,maximum}}{[APT]_{initial}}[P - APT] \tag{4.12.1}$$

$$F_t = a + b([APT]_{initial} - [APT]_{bound}) + \frac{F_{t,maximum}}{[APT]_{initial}}[APT]_{bound} \tag{4.12.2}$$

$$[APT]_{bound} = \frac{F_t - a - b[APT]_{initial}}{\frac{F_{t,maximum}}{[APT]_{initial}} - b} \tag{4.12.3}$$

Finally, the equation (4.3) could be modified to enable the direct calculation of f_{APT} from experimental fluorescence data:

$$f_{APT} = \frac{\frac{F_t - a - b[APT]_{initial}}{\frac{F_{t,maximum}}{[APT]_{initial}} - b}}{[APT]_{initial}} \quad (4.13)$$

When the RNA aptamer concentration approaches or is greater than K_d ($[APT]_{initial} \geq K_d$), this parameter should not be calculated using equation (4.6) since $[P]$ cannot be considered equal to $[P]_t$ and so, in equation (4.6) the free protein concentration should be replaced by:

$$[P] = [P]_t - [P]_{bound} = [P]_t - [P - APT] \quad (4.14)$$

Similarly,

$$[APT] = [APT]_{initial} - [APT]_{bound} = [APT]_{initial} - [P - APT] \quad (4.15)$$

Therefore, by making these replacements in equation (4.2) the following equation for the complex concentration may be derived, as described by Jing et al., (2011):

$$[P - APT] = \frac{[P]_t + [APT]_{initial} + K_d - \sqrt{([P]_t + [APT]_{initial} + K_d)^2 - 4[P]_t[APT]_{initial}}}{2} \quad (4.16)$$

Finally, by replacing these equations in equation (4.4) an expression is obtained for the case where the initial aptamer concentration is not smaller than the dissociation constant:

$$f_{APT} = \frac{[P]_t - \frac{[P]_t + [APT]_{initial} + K_d - \sqrt{([P]_t + [APT]_{initial} + K_d)^2 - 4[P]_t[APT]_{initial}}}{2}}{K_d + [P]_t - \frac{[P]_t + [APT]_{initial} + K_d - \sqrt{([P]_t + [APT]_{initial} + K_d)^2 - 4[P]_t[APT]_{initial}}}{2}} \quad (4.17)$$

Combining equations (4.13) and (4.17) it is then possible to calculate K_d value by applying a non-linear optimization algorithm.

In this study, K_d values were estimated using the Levenberg–Marquardt nonlinear least-squares minimization method. This optimization procedure uses the gradient descent and Gauss–Newton

minimization algorithms, ensuring that a solution is found even if the starting values of the unknown terms are not close to those obtained in the final adjustment. The first algorithm is applied when the sum of squared deviations is large and, the second, when the optimal value is approached (Bloomfield, 2014). The Levenberg–Marquardt method was applied using the package minpack.lm (Timur et al., 2013) of the R software.

4.2.4. RNA aptamer immobilization

The electrochemical-based aptamer biosensor was obtained using a biotinylated RNA aptamer immobilized on a streptavidin-modified gold electrode surface (**Fig. 4.2.A**). The substances, concentrations, temperatures and times used in the RNA aptamer immobilization steps were established based on data reported in the literature (Kim et al., 2010; Xiao et al., 2005a).

First, the gold working electrode surface was cleaned successively with three solutions (0.5 M H_2SO_4, 0.01 M KCl/0.1 M H_2SO_4 and 0.05 M H_2SO_4) under electric potential in the range of -0.3 to 1.5 V, and at scan rate of 100 mV/s. An etching step, with $[Fe(CN)_6]^{3-/4-}$ solution, was carried out to ensure the homogeneity of the gold working electrode surface. Afterwards, a self-assembled monolayer (SAM) was formed through an incubation step, using a 200 mM solution of DPA (30 min at room temperature). The working electrode was then washed with ultra-pure water and treated with 100 mM solution of EDC and 1 mM solution of NHS (1:1 v/v, 60 min at room temperature) to activate the carboxyl groups, which facilitates the binding with the amino group of streptavidin during overnight incubation with streptavidin solution (4 °C). The working electrode was then exposed to ETA (100 mM, pH 8.5, during 20 min at room temperature) to block any remaining activated carboxyl groups. Finally, the biotinylated RNA aptamer was attached to the modified gold surface using the streptavidin–biotin interaction (40 min at room temperature) and the surface was rinsed thoroughly with PBS buffer (pH 7.4) to remove the free aptamers. For the detection of rhOPN, a standard solution of protein in PBS (pH 7.4) was dropped (≈ 5 μL) on the working electrode and incubated for 60 min at room temperature. After washing the electrode with PBS, to further remove non-binding rhOPN, 60 μL of $[Fe(CN)_6]^{3-/4-}$ solution (redox probe) was dropped on the electrodes chip until all three electrodes were immersed. After this procedure CV assay was carried out to assess the level of RNA aptamer binding to the protein tested. All changes obtained in each preparation step of the aptasensor were followed by CV since it is a simple, rapid and sensitivity technique, which gives overall information regarding the reversibility of the oxidation and reduction mechanisms that occur

at the electrode surface (Farghaly and Hameed, 2014). This electrochemical technique worked as a quality control tool and it allowed establishing typical redox probe cyclic voltammograms to monitor the effectiveness of the working electrode surface modification. If in any of the preparation steps, the cyclic voltammogram was not the expected, the sensor was discarded. SWV was also applied, for comparative purposes, to verify if the electrochemical behavior recorded after each preparation step during the aptasensor construction was similar for both techniques.

4.2.5. Electrochemical measurements

CV is widely used in electrochemical analysis to characterize electroactive compounds and electrode surfaces. This method involves linear forward and backward scanning within a fixed potential range, recorded at the working electrode, being the plot of the observed current *versus* the applied potential, the cyclic voltammogram. Anodic and cathodic peak current intensities and the respective potentials, at which these peaks are observed, provide valuable information regarding system reversibility and can be used to elucidate the oxidation/reduction mechanism at the electrode surface. Therefore, all electrodes used were evaluated and further characterized using CV and the electrochemical measurements were performed in the presence of $[Fe(CN)_6]^{3-/4-}$ at room temperature. The CV measurements were performed under a potential range of -0.5 to 0.6 V and at a scan rate of 50 mV/s.

The current decrease was calculated based on the (relative current change, ΔI / %) considering the oxidation peak current values of the cyclic voltammogram recorded after aptamer immobilization and protein solution incubation by using the equation (4.18):

$$\Delta I / \% = (I_0 - I_1)/I_0 \times 100 \qquad (4.18)$$

Where ΔI / is relative current change (%); I_0 and I_1 represents the current before and after the sample incubation, respectively.

The detection limit (LOD) and quantification limit (LOQ) were calculated based on the linear relationship obtained between ΔI / % values of oxidation peak current and different rhOPN concentrations. The detection limit and the quantification limits are calculated by the equations LOD = 3(SD/b) and LOQ = 10(SD/b), respectively, where SD is the standard deviation of the intercept and b is the average slope of the regression line (Ermer and Miller, 2005).

SWV was also used since it is a fast and sensitive pulse method for which a symmetric square wave is superimposed on a staircase potential. The current is measured twice during each square wave cycle, at the end of the forward and reverse pulses, being the current difference plotted against the applied base potential. The SWV response is peak-shaped and the peak potential matches with the half-wave potential for a simple reversible ion transfer mechanism (Farghaly and Hameed, 2014). Under the CV optimized conditions, the SWV signal changes were observed for a potential range of -0.5 V to 0.6 V, at a frequency of 100 Hz, an amplitude of 50 mV and scan increment of 5 mV.

4.3. Results and Discussion

4.3.1. Evaluation of the aptamer-human OPN binding affinity

The aptamer-rhOPN binding evaluation was performed using fluorescence assays. First, fluorescence intensities were measured for increasing concentrations of FAM-RNA aptamer, enabling the establishment of two calibration curves for two incubation periods (30 min and 4 hours), as shown in **Fig. 4.1.A**. Secondly, the aptamer-rhOPN complex formation was followed by measuring the fluorescence intensity after the addition of different rhOPN concentrations to a solution with 20 nM of FAM-RNA aptamer. The **Fig. 4.1.B** shows the titration curve obtained for the two abovementioned incubation periods. This figure shows that total fluorescence increases with increasing rhOPN concentration, thus suggesting that the aptamer-protein complex exhibits fluorescence. Hence, the fluorescence intensity values measured result from the individual contribution of the non-bond aptamer and aptamer-rhOPN complex formed. These fluorescence data (**Fig. 4.1.A** and **4.1.B**) were used together with the equations described in **section 4.2.3** to verify the aptamer-rhOPN complex formation by means of K_d estimation. Since for the RNA aptamer used in this work, a K_d value of 18.0 ± 0.2 nM was already reported by Mi et al., (2009), based in electrophoretic mobility shift assays, the K_d values for the FAM-RNA aptamer were calculated using the mathematical procedure for [APT] ≥ K_d (equations (4.13) and (4.17)). Assuming only one aptamer-rhOPN high affinity-binding site, K_d values of 1.6 nM and 8.5 nM were estimated for 30 min and 4 hours, respectively. These results pointed out that with an incubation of 30 min the binding site seems to have a higher affinity for rhOPN (lower K_d value), showing that this time-period is sufficient to ensure the aptamer-rhOPN binding.

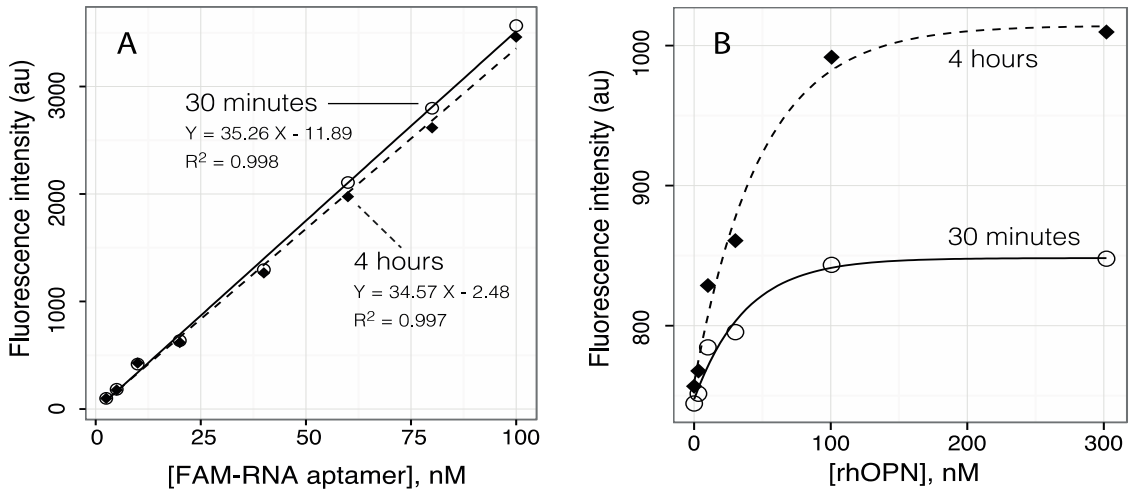

Fig. 4.1. A) Calibration curves of FAM-RNA aptamer for two incubation periods (30 min and 4 hours), and B) Titration curve of 6-carboxyfluorescein-labelled RNA aptamer with increasing rhOPN concentrations in PBS buffer pH 7.6 at 30 min and 4 hours of incubation time. The concentration of RNA aptamer probe was fixed in 20 nM.

4.3.2. Electrochemical evaluation of the electrode surface

The voltammetry assays were conducted to verify the electrochemical behavior of the electrode surface after each preparation step of the aptasensor. CV is a valuable and convenient tool to monitor the barrier of the modified electrode. This tool allows measuring electron transfer between the solution species and the electrode that must occur by tunnelling either through the barrier or through the defects in the barrier (Olowu et al., 2011). The SWV is a more sensitive technique and it was used to confirm the CV results in each step of the aptamer preparation. For these electrochemical studies, a 5 mM solution of $[Fe(CN)_6]^{3-/4-}$ was used as the redox probe.

Fig. 4.2 shows the various immobilization steps towards RNA aptamer onto a working gold electrode (**Fig. 2A**) and the sensor voltammograms obtained in each preparation steps using CV (**Fig. 4.2.B**) and SWV (**Fig. 4.2.C**). Using the cyclic voltammograms data, electrochemical parameters were calculated namely, the potential variation between cathodic and anodic peaks (ΔEp), the cathodic peak current value (Ipc) and anodic peak current value (Ipa), which are given in **Table 4.1**. The results shown are mean values obtained from assays using different SPGEs and prepared in different days.

Table 4.1. Electrochemical parameters obtained after each electrode surface preparation steps.

Steps	ΔEp (mV)	Ipa (µA)	Ipc (µA)
Bare Au electrode	100 ± 10	6.9 ± 0.6	6.9 ± 0.4
Cleaning	175 ± 8	6.0 ± 0.2	5.9 ± 0.3
DPA	200 ± 10	5.68 ± 0.04	5.38 ± 0.04
EDC-NHS	87 ± 5	7.4 ± 0.4	7.6 ± 0.4
Strepatvidin	118 ± 8	5.8 ± 0.5	6.4 ± 0.6
ETA	137 ± 15	5.9 ± 0.5	6.6 ± 0.4
RNA aptamer	143 ± 10	5.6 ± 0.2	6.4 ± 0.2
rhOPN	245 ± 17	4.14 ± 0.08	4.8 ± 0.2

CV - Cyclic voltammogram; ΔEp - potential variation between cathodic and anodic peaks; Ipc - cathodic peak current value; Ipa - anodic peak current value. Mean values ± standard deviation of three or more replicas are presented.

The first cyclic voltammogram in **Fig. 4.2.B1**, recorded with the $[Fe(CN)_6]^{3-/4-}$ redox solution, shows the quasi-reversible electrochemical behavior of the gold electrode surface without any treatment, with peaks separation of 100 mV (ΔEp) and with similar cathodic and anodic peaks current intensities (**Table 4.1**). The current response decreased slightly after the cleaning steps with different H_2SO_4 solutions, which may be due to achieving a homogeneous surface. After the DPA self-assembled monolayer formation on the electrode surface, an expected decrease of the peaks current intensities was observed, as well as an increase of ΔEp, which may be due to the electron transfer blocking. Subsequently, the electrode surface was activated with EDC-NHS (activation of the carboxyl groups), which resulted in an increase of the peaks current intensities (**Fig. 4.2.B2**) and a decrease in the ΔEp giving a voltammogram close to a reversible behavior. The activated carboxylic groups on the electrode surface facilitate the binding of the streptavidin amine's groups. The streptavidin layer in the electrode surface increased the ΔEp value and decreased the current peaks intensities, when compared to the previous step. After exposing the working surface electrode to ETA, aiming to block any remaining activated carboxyl groups, the cyclic voltammogram obtained showed an increase in the ΔEp and in the current peaks as compared with the previous one, which may be due to some non-specific blocking of the remaining free carboxylic groups.

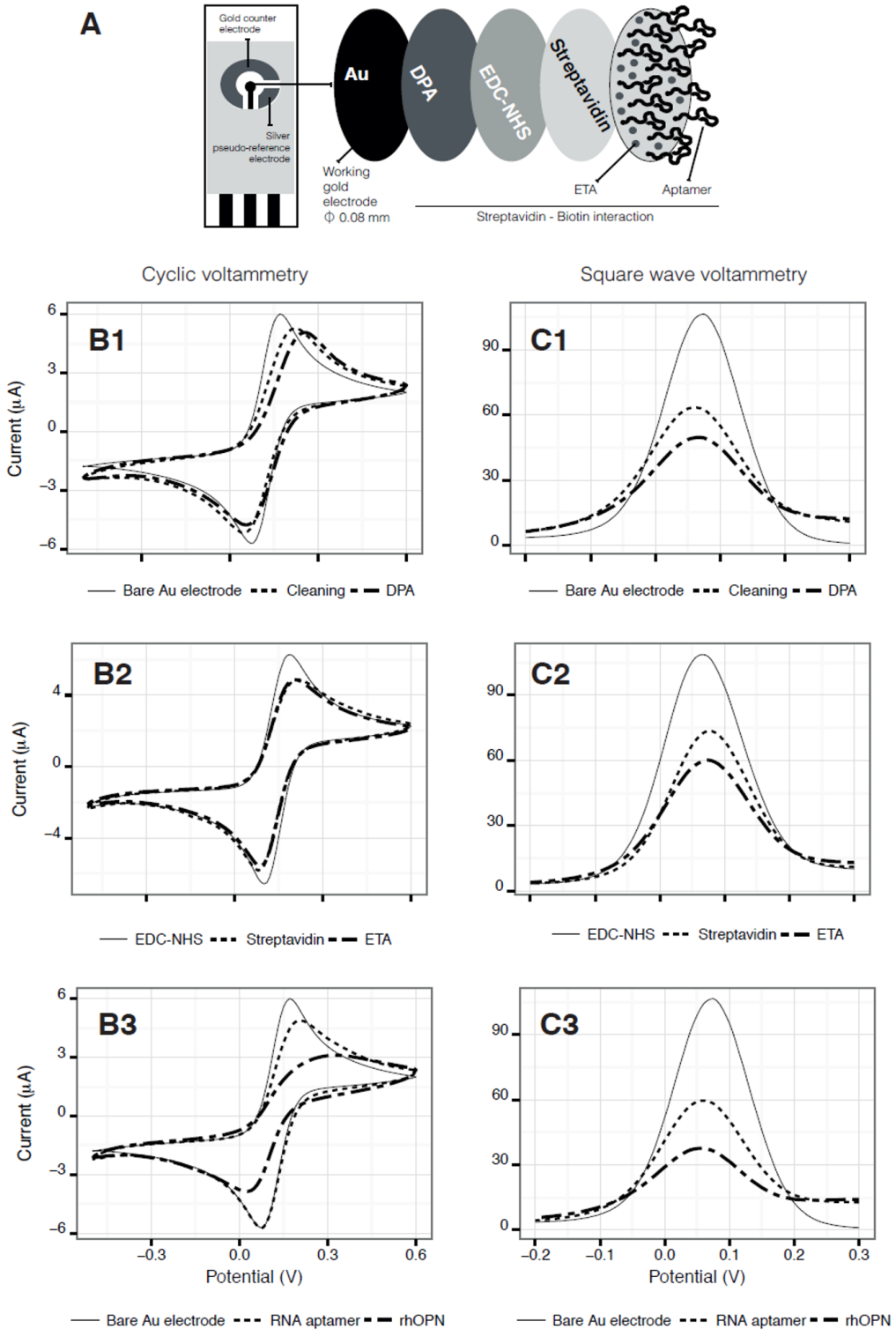

Fig. 4.2. A) Schematic illustration of an RNA aptamer immobilized onto a working gold electrode through streptavidin-biotin interaction. B) Cyclic voltammograms and C) Square wave voltammograms of 5 mM $[Fe(CN)_6]^{3-/4-}$ probe in PBS buffer solution of pH 7.4 at scan rate of 50 mV/s for all aptasensor preparation steps: bare Au electrode, cleaning, DPA, EDC/NHS, streptavidin, ETA, RNA aptamer and RNA aptamer-rhOPN protein.

After the aptamer immobilization on electrode surface, the typical cyclic voltammogram (**Fig. 4.2.B3**) showed similar ΔEp and lower current peaks comparing to the previous steps. Because of the negative charges of the aptamer backbone phosphate group and $[Fe(CN)_6]^{3-/4-}$ redox probe, the electrostatic repulsive interaction is expected to block the electron transfer (Bang et al., 2005). This experiment clearly demonstrated the effective immobilization of the aptamer onto the working electrode surface. The differences between the cyclic voltammograms obtained after the aptasensor preparation and after its incubation with a standard rhOPN solution (1540 nM) are significant. Indeed, for the rhOPN analysis, the cyclic voltammogram showed the highest potential variation between peaks and the lowest current peaks comparing with all the seven previous steps. The decrease of peak current intensities is an evidence of the aptamer-rhOPN complex formation, by means of the specific recognition increased hindered electron transfer. This "signal-off" sensing mechanism (negative readout signal) in the current after aptamer-target interaction could be attributed to a change of the aptamer conformation.

SWV was also used for monitoring each biosensor construction step (**Fig. 4.2.C**). From the visual comparison of the cyclic voltammograms and SWV voltammograms plots (**Fig. 4.2.B and 4.2.C**, respectively) it can be concluded that the order of the peak current intensities for all the biosensor's preparation steps is equivalent, showing that both techniques allow monitoring the electrochemical changes occurred during the electrode surface preparation. However, the differences observed in the plots for SWV (of **Fig. 4.2.C**) are more evident, which was expected considering its higher sensitivity compared to CV. The maximum current intensities of all SWV voltammograms were recorded at a potential range from 0.06 to 0.075 V. As expected, **Fig. 4.2.C1** shows that at the bare Au electrode, the redox probe exhibited maximum peak intensity at the potential 0.075 V and a decrease of 50 % in current intensity after the cleaning step with different H_2SO_4 solutions (current intensity maximum at potential 0.060 V) and a decrease of 64 % after the DPA immobilization (current intensity maximum at potential 0.065 V). After the electrode surface activation with EDC-NHS (**Fig. 4.2.C2**), the current intensity attained was slightly lower comparing to the result for the bare Au electrode (signal decrease of 7 %). The **Fig. 4.2.C2** also showed the current intensity decrease due to the binding of the streptavidin amine's groups in the electrode surface (corresponding to 40 % decrease compared to the bare Au electrode signal) and a shift to a higher potential (0.075 V). As the result of the application of the ETA, to block any remaining activated carboxyl groups, the SWV showed a reduced current intensity peak compared with the previous step, but at the same potential value. In the **Fig. 4.2.C3**,

it is clear the difference between the surface response of the bare gold electrode after the aptamer immobilization on the electrode surface (considering all the described previous steps) and after rhOPN incubation (with a standard solution of 1540 nM). The current intensity of the voltammograms recorded after the aptamer immobilization decreased 56 % compared with the signal observed for the bare gold surface, with a potential shift to lower value (0.07 V) and, for after rhOPN analysis incubation an even higher decrease was observed (78 % compared to that of the bare gold surface), showing a potential shift to an even lower potential value (0.06 V). These last variations, as in CV results, demonstrate the aptamer-rhOPN complex formation and the existence of a current signal-off sensing mechanism (negative readout signal).

The CV technique was chosen to evaluate the quality control of the aptasensor preparation and to evaluate its analytical performance in the detection of proteins since it allowed obtaining information about the sensor surface's oxidative and reducing process. Overall, these two electrochemical techniques enable monitoring each immobilization step used in construction of the RNA aptamer into the working gold electrode and that aptamer-protein interaction results in a decrease of the current response.

4.3.3. Optimization of experimental conditions

The experimental conditions were optimized in order to obtain an aptasensor with a high sensitivity. Several RNA aptamer concentrations, times and temperatures were evaluated to improve the aptamer immobilization on the working gold modified surface. Also, the incubation time of rhOPN with the aptamer, was optimized.

For the RNA aptamer concentration studies, several SPGEs aptasensors were prepared with different concentrations of RNA aptamer (2.5 nM, 4 nM, 0.1 μM, 0.5 μM and 1 μM) for 40 min at room temperature, as described in section 2.5. Afterwards, each aptasensor was incubated with a rhOPN solution (1540 nM) for one hour at room temperature. **Fig. 4.3.A** shows the current relative change ($\Delta I/\%$) obtained from the redox solution probe CV after the rhOPN incubation step. The results showed that the highest $\Delta I/\%$ values were obtained for the aptasensor prepared with an RNA aptamer concentration of 4 nM. For concentrations higher than 4 nM there was a decrease in the $\Delta I/\%$ values. Therefore, the immobilization with an RNA aptamer concentration of 4 nM was chosen for the following studies as it promoted a greater difference between the signals after immobilization of aptamer and after protein inoculation. The incubation time of the RNA aptamer in the gold working

electrode was also evaluated, namely for 40 min and 2 hours (*data not shown*). The ΔI/% values obtained for the two incubation times were also very similar, being the incubation time set equal to 40 min. Regarding the temperature selection for the immobilization of the aptamer, two temperatures were evaluated, namely 4 °C and room temperature. The assays were conducted using a 4 nM RNA aptamer solution that was incubated during 40 min in the SPGEs modified surfaces. The ΔI/% values obtained from the cyclic voltammograms after incubation of rhOPN (1540 nM) were similar for both temperatures. Thus, all experiments were further carried out at room temperature.

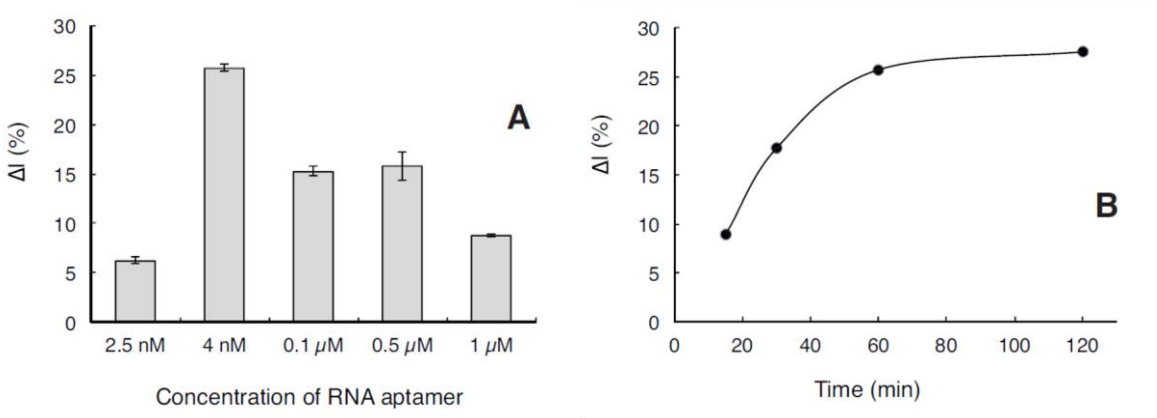

Fig. 4.3. Optimization of the biotin-RNA aptamer concentration: several concentrations of aptamer have been tested (2.5 nM, 4 nM, 0.1 μM, 0.5 μM and 1 μM). The aptamer concentration has been chosen comparing the relative current signals measured in presence and in absence of rhOPN. Mean values ± standard deviation of three or more replicas are presented; B) Effect of the incubation time of the rhOPN solution.

Another important parameter to increase the sensitivity and selectivity of the aptasensor is the incubation time of the target protein. This factor can affect the formation of the aptamer-target complex and therefore must be evaluated. A series of modified electrodes prepared with 4 nM biotin-RNA aptamer were incubated with 1540 nM of rhOPN solution for 15, 30, 60 and 120 min at room temperature. As shown in **Fig. 4.3.B**, the ΔI/% values increased gradually with the increase of the incubation time, and it was found to remain almost constant after 60 min of protein incubation. Thus, an incubation time of 60 min was chosen as the optimal time for the aptamer-protein complex formation and it was used in the following experiments.

4.3.4. Electrochemical detection of human OPN

The performance of the aptasensor was evaluated under the experimental conditions selected, taking into account its response (ΔI/% values) to standard solutions containing different concentrations of rhOPN. Each rhOPN determination was carried out using different SPGEs.The cyclic voltammograms of the $[Fe(CN)_6]^{3-/4-}$ solution (redox probe) showed an electrochemical response that could be related to the aptamer surface modification and, in this case, to the amount of aptamer–rhOPN interactions, which is dependent on the rhOPN concentrations. The CV assays showed a decrease in the current response (Ipa and Ipc) as a consequence of the increase of the rhOPN concentration (**Fig. 4.4.A**). **Fig. 4.4.B** illustrates the ΔI/% values as a function of the rhOPN concentration. The results suggest that the increasing values of ΔI/% with the increase of the rhOPN concentration, in the rhOPN concentration range between 25 nM and 2402 nM, reaching signal saturation near 800 nM. A linear correlation could be established for a dynamic concentration range from 25 nM and 200 nM (ΔI/% = 0.0591(± 0.0007) × [rhOPN, nM] + 1.81(± 0.08), **Fig. 4.4.B**).

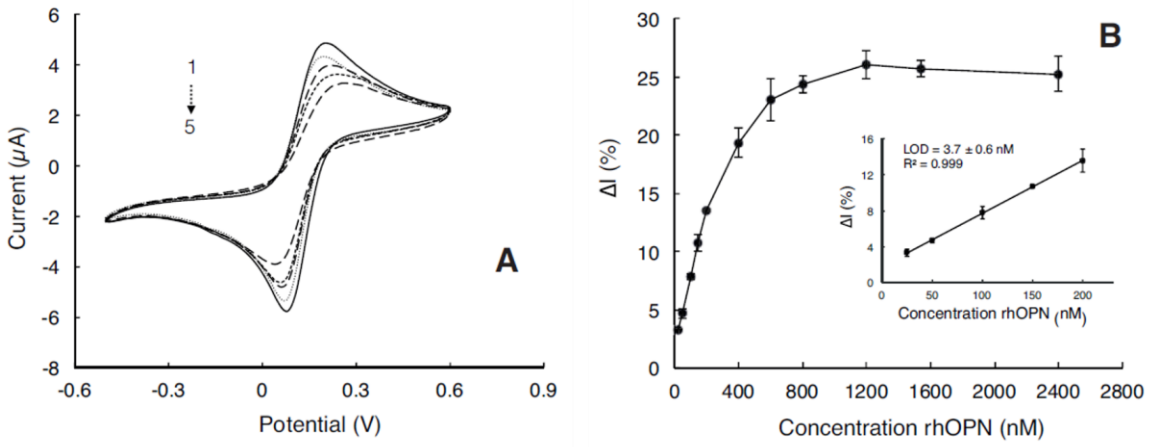

Fig. 4.4. A) CV response for rhOPN detection at different concentrations: (1) RNA aptamer immobilized, (2) 100.1 nM, (3) 200.2 nM, (4) 800.8 nM and (5) 2402.4 nM. B) Electrochemical aptasensor sensitivity analysis of rhOPN using an aptamer-immobilized gold working electrode. Error bars indicate the relative standard deviation of three independent experiments. The insert shows the linear relationship between the ΔI/(%) and the rhOPN concentrations.

The linear correlation coefficient was 0.999 and the calculated detection and quantification limits were 3.7 ± 0.6 nM and 11 ± 2 nM (240 ng/mL and 715 ng/mL, assuming a molecular weight of 65 kDa), respectively. This detection limit was quite improved compared to the preliminary work

presented in chapter 3 (520 ng/mL) (Meirinho et al., 2014), but higher than those previously reported for the detection of human OPN (7.48 ng/mL (Chen et al., 2014) and 10.7 ng/mL (Cao et al., 2014)), obtained using different measurement techniques, type of electrodes and biosensor preparation methodology. Considering the reported range of plasma OPN concentrations in patients with metastatic breast cancer (up to 290 ng/mL) (Bramwell et al., 2014) the proposed aptasensor still could be applied in OPN detection. Also, in the present study, a smaller gold working electrode was used, compared to previous works (Cao et al., 2014; Chen et al., 2014), contributing to the miniaturization of the sensor, as well as the reduction of the amount of reagents and samples' volumes required for the detection. On the other hand, the future application of other voltammetry techniques, such as square wave voltammetry (SWV) and differential pulse voltammetry (DPV), could increase the sensitivity of the proposed analysis. Indeed, the SWV compared to CV is a technique that presents broader dynamic range and lower limit of detection. Also, SWV enables a faster analysis with less consumption of electroactive compounds that DPV, consequently reducing blocking problems of the electrode surface (Dogan-Topal et al., 2010).

Finally, the use of aptamers as bioreceptors instead of antibody or antigen (immunological detection) makes the proposed method less expensive and therefore, an interesting commercial alternative. Additionally, the use of aptamers presents some advantages such as ease and reduced cost of production, as well as the possibility of introducing some chemical modifications to enhance stability, affinity and specificity towards the target. Moreover, aptamers can be immobilized on a large number of transducers surfaces (Balamurugan et al., 2008; Hianik and Wang, 2009; Radi, 2011; Song et al., 2012; S. Song et al., 2008; Strehlitz et al., 2008). On other hand, the possible use of new materials or nanoparticles could contribute to reduce the detection limits, since the electrode surface area could be greatly increased and consequently more aptamers could be immobilized, thus contributing to an increase of the sensitivity and specificity.

4.3.5. Specificity of aptasensor

A highly selective response to the target protein over other non-specific proteins is crucial when developing biosensors. Selectivity is a key factor to evaluate the aptasensor performance. The selectivity test was carried out by measuring and comparing the response of the RNA aptamers to rhOPN and to some other non-specific proteins (THR, BSA, LYS and rbOPN), all at a concentration of 200 nM. The THR was analyzed as a possible interferent because it is a secreted serine protease

found in the blood (Beausileil et al., 2011). The other proteins, though not present in human body fluids were also analyzed. The rbOPN was analyzed because it exhibits a cDNA sequence with high degree of homology with that of rhOPN (Wai and Kuo, 2004). The BSA and LYS were used to analyze if the effect of the proteins molecular weight could affect the detection. For each individual protein determination, different SPGE were used. **Fig. 4.5** illustrates the ΔI/% obtained for rhOPN and also for the non-specific proteins tested.

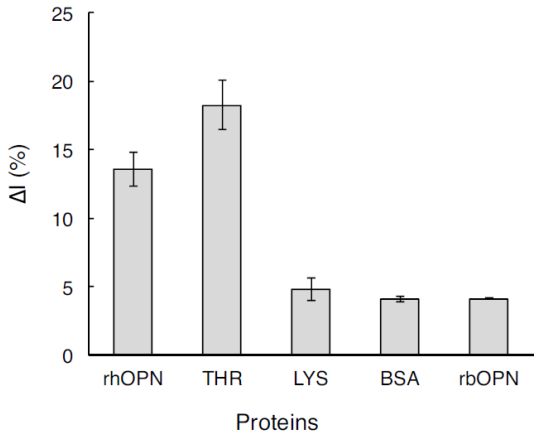

Fig. 4.5. Bar chart of CV response (ΔI/%) to non-specific proteins (200 nM): BSA – bovine serum albumin, LYS – lysozyme, rbOPN – bovine osteopontin and THR-thrombin and for specific-protein rhOPN – human osteopontin. Error bars indicate the relative standard deviation of three independent experiments.

The results showed that the RNA aptamer had a good sensitivity to rhOPN when compared with the proteins BSA, LYS and rbOPN. However, their ΔI/ % values cannot be neglected and a more pronounced response was observed in the presence of THR. Aptamers are described as small single-stranded RNA or DNA with high affinity and specificity for a given target molecule. However, some aptamers can also bind to other molecules presenting similar structures without losing their specificity (Lakhin et al., 2013). The possible aptamer cross-reactivity may explain the results obtained for THR. The rhOPN and THR structures are not similar. Nonetheless, the rhOPN contains several conserved domains including THR cleavage domain RSK site, leading to the breakdown of the protein into two fragments (Beausoleil et al., 2011; Sivakumar and Niranjali Devaraj, 2014). Thus, during the process of RNA aptamer selection, the cleavage of OPN might have occurred, and therefore the RNA aptamer could hold a site that is able to recognize THR. The results obtained

suggest that the RNA aptamer used in this work may have two recognition sites, one for rhOPN and another for THR.

To assess the possible RNA aptamer binding affinity towards THR, fluorescence assays were also performed using the same procedure described in sections 4.2.3 (experimental conditions) and 4.2.4 (mathematical procedure). For FAM-RNA aptamer-THR complex formation, a Kd value of 1.3 nM was obtained for 4 hours of incubation. This result suggests that the RNA aptamer may have a binding site for THR, with a higher affinity than that observed for rhOPN ($Kd_{,THR} < Kd_{,rhOPN}$).

4.3.6. Reproducibility and stability of the aptasensor

To evaluate the reproducibility of the aptasensor, four different SPGEs were prepared in the same day, under the same conditions and tested using a solution with a concentration of 1540 nM of rhOPN. Also, seven other SPGEs were prepared in different days and tested with 200 nM rhOPN. The current response obtained from the aptasensors prepared in the same and different days showed a relative standard deviation (RSD %) of 4.2 % and 5.7 %, respectively, thus suggesting that the aptasensor preparation method was reproducible and precise. The overall experimental results indicate that the aptasensor used in this work had a good reproducibility (RSD % less than 6 %).

The aptasensor stability was also evaluated since this is another important parameter for the practical application of a sensor. To evaluate this parameter, the RNA aptamer half-life was studied. Our results were compared with the ones reported by Mi et al., (2009) and Talbot et al., (2011), that reported half-lives of 8 hours and more than 24 hours for *in vitro* assays and human serum, respectively (Mi et al., 2009; Talbot et al., 2011). The aptasensor stability was evaluated by comparing the ΔI/% of three SPGEs, prepared under the same experimental conditions, and stored during 2, 4, 6, 8 hours and 10 days. When compared with the initial ΔI/% value, the response after 8 hours and 10 days, was still 95 % and 88 %, respectively, showing a satisfactory stability of the aptasensor response along time. This result may explain the difficulty in regenerating the aptamer, even when using different regeneration solutions (e.g. 2 M of NaCl or 7 M of urea).

4.4. Conclusion

This chapter presents a proof-of-principle that the proposed electrochemical aptasensor is a simple and sensitive tool with satisfactory performance, reproducibility and stability for the detection of human OPN. However, the developed aptasensor is not fully specific for the target protein when other interfering species are present. Therefore, further studies are required, namely in the selection of new and more specific aptamers against human OPN, in order to improve its detection performance and selectivity, as well as the implementation of other voltammetric techniques such as square wave voltammetry (SWV) and differential pulse voltammetry (DPV), which are also used in the development of aptasensors.

4.5. References

Ahmed, M., Kundu, G.C., 2010. Mol. Cancer 9, 101–114.

Anborgh, P.H., Mutrie, J.C., Tuck, A.B., Chambers, A.F., 2011. J. Cell Commun. Signal. 5, 111–122.

Arshak, K., Velusamy, V., Korostynska, O., Oliwa-Stasiak, K., Adley, C., 2009. IEEE Sens. J. 9, 1942–1951.

Bache, M., Kappler, M., Wichmann, H., Rot, S., Hahnel, A., Greither, T., Said, H.M., Kotzsch, M., Würl, P., Taubert, H., Vordermark, D., 2010. BMC Cancer 10, 132-148.

Balamurugan, S., Obubuafo, A., Soper, S. a, Spivak, D.A., 2008. Anal. Bioanal. Chem. 390, 1009–1021.

Bang, G.S., Cho, S., Kim, B., 2005. Biosens. Bioelectron. 21, 863–870.

Beausoleil, M.S., Schulze, E.B., Goodale, D., Postenka, C.O., Allan, A.L., 2011. BMC Cancer 11, 25-37.

Bloomfield, V.A., 2014. Using R for Numerical Analysis in Science and Engineering. Chapman & Hall/CRC.

Bramwell, V.H.C., Doig, G.S., Tuck, A.B., Wilson, S.M., Tonkin, K.S., Perera, F., Vandenberg, T.A., Chambers, A.F., 2006. Clin. Cancer Res. 12, 3337–3343.

Bramwell, V.H.C., Tuck, A.B., Chapman, J.-A.W., Anborgh, P.H., Postenka, C.O., Al-Katib, W., Shepherd, L.E., Han, L., Wilson, C.F., Pritchard, K.I., Pollak, M.N., Chambers, A.F., 2014. Breast Cancer Res. 16, R8.

Cao, Y., Chen, D., Chen, W., Yu, J., Chen, Z., Li, G., 2014. Anal. Chim. Acta 812, 45–54.

Centi, S., Sanmartin, B., Tombelli, S., Palchetti, I., 2009. Electroanal. 21, 1309–1315.

Chen, H., Mei, Q., Jia, S., Koh, K., Wang, K., Liu, X., 2014. Analyst 139, 4476–4481.

Dogan-Topal, B., Ozkan, S.A., Uslu, B., 2010. Open Chem. Biomed. Methods J. 3, 56–73.

Ermer, J., Miller, J., 2005. Wiley: New York. Wiley-VCH GmbH and co. KGaA. Weinheim, ISBN: 3-527-31255-2.

Farghaly, O. a, Hameed, R.S.A., 2014. Int. J. Electrochem. Sci. 9, 3287–3318.

Ferlay, J., Soerjomataram, I., Ervik, M., Dikshit, R., Eser, S., Mathers, C., Rebelo, M., Parkin, D.M., Forman, D., Bray, F., 2013. GLOBOCAN 2012 v1.0, IARC CancerBase. No. 11.

Hianik, T., Wang, J., 2009. Electroanal. 21, 1223 – 1235.

Jing, M., Brwser, M.T., Bowser, M.T., 2011. Anal. Chim. Acta 686, 9–18.

Kim, Y.-J., Kim, Y.S., Niazi, J.H., Gu, M.B., 2010. Bioprocess and Biosyst. Eng. 33, 31–38.

Lai, R.Y.R.Y., Plaxco, K.W.K.W., Heeger, A.J.A.J., 2007. Anal. Chem. 79, 229–233.

Lakhin, A. V, Tarantul, V.Z., Gening, L. V, 2013. Acta Nat. 5, 34–43.

Macrì, A., Versaci, A., Lupo, G., Trimarchi, G., Tomasello, C., Loddo, S., Sfuncia, G., Caminiti, R., Teti, D., Famulari, C., 2009. Tumori 95, 48–52.

Meirinho, S.G., Dias, L.G., Peres, A.M., Rodrigues, L.R., 2014. Procedia Eng. 87, 316–319.

Mi, Z., Guo, H., Russell, M.B., Liu, Y., Sullenger, B. a, Kuo, P.C., 2009. Mol. Ther. 17, 153–161.

Mirza, M., Shaughnessy, E., Hurley, J.K., Vanpatten, K.A., Pestano, G. a, He, B., Weber, G.F., 2008. Int. J. Cancer 122, 889–897.

Olowu, R.A., Ndangili, P.M., Baleg, A.A., Ikpo, C.O., Njomo, N., Baker, P., Iwuoha, E., 2011. Int. J. Electrochem. Sci. 6, 1686–1708.

Potty, A.S.R., Kourentzi, K., Fang, H., Jackson, G.W., Zhang, X., Legge, G.B., Willson, R.C., 2009. Biopolymers 91, 145–156.

Radi, A.-E., 2011. Int. J. Electrochem. 2011, 1–17.

Rodrigues, L.R., Lopes, N., Sousa, B., Vieira, D., Milanezi, F., 2009. Open Breast Cancer J. 1, 1–9.

Rodrigues, L.R., Teixeira, J.A., Schmitt, F.L., Paulsson, M., Lindmark-Mansson, H., 2007. Cancer Epidemiol. Biomark. Prev. 16, 1087–1097.

Rudland, P.S., Platt-Higgins, A., El-Tanani, M., De Silva Rudland, S., Barraclough, R., Winstanley, J.H.R., Howitt, R., West, C.R., 2002. Cancer Res. 62, 3417–3427.

Saberian, M., Hamzeiy, H., Aghanejad, A., Asgari, D., 2011. Bioimpacts 1, 31–37.

Sivakumar, S., Niranjali Devaraj, S., 2014. J. Diabetes Metab. Disord. 13, 1-14.

Song, K.-M., Lee, S., Ban, C., 2012. Sensors 12, 612–631.

Song, S., Wang, L., Li, J., Zhao, J., Fan, C., 2008. Anal. Chem. 27, 108–117.

Strehlitz, B., Nikolaus, N., Stoltenburg, R., 2008. Sensors 8, 4296–4307.

Talbot, L.J., Mi, Z., Bhattacharya, S.D., Kim, V., Guo, H., Kuo, P.C., 2011. Surgery 150, 224–30.

Thorat, D., Sahu, A., Behera, R., Lohite, K., Deshmukh, S., Mane, A., Karnik, S., Doke, S., Kundu, G.C., 2013. Oncol. Lett. 6, 1559–1564.

Timur V. Elzhov, Katharine M. Mullen, A.-N.S. and Ben, Bolker, 2013. Minpack. lm: R interface to the Levenberg-Marquardt nonlinear least-squares algorithm found in MINPACK, plus support for bounds. R package version 1.1-8.

Tran, D.T., Janssen, K.P.F., Pollet, J., Lammertyn, E., Anné, J., Van Schepdael, A., Lammertyn, J., 2010. Molecules 15, 1127–1140.

Tuck, A.B., Chambers, A.F., Allan, A.L., 2007. J. Cell. Biochem. 868, 859–868.

Velasco-Garcia, M.N., Missailidis, S., 2009. Gene Ther. Mol. Biol. 13, 1–9.

Velusamy, V., Arshak, K., Korostynska, O., Oliwa, K., Adley, C., 2010. Biotechnol. Adv. 28, 232–254.

Wai, P., Kuo, P., 2008. Cancer Metastasis 27, 103–118.

Weber, G.F., Lett, G.S., Haubein, N.C., 2010. Br. J. Cancer 103, 861–869.

Weber, G.F., Lett, G.S., Haubein, N.C., 2011. Oncol. Rep. 25, 433–441.

Xiao, Y., Lubin, A.A., Heeger, A.J., Plaxco, K.W., 2005a. Angew. Chem. 44, 5456–5459.

Xiao, Y., Piorek, B.D., Plaxco, K.W., Heeger, A.J., 2005b. J. Am. Chem. Soc. 127, 17990–17991.

Xu, Y., Cheng, G., He, P., Fang, Y., 2009. Electroanal. 21, 1251–1259.

Yu, T., Li, J., Liu, Q., Cheng, W., Zhang, D., Ju, H., 2012. J. Electrochem. Sci. 7, 8533–8542.

CHAPTER 5

Electrochemical Aptasensor for Human Osteopontin Detection using a DNA Aptamer Selected by SELEX

A DNA aptamer with affinity and specificity for human osteopontin (OPN), a potential breast cancer biomarker, was selected using an iterative *in vitro* process so-called SELEX (Systematic Evolution of Ligands by Exponential Enrichment). The DNA aptamer exhibited a satisfactory affinity towards human OPN, showing low dissociation constants (2.49 nM and 1.05 nM for 30 min and 4 hours, respectively). It was used to develop a simple, label-free electrochemical aptasensor for the detection of rhOPN. For that purpose, it was immobilized on the surface of a screen-printed gold working electrode via biotin-streptavidin interaction and it was characterized using cyclic and square wave voltammetry. Cyclic voltammetry was used to quantify human OPN in the presence of a $[Fe(CN)_6]^{3-/4-}$ electrochemical probe. Detection and quantification limits of 2.3 ± 0.3 nM (150 ± 20 ng/mL) and 7 ± 1 nM (448 ± 65 ng/mL), respectively, were obtained. The aptasensor showed a good reproducibility and an acceptable selectivity towards human OPN, exhibiting low signal interferences from other proteins, such as thrombin, with quite lower current signals-off (2.6 to 10 times lower than that observed for human OPN). Therefore, the aptasensor herein developed represents a promising alternative for the detection of a protein with relevance for the diagnosis and prognosis of breast cancer.

The information presented in this Chapter was submitted in Biosensors and Bioelectronics:

Meirinho, Sofia G., Dias, Luís G., Peres, António M., Rodrigues, Lígia R. Electrochemical Aptasensor for Human Osteopontin Detection using a DNA Aptamer Selected by SELEX. Biosens. Bioelectron. (submitted in September 2015).

5.1 Introduction

Osteopontin (OPN) is a matricellular protein, expressed by a variety of cell types and found in several biological fluids and tumor tissues (Anborgh et al., 2011; Sase et al., 2012). The human OPN contains around 314 amino acid residues subject to multiple post-translational modifications, thus resulting in a molecular weight range between 41-75 kDa (Anborgh et al., 2011; Tuck et al., 2007; Wai and Kuo, 2008). The OPN is rich in aspartate, glutamate and serine residues. Besides, it contains several functional domains such as arginine-glycine-aspartate (RGD), serine-valine-valine-tyrosine-glutamate-leucine-arginine (SVVYGLR) and the thrombin cleavage site (RSK) (Beausoleil et al., 2011; Gursoy et al., 2010; Scatena et al., 2007; Wai and Kuo, 2008). High levels of OPN in serum or plasma have been detected in people suffering from cancer and may be associated with tumor progression, aggressiveness and metastasis (Ahmed and Kundu, 2010; Bache et al., 2010; Bramwell et al., 2014; Likui et al., 2010; Mirza et al., 2008; Ohno et al., 2010; Rodrigues et al., 2007). Specifically in breast cancer, its overexpression has been related with a decrease of the patients survival rate (Bramwell et al., 2006), as well as with a poor prognosis, disease progression, aggressiveness and metastasis (Bramwell et al., 2014; Ohno et al., 2010; Rodrigues et al., 2007; Weber et al., 2010; Xu et al., 2015). Indeed, OPN has been pointed as a potential biomarker in a number of cancers including breast, ovarian, prostate, lung, liver and colon (Macrì et al., 2009; Ohno et al., 2010; Rodrigues et al., 2007; Tuck et al., 2007; Weber et al., 2011, 2010). Moreover, OPN has been considered as a possible therapeutic target for blocking tumor growth and subsequent metastasis (Anborgh et al., 2009; Mi et al., 2009; Rodrigues et al., 2009). Therefore, the detection of OPN can be used to monitor the disease progression and provide useful information about its prognosis (Anborgh et al., 2011). Commonly, OPN detection in plasma samples is performed through enzyme-linked immunosorbent assay (ELISA). Bramwell et al., (2014), quantified human OPN in plasma samples of patients with metastatic breast cancer using ELISA. The average OPN concentration determined was 46 ng/mL (ranging from 22.6 to 290 ng/mL). Despite the usefulness of ELISA, alternative methods ought to be developed for the detection of OPN at the lower concentrations that are usually found in early stages of the disease. Advances in the biosensors field, namely the possibility of designing new and extremely specific bioreceptors (e.g. aptamers), make them very promising for the detection of low levels of protein biomarkers, such as OPN, in plasma or blood samples (Prieto-Simón et al., 2010; Strehlitz et al., 2008).

Aptamers are short single-strand DNA (ssDNA) or RNA oligonucleotides (20 to 100 nucleotides) that can fold into unique tertiary structures (Kanwar et al., 2010; Stoltenburg et al., 2012). It is possible to isolate aptamers, from a large oligonucleotide library, with high affinity and specificity to a wide variety of targets, ranging from small molecules to large proteins, using the Systematic Evolution of Ligands by Exponential Enrichment (SELEX) methodology (Sett et al., 2012; Ye et al., 2012). This methodology can be used for the isolation of both RNA and DNA aptamers. For the selection of RNA aptamers, the chemically modification of the oligonucleotide library in the 2'-position is necessary to increase its nuclease resistance and also additional steps are required for transcription and reverse transcription. Thereby, the production of RNA aptamers is more expensive, complex and time consuming in comparison with the production of DNA aptamers (Dua et al., 2011; Tombelli et al., 2005). The use of aptamers as bioreceptors in biosensors is gaining an increased interest, especially as alternatives to antibodies, mainly due to their unique features. Aptamers are easy to produce and synthesize; present a good stability over a wide range of pH, temperature and/or storage conditions; are resistant to denaturation and degradation; are amenable to chemical modifications, thus enabling their immobilization in several surfaces; and can be labelled with fluorophores, and other tags facilitating their applications as bioreceptors in biosensors (Hianik and Wang, 2009; Radi, 2011; Song et al., 2012; Strehlitz et al., 2008). The main limitation on the use of aptamers (especially RNA aptamers) as bioreceptors is their susceptibility to degradation by nucleases, which is critical for *ex vivo* and *in vivo* applications (Prieto-Simón et al., 2010; Tombelli et al., 2005). Since, DNA aptamers are usually highly chemically stable than RNA aptamers due to the absence of the hydroxyl group at the 2'-end of the DNA molecules (Marimuthu et al., 2012); and to increase RNA aptamers stability in real samples some chemical modifications have be introduced in the 2' positions of pyrimidine nucleotides such as amino/fluoro groups (Strehlitz et al., 2008).

Mi et al., (2009) described the first RNA aptamer against OPN that was used by Cao et al., (2014) to develop an electrochemical aptasensor using a pyrolytic graphite disk electrode (3.0 mm diameter), functionalized with AuNPs. The human OPN detection limit achieved by SWV was 10.7 ng/mL. The aptasensor high sensitivity could be attributed to the use of nanoparticles that increase the superficial area available for aptamers immobilization (Palchetti and Mascini, 2012). However, these strategies increase the biosensor cost and can affect its reproducibility and performance when complex samples are used (Yu et al., 2012). Recently, a voltammetric aptasensor, based on the same RNA aptamer, was used to detect human OPN in standard solutions (Meirinho et al., 2015).

The proposed electrochemical aptasensor is a simple tool with suitable performance, reproducibility and stability. However, it exhibited a greater detection limit (3.7 ± 0.6 nM). Also, the RNA aptasensor was sensitive to thrombin, a protein that is also present in human blood and serum, which could be a drawback when real samples are used.

Hence, herein it is reported for the first time the isolation and characterization of a high affinity DNA aptamer for human OPN, through SELEX. The binding affinity of the selected DNA aptamer was determined by fluorescence assays. Moreover, this aptamer was used as bioreceptor for the design of a label-free electrochemical DNA aptasensor to detect human OPN.

5.2 Materials and Methods

5.2.1 Material and reagents

Nitrocellulose membranes (0.45 μm) were purchased from Whatman. dNTP mix (containing dATP, dCTP, dGTP, and dTTP (4 mM each)) and Taq DNA polymerase (5 U/μl) were obtained from New England Biolabs. TOPO TA cloning Kit was acquired from Invitrogen. GRS Plasmid Purification Kit was purchased from Grisp Research Solutions. Kieselgur, sodium acetate, urea were obtained from Sigma-Aldrich. 3,3-dithiodipropionic acid (DPA), N-(3-dimethylaminopropyl)-N-ethylcarbodiimide hydrochloride (EDC), N-hydroxysuccinimide (NHS), ethanolamine (ETA) and sulfuric acid (purity = 99.999 %) were obtained from Sigma-Aldrich. Potassium hexacyanoferrate (III) [$K_3Fe(CN)_6$] and potassium hexacyanoferrate (II) [$K_4Fe(CN)_6$] were obtained from Acros Organics and potassium dihydrogen phosphate (KH_2PO_4) from Merck. Sodium chloride (NaCl), potassium chloride (KCl), sodium hydrogen phosphate (Na_2HPO_4) and Ethanol were acquired from Panreac. Recombinant human osteopontin (rhOPN, 65 kDa, p/= 3.5) and recombinant bovine osteopontin (rbOPN, 60 kDa, p/= 3.59 – 4.46) were purchased from R&D Systems. Thrombin from human plasma (THR, 37.4 kDa, p/7 - 7.6), bovine serum albumin (BSA, 66 kDa, p/= 4.7), lysozyme from chicken egg white (LYS, 14.3 kDa, p/= 10 - 11) and streptavidin were obtained from Sigma-Aldrich.

5.2.1.1 Solutions

All solutions were prepared using Milli-Q grade water (18.2 MΩ) purified by a milli-QTM system (Millipore). Phosphate buffer saline (PBS) solution (137 mM NaCl, 2.7 mM KCl, 8.1 mM Na_2HPO_4 and 1.47 mM KH_2PO_4) with an adjusted pH 7.6 was used for the selection/isolation and characterization of the DNA aptamer and with pH 7.4 for the development of the electrochemical aptasensor. A solution of urea (7 M) was prepared in PBS buffer pH 7.6 (elution buffer). EDC (200 mM) and NHS (100 mM) stock solutions were prepared and stored at -20 °C until use. Stock solution of streptavidin (1 mg/ml) was prepared in PBS (pH 7.4) and stored at -20 °C. The ferro/ferricyanide redox probe (5 mM $K_3Fe(CN)_6$ and $K_4Fe(CN)_6$ (1:1) and 10 mM KCl in 100 mL of PBS), with an adjusted pH of 7.4, was daily prepared. Stock solutions of rhOPN protein were prepared according to the manufacturer specifications and stored at -20 °C. The protein working solutions were obtained by adequate dilutions with PBS buffer (pH 7.6) and stored at 4 °C until use. Before the fluorescence assays and immobilization on the gold working electrode, the DNA aptamer was subjected to a temperature treatment (95 °C during 5 min; 4 °C for 5 min and 10 min at room temperature) to obtain an adequate structure flexibility of the aptamer.

5.2.1.2. ssDNA library, primer and aptamer sequences

A 70-base random single-stranded DNA (ssDNA) library purified by polyacrylamide gel electrophoresis (PAGE) and the primer-binding sites were synthesized by Alfagene (Portugal). Each sequence of the library contains a central region of 30 random nucleotides (nt) flanked by two 20 nt primer hybridization sites (5'- GGG GGT GGT ACC AGA GAT GC - N_{30} - CAG AGA GGA GGT ACC GTG GG-3'). A forward primer (5'- GGG GGT GGT ACC AGA GAT GC-3') and a reverse primer (5'- CCC ACG GTA CCT CCT CTC TG-3') were used in the PCR amplification of the selected aptamer pool. The DNA aptamer used to design the aptasensor possesses 30 nt and was isolated through SELEX. The selected DNA aptamer sequence was modified with 6-carboxyfluorescein (5'-6-FAM- TGT GTG CGG CAC TCC AGT CTG TTA CGC CGC-3') and biotinylated in the 5'-end (5'-Biotin-TGT GTG CGG CAC TCC AGT CTG TTA CGC CGC-3'). These modified sequences were provided by Integrated DNA Technologies (Belgium).

5.2.1.3. Apparatus and electrodes

The pH was measured using a pH meter (iHANNA instruments pH 211). ssDNA and DNA plasmid were quantified using a Nanodrop 1000 (Thermo Scientific). The fluorescence measurements were conducted in 96-dark-well plates using an ELISA reader (Synergy HT, BIO-TEK, IZASA) equipped with thermostat holding temperature control (accuracy of ± 0.1 °C) and filters configured to a wavelength of 492 nm for excitation and 518 nm for emission. The Gen5™ data analysis software was used for collecting microplate data. Electrochemical measurements were carried out at room temperature with a Potentiostat-Galvanostat device (PG580, Uniscan Instruments). Screen printed gold electrodes (SPGEs) were purchased from Dropsens (Spain) and consisted in a three-electrode system with a gold working electrode (diameter of 0.8 mm), a gold counter or auxiliary electrode and a silver pseudo-reference electrode.

5.2.2. SELEX methodology

The selection of aptamers able to specifically bind rhOPN demands several cycles of binding, partitioning/separation, target-bound elution/enrichment, and amplification (Hoinka et al., 2012; Stoltenburg et al., 2012). Usually 10 to 15 iterations are necessary to isolate one or few aptamers that possess the highest affinity and specificity to the desired target (Szeto et al., 2013). The process starts with the synthesis of a random ssDNA library with a large number of unique sequences to increase the probability of some sequences being able to interact with the protein (previously immobilized on a Kieselgur support) with high affinity and specificity (Ye et al., 2012). For the protein immobilization, Kieselgur (25 mg) was used in each cycle. Before immobilization, this support was washed three times with PBS buffer (pH 7.6) and centrifuged at 13500 rpm during 5 min. Decreasing rhOPN concentrations were used depending on the selection cycle: 154 nM for the 1st to the 4th cycle; 77 nM for the 5th to the 8th; and 38 nM for the last two cycles. The pre-washed Kieselgur support was inoculated with the adequate rhOPN concentrations for 6 hours at 37 °C with gentle agitation (130 rpm). Then, it was washed three times with PBS buffer (pH 7.6) and centrifuged at 13500 rpm for 5 min. To confirm the success of the immobilization step, the supernatant was collected and analyzed by PAGE. The Kieselgur support with immobilized rhOPN was dried at 37 °C (≈ 18 hours) and was then ready to inoculate with the ssDNA library. In each selection cycle, the ssDNA pool was prepared as follows. First, the ssDNA pool in PBS buffer (pH 7.6) was denatured (heating to 95 °C for 5 min) and then immediately cooled to 4 °C for 15 min, and finally kept at room

temperature for 5 min. Second, the re-natured ssDNA pool was filtered through a 0.45-µm nitrocellulose filter to remove all filter-binding molecules (negative selection). Afterwards, the ssDNA library (1st cycle) or the DNA bound rhOPN (2nd to 9th cycle) was incubated with the immobilized rhOPN. These DNA samples contained approximately 5 µM in the 1st cycle; 7 µM in the 2nd to the 5th cycles; 3 µM in the 6th to the 9th cycles; and 1 µM in the 10th cycle. Following 4 hours of incubation with the rhOPN (37 °C and 130 rpm), three washing steps with PBS buffer (pH 7.6) (centrifuged at 13500 rpm during 5 min) were performed to remove the unbound ssDNA. The bound ssDNA was eluted using a urea solution (7 M) and heat treatment (95 °C for 5 min) twice. The eluted ssDNA was precipitated by adding one-tenth volume of sodium acetate (0.3 M final concentration) and 2.5 volumes of 95 % ethanol; centrifuged at 13500 rpm, at 4 °C for 5 min, and the pellet was washed twice with 70 % ethanol. The recovered ssDNA was then amplified by PCR, ethanol-precipitated (as described above), and separated into single-stranded sequences using thermal denaturation (95 °C for 10 min) for the next selection cycle. The final concentrations used in the PCR reaction were as follows: PCR buffer (1x), dNTP mix (200 µM), forward primer and reverse primer (0.4 µM each), ssDNA pool (10 - 100 ng/µL), and Taq DNA polymerase (2.5 U/µL). The initial denaturation step was conducted at 95 °C for 90 s, proceeded by 30 cycles (denaturation, annealing and extension) at 95 °C for 1 min, 53 °C for 30 s and 72 °C for 30 s, followed by a final extension at 72 °C for 2 min and then temperature was lowered to 4 °C. The recovered ssDNA pool from the 10th cycle of selection was cloned with the TOPO TA Cloning kit. Nineteen colonies were randomly picked, purified and sequenced. Plasmids were purified using the GRS Plasmid Purification Kit and were sequenced at Macrogen Corporation (The Netherlands). The secondary structure analysis of the isolated aptamers was established using the MFold online available tool (http://mfold.rna.albany.edu/?q=mfold/DNA-Folding-Form) setting up the conditions NaCl (0.146 M) at 37 °C (Zuker, 2003).

5.2.3. Determination of the isolated DNA aptamer affinity to rhOPN

The DNA aptamer C10K2 modified with 6-carboxyfluorescein (FAM) in the 5'-end was subjected to heat treatment (95 °C during 5 min, 4 °C for 5 min and 10 min at room temperature) before each fluorescence assay. Initially, different concentrations of FAM-DNA aptamer were used to determine the contribution of the free aptamer to the overall fluorescence and to later estimate its concentration in the aptamer-protein complex studies. The DNA aptamer concentrations (varying from 2.5 to 100 nM) were stored/incubated for 30 min or 4 hours at room temperature. Afterwards, these solutions

were excited at 492 nm and the fluorescence was measured at 518 nm. These assays allowed establishing the calibration curves that relate the fluorescence intensity and FAM-DNA aptamer concentrations for both incubation times. To determine the fluorescence intensity of the aptamer-protein complexes, the FAM-DNA aptamer concentration was fixed by varying the rhOPN concentrations. In each fluorescence assay, 60 µL solution of FAM-DNA aptamer (20 nM) were incubated with the same volume of different concentrations of rhOPN (0, 3, 10, 22, 100, 300, 370 nM) prepared in the same buffer (Potty et al., 2009; Tran et al., 2010), in 96-dark-well plates. The mixtures were incubated at room temperature for two different incubation times. The mixture was excited at 492 nm and the fluorescence was measured at 518 nm. The analysis of the fluorescence data and the confirmation of the aptamer-rhOPN complex formation by means of dissociation constant (*Kd*) estimation was performed as previously described (Meirinho et al., 2015). To establish the specificity of the isolated DNA aptamer towards the desired target (i.e. rhOPN), the same affinity assays were conducted using other proteins (THR, rbOPN and BSA).

5.2.4. Development of the DNA aptasensor

The DNA aptasensor was developed according to the procedure described by Meirinho et al., (2015) Briefly, it includes the cleaning and functionalization with streptavidin and immobilization of the isolated DNA aptamer onto the working electrode surface via streptavidin-biotin interaction, followed by the incubation of the rhOPN protein with the aptamer (**Fig. 5.1**).

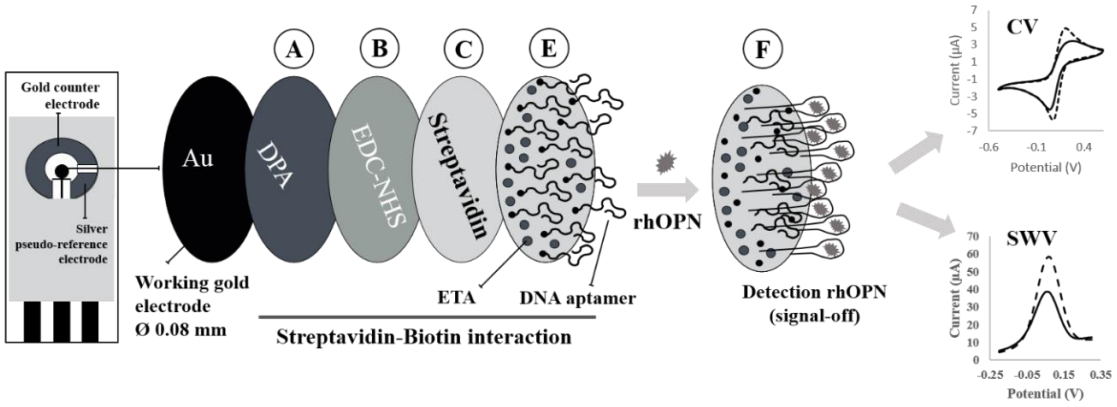

Fig. 5.1. Schematic representation of the construction of electrochemical aptasensor and the principle of rhOPN detection. A) SPGE-self-assemble monolayer, B) activation carboxyl groups, C) Binding amine group of streptavidin, D) blocking step with ETA, E) immobilization of DNA aptamer, and F) rhOPN binding event and detection by cyclic voltammetry (CV) and square-wave voltammetry (SWV).

5.2.4.1. Cleaning and functionalization of the working electrodes

The electrode was electrochemically cleaned by a series of oxidation and reduction cycles using three solutions (H_2SO_4 (0.5 M), KCl (0.01 M)/H_2SO_4 (0.1 M) and H_2SO_4 (0.05 M)), under a potential range between -0.3 and +1.5 V at a scan rate of 100 mV/s until a representative cyclic voltammogram of a clean gold electrode was obtained. To functionalize the cleaned working electrode surface for the DNA aptamer immobilization, the electrode was incubated with DPA during 30 min at room temperature and then rinsed with deionized water for 1 min. The carboxylic groups of the self-assembled monolayer formed were activated with EDC and NHS (1:1 v/v) during 60 min at room temperature. Then, the working electrode surface was exposed to a streptavidin solution overnight at 4 °C, enabling the binding of the amine groups. Finally, the functionalized working electrode surface was exposed with ETA during 20 min at room temperature to block any remaining active carboxyl groups.

5.2.4.2. Immobilization of the DNA aptamer and interaction with the protein

Prior to the immobilization, the DNA aptamer solution prepared in PBS buffer was subjected to heat treatment (95 °C during 5 min, 4 °C for 5 min and 10 min at room temperature) to obtain an adequate flexible aptamer structure for interacting with the streptavidin on the working electrode surface. Then, the DNA aptamer (5 µL, 4 nM) was placed on the cleaning working electrode, followed by a rinsing step with PBS buffer (pH 7.4) to remove the unbound DNA aptamer. Next, rhOPN (5 µL, 1540 nM) was dropped on the working electrode and kept during 60 min (incubation time) for enabling the formation of aptamer-protein complex. After that, the electrode surface was washed with PBS solution to remove the unbound protein.

5.2.4.3. Optimization of the aptasensor

Different concentrations of DNA aptamer were evaluated to optimize the electrode surface coverage with aptamers towards an improvement of the detection sensitivity. SPGEs aptasensors were prepared with different concentrations of DNA aptamer (4 nM, 0.1 µM, 0.5 µM and 1 µM) at an incubation time of 40 min and RT. Afterwards, the surface of the SPGE was washed with PBS buffer and incubated with rhOPN (1540 nM).

Additionally, the incubation time of the aptamer with the protein was studied in order to optimize the formation of the aptamer-protein complex. All SPGEs were prepared using a fixed aptamer

concentration of 4 nM and of 1540 nM rhOPN at room temperature. The incubation times studied were 15, 30, 60 and 120 min.

5.2.4.4. Sensitivity of the DNA aptasensor

The sensitivity of the aptasensor was evaluated using rhOPN solutions prepared by serial dilutions in PBS at pH 7.4. The concentrations tested were 25, 50, 100, 200, 400, 801 and 1540 nM. Several SPGEs modified with DNA aptamer (4 nM) were incubated with different rhOPN standard solutions during 60 min at room temperature. The sensitivity of aptasensor was evaluated through the calculation of the detection limit (LOD) and quantification limit (LOQ), based on the linear relationship obtained between relative current change ($\Delta I/\%$) values of the oxidation peak current and the different rhOPN concentrations through the equations LOD = 3 x SD/b and LOQ = 10 x SD/b, respectively, where SD is the standard deviation of the intercept and b is the average slope of the regression line (Ermer and Miller, 2005).

5.2.4.5. Evaluation of the DNA aptasensor

The specificity, stability, repeatability and reusability of the aptasensor were analyzed by CV. The specificity of the aptasensor was established by measuring and comparing the response of the DNA aptamer to rhOPN and to other non-specific proteins with different molecular weights (MW) and isoelectric points (p*I*). Different SPGE modified with DNA aptamer (4 nM) were tested with each individual protein, all at a concentration of 200 nM. The non-specific proteins tested include BSA, THR, LYS and rbOPN. The stability of the aptasensor was investigated over time during 20 days by using three SPGE modified with 4 nM DNA aptamer and further incubated with 1540 nM rhOPN. The aptasensor was stored at 4 °C and subjected to electrochemical measurements every 5 days. The reproducibility of the aptasensor was studied at a rhOPN concentration of 200 nM and 1540 nM using five different SPGE prepared in different days and three different SPGE prepared in the same days. The reusability of the aptasensor was evaluated through the analysis of successive cycles of regeneration of the binding surfaces. To regenerate the aptasensor, NaCl (2 M) and urea (7 M) were evaluated. Three different SPGE modified with DNA aptamer were incubated with rhOPN (1540 nM), then incubated with the regenerate reagent (2 min at room temperature) and then again incubated with rhOPN for 5 times. The cyclic voltammogram was recorded before and after the incubations with the regeneration reagent.

5.2.4.6. Electrochemical measurements

All electrochemical measurements were performed at room temperature, using $[Fe(CN)_6]^{3-/4-}$ solution (60 µL) as electrochemical probe, dipping them the three electrodes. The electrochemical analysis was performed using CV and SWV. The CV was used in all stages of the development of the aptasensor using a potential range of -0.5 to 0.6 V and with a scan rate of 50 mV s^{-1}, while SWV was only used to confirm the electrochemical behavior after each preparation step of the aptasensor development using the following conditions: amplitude 50 mV; potential range -0.5 V to 0.6 V; scan increment 5 mV and frequency 100 Hz.

In both techniques, the decrease in peak current was calculated based on the relative current change (ΔI %) considering the oxidation peak current values obtained after aptamer immobilization and protein incubation of the cyclic and SWV voltammograms recorded using the equation (5.1):

$$\Delta I\% = (I_0 - I_1)/I_0 \times 100 \quad (5.1)$$

where ΔI is relative current change (%); I_0 and I_1 represents the current before and after the sample incubation, respectively.

5.3. Results and Discussion

5.3.1. Isolation of DNA aptamers against rhOPN

In the current work, 10 selection cycles were conducted. The bound aptamers sequences were cloned in the vector pCR2.1-TOPO and 19 clones were isolated and sequenced. These aptamers can potentially be used as bioreceptors for the development of OPN aptasensors. The sequences of the isolated aptamers are typically examined taking into account their homology, lowest Gibbs energy and ability to form stable secondary structures considering the aptamer full-sequence (70 nucleotides (nt)) or the random region (30 nt). All the 19 DNA aptamer sequences exhibited a variable region with 30 nt (**Table 5.1**). These sequences were further aligned based on the common trinucleotide sequence (TGT) and were classified into seven groups taking into account their homology. Although the clones C10K9, C10K3 and C10K5 only presented a partial TG nucleotide, given their homology with the group (inserted in groups II, III and V, respectively), they were included in the analysis (**Table**

5.1). Since the trinucleotide was not found in the constant regions of the sequences, these regions were not considered in the analysis. Sequences C10K2, C10K12, C10K5 and C10K20 present a higher homology compared to sequences of the same group. The sequence C10K2 exhibits 80 % of homology with the clones C10K1 and C10K10. The aptamer sequences can be analyzed using the MFold online tool (Zuker, 2003). This tool predicts their potential secondary structures calculating the lowest Gibbs free energies and the number of structures that can be formed using the same conditions as those used for the selection. As previously mentioned, aptamers are short single-stranded oligonucleotides that are able to bind their target molecules with high affinity and specificity. Binding occurs due to their specific and complex three-dimensional shapes that are characterized by stems, loops, bulges, hairpins, pseudoknots, triplexes, or quadruplexes. The aptamer-target binding is the result of structure compatibility, stacking of aromatic rings, electrostatic and van der Waals interactions, hydrogen bonding, or a combination of these effects (de-los-Santos-Álvarez et al., 2008; He et al., 2011; Lönne et al., 2014; Stoltenburg et al., 2007; Strehlitz et al., 2012). **Table 5.1** also shows the lowest Gibbs free energy values calculated taking into account both the random (30 nt) and full sequence with conserved regions (70 nt) for all the DNA aptamers isolated. The sequences exhibiting higher Gibbs free energy values (ΔG) (i.e. lower stability) and with multiple possible secondary structures were not chosen for further characterization. Moreover, although the sequences C10K2, C10K7, C10K3, C10K5, C10K9, C10K15 and C10K18 exhibited the lowest ΔG values in the analysis with 70 nt, multiple structures could be formed. Analyzing only the random region (30 nt), the sequences with the lower ΔG values were C10K2, C10K7 and C10K15 and these were found to form a stable secondary structure **(Appendix A1)**. On the other hand, the sequence corresponding to the constant regions could be involved in the aptamers functional secondary structure conferring it stability (Kim et al., 2013; Ozer et al., 2014), thus an analysis comprising these regions was also conducted. When adding parts of the conserved region to the random region it was found that only the sequences C10K2, C10K7, C10K15 and C10K18 presented an increase in the ΔG value (-4.41 (35 nt), -3.18 (50 nt), -2.65 (35 nt) and -3.92 (40 nt) Kcal/mol, respectively) and the formation of a single secondary structure **(Appendix A2)**.

Table 5.1. Nucleotide sequences of the clones obtained from the 10th cycle of selection. The sequences listed correspond to the 30 nucleotides random region (30 nt) of each ssDNA aptamer isolated. The regions were aligned based on the TGT trinucleotide.

Clone Name	Variable region (5' to 3')	Homology (%)	Full *vs* random aptamer sequence 70 nt / 30 nt	
			Possible structures	*ΔG* (Kcal mol^{-1})
	Group I			
C10K1	GAAGT–CGGTCTAT–ATGTCTGTACGGCCATC	67	2 / 5	-2.81 / 0.62
C10K2	T–G–TGTGCGG–CACTCCAGTCTGTTACGCCG–C	80	4 / 1	-4.89 / -4.21
C10K10	TCGTTGTGTCGTTGCTAAAGACTGTGGCTC	63	3 / 3	-3.99 / -0.02
	Group II			
C10K9	GGGACGGTTTAGACGTTG–GTCTTGGCTTGC	57	1 / 2	-4.31 / -1.49
C10K4	ATATCCTATGGATGATGATCTAG–TGTGTCC	60	3 / 1	-2.15 / -0.80
C10K12	GGGTTGG–TGGGCGTCTAGTTGTGCCTTGAC	70	4 / 1	-3.01 / -1.20
	Group III			
C10K3	GTGCAGGTGAAATACTTG–CCGTTTCCTCAC	63	3 / 1	-4.07 / -1.54
C10K16	CACTCA–GTAGTAGAGTTGTCCCTA–AGGCCC	63	7 / 3	-2.29 / -0.50
C10K17	CCAGCA–GTGATT–GGATTGTCGGTGGTGTGTC	63	5 / 1	-3.04 / -1.96
	Group IV			
C10K7	CATAAC–ACGGTAATTGTGTGAACCGCTGTG	53	2 / 2	-3.66 / -2.06
C10K11	GCCCCGTGGCAGAATGTGTTTGGTGGTGTG	53	4 / 1	-2.43 / -1.55
C10K6	TGCTGTGTGTGTCAGGCCATGTTTCGTGTC	50	5 / 3	-1.08 / 0.17
	Group V			
C10K20	TGCTACAACACTTGGAATGTCACGCTGGTC	73	9 / 3	-1.19 / -0.01
C10K14	AGGTAGGTCTACTG–TATGT–AT–G–TGC–CTGCC	57	1 / 4	-3.18 / -0.49
C10K5	GCAAGCCCACCATCAGTAATG–G–CGTTGGTC	77	2 / 2	-4.58 / -1.66
C10K15	GGGACCAAGGCTAACCACTGTGGCCC	60	2 / 1	-5.03 / -2.64
	Group VI			
C10K8	CACT–ATG–CTGTCCGTTCTAGTCTTGCTGCC	67	1 / 4	-2.38 / 0.40
C10K18	CA–TCACCTCTGTCAGAGTAAGTGG–ACTCTC	67	3 / 2	-4.48 / -1.26
C10K22	TG–TGCATGT–AGGCTTCCCCTATACCGTTTAC	47	2 / 2	-3.42 / -0.70

[a] Aptamers selected by Systematic Evolution of Ligands by Exponential enrichment (SELEX). [b] MFold program was used to calculate the Gibbs free energy (*ΔG*) (Kcal/mol), number of predicted structure using [Na^+] = 0.146 mol/L, [Mg^{2+}] = 0 mol/L and 37 °C. [c] The percentage of homology was estimated as the ratio between the number of highlighted nucleotides and the length of the random region. The gaps shown here are indicated by hyphens.

In the stem-loop structure of this sequence, it could be observed the common trinucleotide (TGT), thus suggesting that this trinucleotide could be involved in the specific binding site to the rhOPN protein. Therefore, the C10K2 clone sequence was chosen for the following studies since it showed the lowest ΔG value and the same stable stem-loop secondary structure taking into account the analysis using 70 nt, 30 nt and 35 nt of the whole isolated and identified sequence (**Fig. 5.2**).

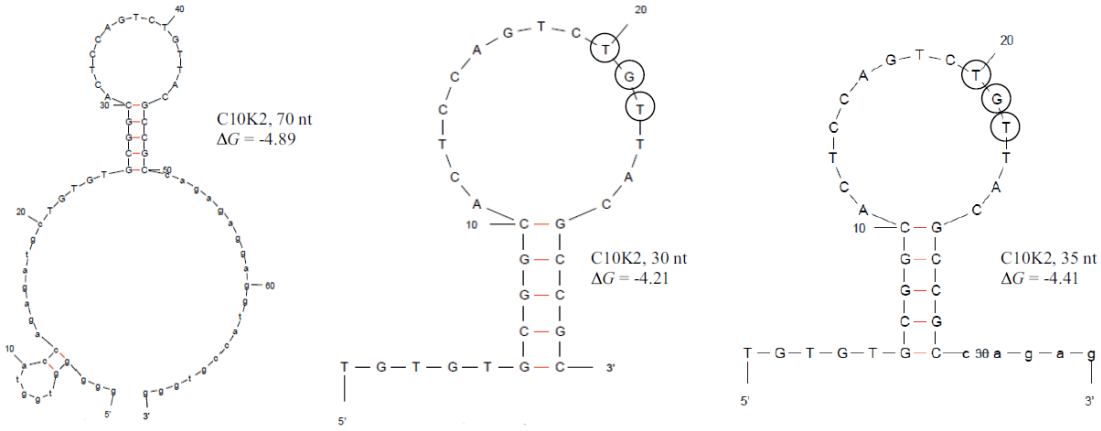

Fig. 5.2. Secondary structure of the selected DNA aptamer. The DNA aptamer sequence of C10K2 with 70, 30 and 35 nucleotides were analyzed using the MFold software. The operational conditions considered were a temperature of 37 °C and a Na^+ concentration of 0.146 M. The resultant stem-loop secondary structures with the lowest free energy folding are shown. The conserved regions are displayed in lowercase.

Stem-loop structures are important as binding regions of the DNA or RNA aptamers to their targets and the consensus motifs are often located in these structures (Stoltenburg et al., 2007). To date, only one RNA aptamer presenting a stem-loop secondary structure was reported to specifically recognize OPN (Mi et al., 2009). RNA is considered more reliable for aptamer identification, since structures are more diverse than those obtained with DNA, mainly due to the presence of 2'-OH group and non-Watson–Crick base pairing in RNA. RNA aptamers are more flexible than the DNA molecules and can offer a wider range of conformational diversity. However, as previously mentioned, RNA is more susceptible to nuclease degradation, which can restrict its use in the presence of biological fluids. On the other hand, the DNA aptamers are considered naturally more robust than RNA aptamers due to the absence of the hydroxyl group at their 2'-end (Marimuthu et al., 2012), displaying high stability for biological applications (Dua et al., 2011; Kim et al., 2013; Ruigrok et al., 2011; Tombelli et al., 2005).

5.3.2. Determination of the isolated DNA aptamer affinity to rhOPN

Aptamers show high affinity for their target with dissociation constants typically ranging from the low micromolar to high picomolar levels (Labuda et al., 2010; Jing et al., 2011; Kim et al., 2013). The determination of the aptamer-protein interaction is very important for the clinical application of aptamers. The fluorescence binding assays are suitable methods for determining the dissociation constants of aptamer-protein complexes, and are very simple methods that only require the modification of the aptamer with a fluorescent dye molecule (Fang et al., 2001; Tran et al., 2010).

The dissociation constant (*Kd*) of the isolated DNA aptamer (C10K2) was determined taking into account the fluorescence intensity of the free aptamer and the aptamer-protein complex formed, using the method previously described by Meirinho et al., (2015). The DNA aptamer (C10K2) was modified with 6-carboxyfluorescein (FAM). The fluorescence intensity of the free aptamer was measured at increasing concentrations of FAM-DNA aptamer in solution. **Fig. 5.3.A** shows the two calibration curves established for the incubation time of 30 min and 4 hours, respectively. The calibration curves obtained at the two time periods for the free aptamer were similar. The fluorescence intensity of the aptamer-protein complex was measured after the aptamer inoculation with different rhOPN concentrations. The total fluorescence of the aptamer-protein complex formed *versus* the rhOPN concentration is plotted in **Fig. 5.3.B**. As can be inferred, the fluorescence increased with increasing rhOPN concentrations for the two abovementioned incubation periods. Moreover, it was found that the total fluorescence was greater for the assays in which 4 hours of incubation was used, thus proving an increased formation of the aptamer-protein complex. However, 30 min of incubation was sufficient to obtain an aptamer-protein interaction. These results suggest that the total fluorescence is due to both non-bound aptamer and aptamer-rhOPN complex. Therefore, assuming that only one aptamer-rhOPN high affinity-binding site, *Kd* values of 2.5 and 1.1 nM were estimated for 30 min and 4 hours, respectively. The relative standard deviation (RDS) of three experiments was lower than 5 % for the two incubation periods, demonstrating that the DNA aptamer has a high affinity for rhOPN for both incubation periods studied.

To confirm the specificity of DNA aptamer for rhOPN, the same fluorescence experiments were conducted with other proteins (THR, BSA and rbOPN). In these experiments, 20 nM of DNA aptamer was incubated with different concentrations of THR, BSA and rbOPN for 30 min and 4 hours, respectively. No titration curves could be obtained using the total fluorescence measured after

interaction of the DNA aptamer with those proteins and so, it was not possible to estimate the respective dissociation constants. Thus, it can be concluded that the DNA aptamer exhibits high specificity for rhOPN.

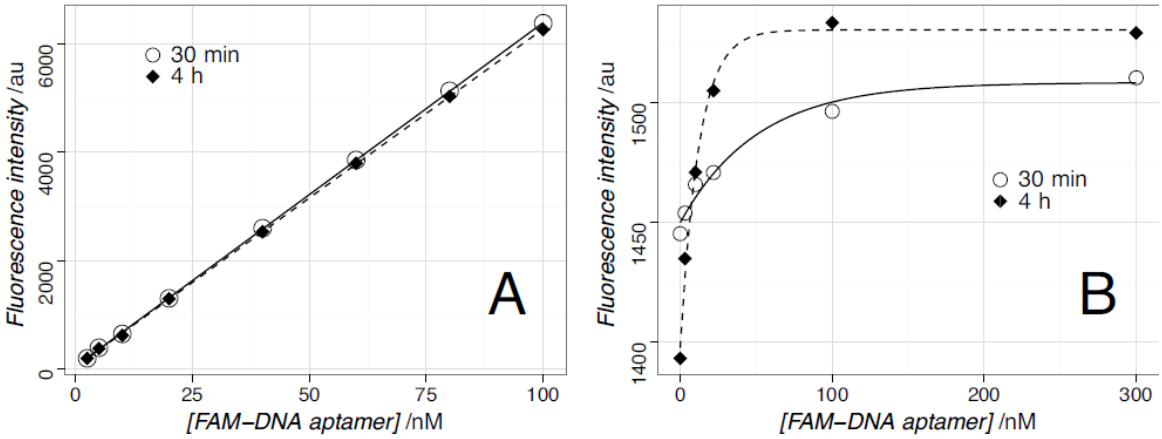

Fig. 5.3. Fluorescence assays. (A) Calibration curves of FAM-DNA aptamer for two incubation times (30 min and 4 hours), and (B) Titration curve of FAM-DNA aptamer with increasing rhOPN concentrations in PBS buffer pH 7.6 at 30 min and 4 hours. The concentration of the DNA aptamer was 20 nM.

5.3.3 Optimization of the experimental conditions for the development of the aptasensor

Several experimental conditions were optimized to improve the aptasensor sensibility and specificity. The success of an aptasensor greatly depends on an efficient immobilization of the biotinylated aptamer onto the small gold working electrode (0.8 mm diameter). To evaluate this effect, different aptamer concentrations were used to obtain different electrode surface coverages, allowing evaluating its effect on the rhOPN detection. The optimal concentration of DNA aptamer to be immobilized onto the working electrode surface, as well as the best incubation time for enhancing the rhOPN interaction with the surface-bound aptamer were evaluated as previously described (Meirinho et al., 2015). **Fig. 5.4.A** shows the $\Delta I/\%$ obtained for the electrodes with different aptamer concentrations and after the incubation with rhOPN. The results demonstrate that the highest $\Delta I/\%$ values were obtained when the SPGE were modified with an aptamer concentration of 4 nM. For the higher aptamer concentrations, a decrease of the $\Delta I/\%$ values was observed. In another study, in which a RNA aptamer was used with the same SPGE, this concentration was also the one that led to

the best results. Therefore, these results suggest that for small working gold electrodes, an aptamer concentration of 4 nM is adequate to achieve a high coverage of the electrode surface.

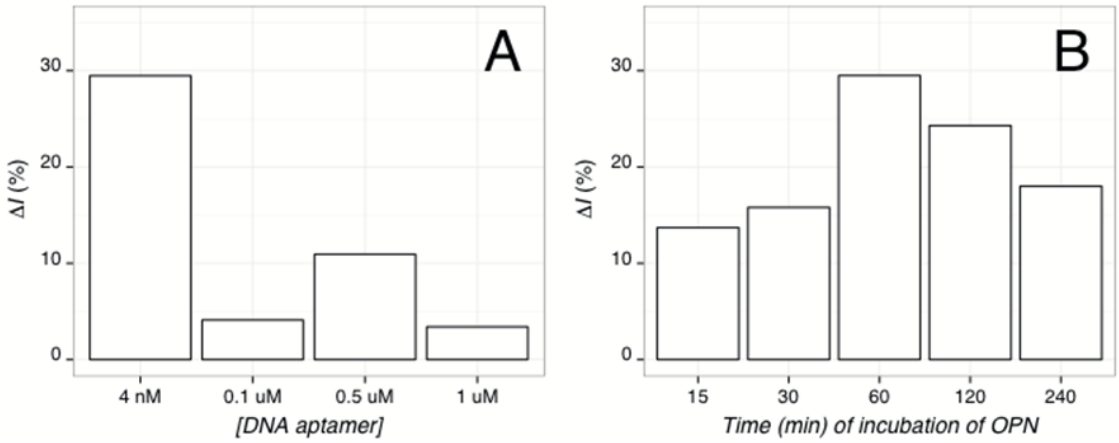

Fig. 5.4. A) Optimization of the biotinylated DNA aptamer concentration. B) Effect of the incubation time of the rhOPN solution.

The incubation time of the DNA aptamer with rhOPN was also optimized. For that purpose, the SPGE modified with DNA aptamer was incubated with 1540 nM of rhOPN for different time points. The *ΔI* % increased sharply and tended to a steady value after 60 min with increasing incubation times. Longer incubation times did not markedly improve the response (**Fig. 5.4.B**). Hence, 60 min was chosen as the optimal incubation time for the formation of the aptamer-protein complex.

5.3.4 Characterization of DNA aptasensor

The CV is a simple, sensitive and convenient technique that gives an overall information regarding the reversibility of the oxidation and reduction mechanisms that occur at the electrode surface (Farghaly and Hameed, 2014). This electrochemical technique may be used as a quality control tool allowing monitoring the effectiveness of the working electrode surface modification and establishing the typical cyclic voltammogram. If in any of the preparation steps, the cyclic voltammogram was distinct from the typical cyclic voltammogram, then the SPGE was discarded. Likewise, the SWV was used to evaluate the changes of the electrode behavior after each preparation step of the aptasensor development. The SWV enables a fast analysis with excellent sensitivity, usually higher than that of the CV (Li et al., 2011). The **Fig. 5.5** illustrates the voltammograms obtained by CV (**Fig. 5.5.A**) and

SWV (**Fig. 5.5.B**) analyzes after each step, using a 5 mM solution of $[Fe(CN)_6]^{3-/4-}$ as an electrochemical probe. The voltammograms profiles for CV and SWV showed a similar order of peak current intensities for all the biosensor's preparation steps, thus evidencing that both techniques are adequate to monitor the electrochemical changes occurring during the preparation of the electrode surface. However, since SWV (**Fig. 5.5.B**) is more sensitive than CV (**Fig. 5.5.A**), the differences observed in the plots for each step using SWV are more pronounced. The maximum current intensities of all SWV voltammograms were recorded at a potential range from 0.06 to 0.075 V. **Table 5.2** summarizes the electrochemical parameters obtained after each electrode surface preparation step, namely the potential variation between cathodic and anodic peaks (ΔEp), the cathodic peak current value (Ipc) and anodic peak current value (Ipa) calculated using the cyclic voltammograms and the peak current (Ip) calculated using the forward and reverse current the SWV voltammograms. The results shown correspond to the mean values (± standard deviation) obtained from assays using different SPGEs and prepared in different days.

Table 5.2. Electrochemical parameters obtained after each electrode surface preparation step obtained using the cyclic voltammetry (CV) and square wave voltammetry (SWV) techniques.

	CV			SWV
Steps	**ΔEp (mV)**	**Ipa (µA)**	**Ipc (µA)**	**Ip (µA)**
Bare gold	100 ± 10	6.9 ± 0.5	6.9 ± 0.4	102.7 ± 2.9
Cleaning	173 ± 6	6.1 ± 0.1	6.1 ± 0.3	79.1 ± 10.7
DPA	195 ± 7	5.7 ± 0.01	5.4 ± 0.04	66.8 ± 13.9
EDC-NHS	90 ± 0	7.3 ± 0.2	7.6 ± 0.2	134.5 ± 18.1
Strepatvidin	118 ± 8	6 ± 0.5	6.6 ± 0.5	74.1 ± 2.2
ETA	137 ± 15	5.9 ± 0.5	6.6 ± 0.4	60.3 ± 0.01
RNA aptamer	133 ± 6	5.9 ± 0.3	6.5 ± 0.2	59 ± 2
rhOPN	233 ± 9.6	4.1 ± 0.2	4.9 ± 0.3	38.6 ± 0.5

ΔEp - potential variation between cathodic and anodic peaks; Ipc - cathodic peak current value; Ipa - anodic peak current value; Ip – Peak current intensity (Ip = If – Ir); If - forward current; Ir - reverse current

A characteristic quasi-reversible electrochemical cyclic voltammogram of the $[Fe(CN)_6]^{3-/4-}$ redox solution at the bare gold electrode was observed (**Fig. 5.5.A1**) with a peak-to-peak separation ΔEp of 100 mV and similar cathodic and anodic peaks current intensities (**Table 5.2**). After the cleaning steps with different H_2SO_4 solutions, the current response slightly decreased possibly due to achieving a uniformity of the surface. A self-assembled monolayer is formed on the gold working electrode surface by the DPA solution, being characterized by the increase of ΔEp and decrease of the peaks current intensities. **Fig. 5.5.B1** shows that the bare gold electrode presented a high peak current intensity for the redox probe and exhibited maximum peak intensity at the potential 0.070 V. In the following steps, a decrease in the current intensity was observed. After the EDC-NHS step, the activation of carboxyl groups onto the working gold surface was achieved; accordingly a significant decrease in the ΔEp and slightly increase peaks current intensities of the electrode could be observed (**Fig. 5.5.A2**). In SWV, the peak current intensity attained was higher comparing to the result for the bare Au electrode that showed a signal increase of 30.5 % and lower potential (0.06 V) (**Fig. 5.5.B2**). At this stage, the activated surface of the working gold electrode enables the binding of carboxylic groups with the amine groups of streptavidin. Subsequently, in the next steps, the streptavidin binding and the blocking of free carboxylic groups with ETA was achieved, which resulted in an increase of ΔEp and a decrease of the peaks current intensities comparing with the bare gold electrode for both techniques. However, comparing the cyclic voltammograms from the ETA and streptavidin steps it was observed a slight increase in the peaks current intensities (ΔIpa ≈ 0.01 μA, ΔIpc ≈ 0.07 μA). Contrarily, for SWV the current intensities decreased, as expected, from in the expected order, i.e. from the streptavidin step to the ETA step, but at the same potential value. These results confirm the strong streptavidin binding. The step corresponding to the DNA aptamer immobilization on the working gold surface showed an increase of the ΔEp and lower peaks current intensities comparing with the bare gold electrode (**Fig. 5.5.A3 and 5.5.B3**). This probably occurs due to the negative charges of the aptamer backbone phosphate group and $[Fe(CN)_6]^{3-/4-}$ redox probe. Indeed, the electrostatic repulsive interaction is expected to block the electron transfer (Bang et al., 2005). These results suggest that the DNA aptamer was successfully assembled on the working gold surface. Next, the SPGE modified with the DNA aptamer was incubated with a standard rhOPN solution (1540 nM) and significant changes could be observed. The cyclic voltammograms showed the highest potential variation between peaks and the lowest peaks current intensities comparing with all the seven previous steps (**Table 5.2**).

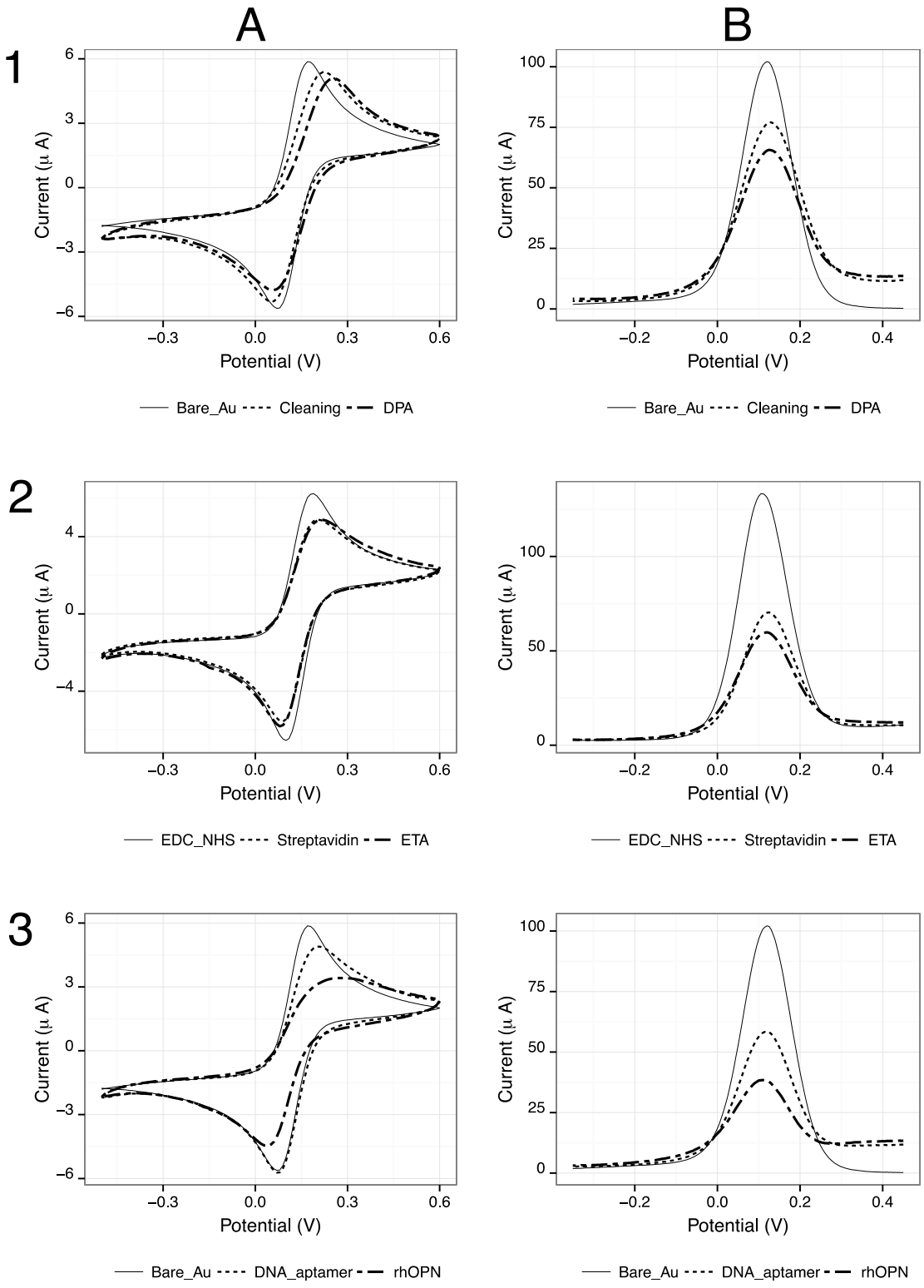

Figure 5.5. Immobilization steps of the DNA aptamer onto the working gold electrode via streptavidin-biotin interaction. A) Cyclic voltammograms and B) Square wave voltammograms of 5 mmol-1 [Fe(CN)6]3−/4− probe in PBS buffer solution of pH 7.4 at a scan rate of 50 mV/s for all aptasensor preparation steps: bare Au electrode, cleaning, DPA, EDC-NHS, streptavidin, ETA, DNA aptamer and DNA aptamer-rhOPN protein.

The cyclic voltammograms showed the highest potential variation between peaks and the lowest peaks current intensities comparing with all the seven previous steps (**Table 5.2**). Similar trends were found for the SWV analysis, in which it was observed a higher decrease of peak current intensity (62.3 % compared to that of the bare gold surface) and a lower potential value (0.06 V). These significant changes observed in the two electrochemical techniques strongly evidence that the formation of the aptamer-rhOPN complex can alter the permeability of the layer towards the charged redox solution and consequently the rate of their diffusion (Kim et al., 2009). The higher decrease (negative readout signal) in the peaks current intensities after rhOPN incubation can be associated with the high specificity of the DNA aptamer to rhOPN and this specific interaction can lead to a change of the aptamer conformation.

5.3.5. Sensitivity of the DNA aptasensor

The sensitivity of the DNA aptasensor was evaluated taking into account its response (ΔI/% values) to standard solutions containing different amounts of rhOPN, using $[Fe(CN)6]^{3-/4-}$ as electrochemical probe. Each rhOPN assay was carried out using different SPGEs. The CV assays showed a decrease in the current response (Ipa and Ipc) with increasing concentrations of rhOPN (**Fig. 5.6.A**). **Fig. 5.6.B** illustrates the ΔI/% values as a function of the rhOPN concentration. The results show the increasing values of ΔI/% with the increase of the rhOPN concentration, in the range between 25 and 1540 nM, reaching signal saturation near 400 nM. A linear correlation could be established for a dynamic concentration range from 25 to 100 nM (ΔI/% = 0.198 (± 0.002) × [rhOPN, nM] + 0.090 (± 0.155), **Fig. 5.6.B)**. The correlation coefficient was 0.999 and, based on the regression parameters (Ermer and Miller, 2005), the detection and quantification limits were calculated as 2.3 ± 0.3 and 7 ± 1 nM (150 ng/mL and 448 ng/mL), assuming a rhOPN molecular weight of 65 kDa), respectively. This detection limit was reasonably improved compared to that of the RNA aptasensor (240 ng/mL) previously developed by Meirinho et al., (2015), but still higher than those reported by other researchers using different techniques, type of electrodes and biosensor preparation methodologies (7.5 ng/mL, Chen et al., (2014) and 10.7 ng/mL, Cao et al., (2014)). Comparing to the works developed by Cao et al., (2014) and Chen et al., (2014), the RNA aptasensor (Meirinho et al., 2015) and DNA aptasensor developed in this chapter use a smaller gold working electrode for the detection of rhOPN aiming at the minimization of the biosensor, as well as the decrease of the amount of reagents and samples' volumes required for the detection. Therefore, the proposed DNA aptasensor

could still be used for rhOPN detection, considering that in patients with metastatic breast cancer the reported range of plasma OPN concentrations is up to 290 ng/mL (Bramwell et al., 2014).

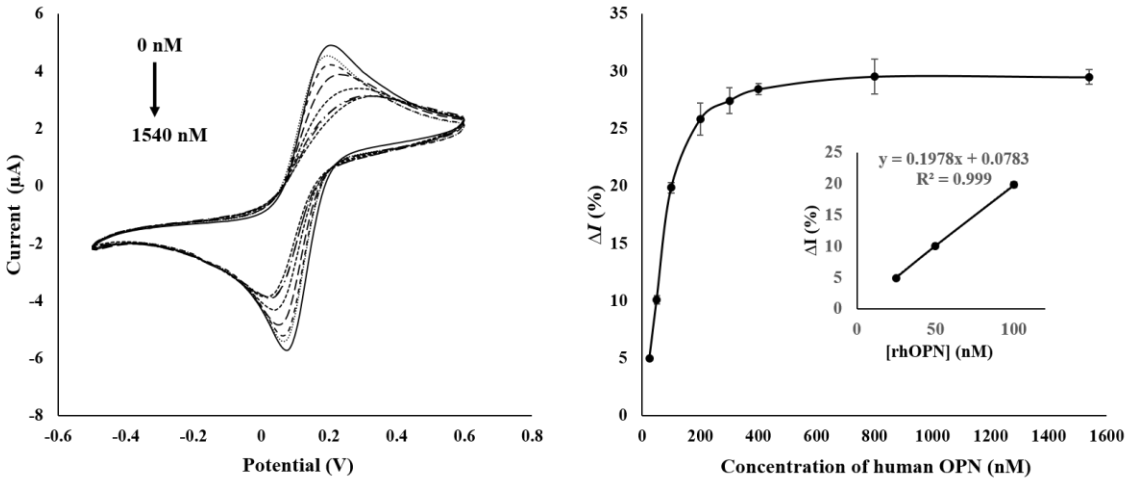

Fig. 5.6. A) CV response for rhOPN detection at different concentrations: (1) DNA aptamer immobilized, (2) 25, (3) 50, (4) 100, (5) 200, (6) 801 and (7) 1540 nM. B) Electrochemical aptasensor sensitivity analysis of rhOPN using an aptamer-immobilized gold working electrode. Error bars indicate the relative standard deviation of three independent experiments. The insert shows the linear relationship between the ΔI (%) and the rhOPN concentrations.

On the other hand, the sensitivity of the proposed analysis can be increased using other voltammetry techniques, such as SWV. In the current work, the use of SWV to characterize the DNA aptasensor and detect rhOPN (1540 nM) led to a decrease in the current (ΔI = 34.2 %), while using CV for the same concentration resulted in a lower decrease (ΔI = 29.7 %, **Fig. 5.6.B**). The SWV technique enables a faster analysis and presents a broader dynamic range and lower limit of detection as compared to CV (Dogan-Topal et al., 2010). Finally, the use of antibody-based biosensors (immunosensors) to detect a protein presents some drawbacks such as their production, stability, modification, washing steps and reagents requirements (i.e. sensitivity to temperature and expensive) (Liu et al., 2010). Therefore, the use of aptamers still is a good alternative. The application of aptamers as biorecognition elements in biosensors presents some advantages in comparison to antibodies such as the ease and reduced cost for their production via chemical synthesis, easy to be labelled and modified with a variety of functional groups or reporter molecules for immobilization onto a diversity of transducers surfaces and different detection strategies. Another interesting feature of aptamers is the excellent affinity by folding themselves in distinct secondary structures and

specificity towards the target (Balamurugan et al., 2008; Farabullini et al., 2007; Hianik and Wang, 2009; Palchetti and Mascini, 2012; Radi, 2011; Song et al., 2012; S. Song et al., 2008; Strehlitz et al., 2008). Another alternative for the development of aptasensors with reduced detection limits can be the application of nanomaterials, such as nanoparticles. This nanomaterial increases the electrode surface area, thus allowing the immobilization of more aptamers, and could also be used as an attractive signal transducer contributing to an increase of the sensitivity and specificity (Palchetti and Mascini, 2012).

5.3.6. Evaluation of DNA aptasensor

The specificity is crucial to evaluate the aptasensor performance and it can be assessed by comparing the DNA aptamer binding with the specific protein (rhOPN) and with non-specific proteins. Non-specific binding to the aptasensor leads to high background signals, decreasing its performance. Four proteins (THR, BSA, rbOPN and LYS) were evaluated as possible interferents. These proteins were chosen taking into account their molecular weights and isoelectric points, as well as their distinctive features that can affect the aptasensor performance. THR was used since the OPN has a conserved thrombin cleavage domain (RSK (arginine^{168}-lysine^{170}) adjacent to the RGD domain) and it is a secreted serine protease found in the human blood (Beausoleil et al., 2011; Gursoy et al., 2010). BSA is inert and similar to the human serum albumin (HSA) also present in human blood (Xie et al., 2012) and in high concentrations in serum samples (Gokulrangan et al., 2005). rbOPN was used since its cDNA sequence holds a high degree of homology with rhOPN (Wai and Kuo, 2008, 2004). Finally, LYS was used as a control protein since it possesses the lowest MW and highest p*I* compared with all the other proteins studied and it is known to non-specifically bind to nucleic acids (Gokulrangan et al., 2005). The relative current response ($\Delta I/\%$) for the interferent proteins tested was found to be negligible as compared to the unique binding response obtained with rhOPN (**Fig. 5.7**). The results clearly demonstrate the great DNA aptamer sensitivity and specificity to rhOPN. This DNA aptasensor showed a better selectivity for THR, LYS and similar for rbOPN than the one obtained with the RNA aptasensor previously reported (Meirinho et al., 2015). The results suggest that this aptasensor could be used to detect rhOPN in biological samples such as blood, plasma or serum.

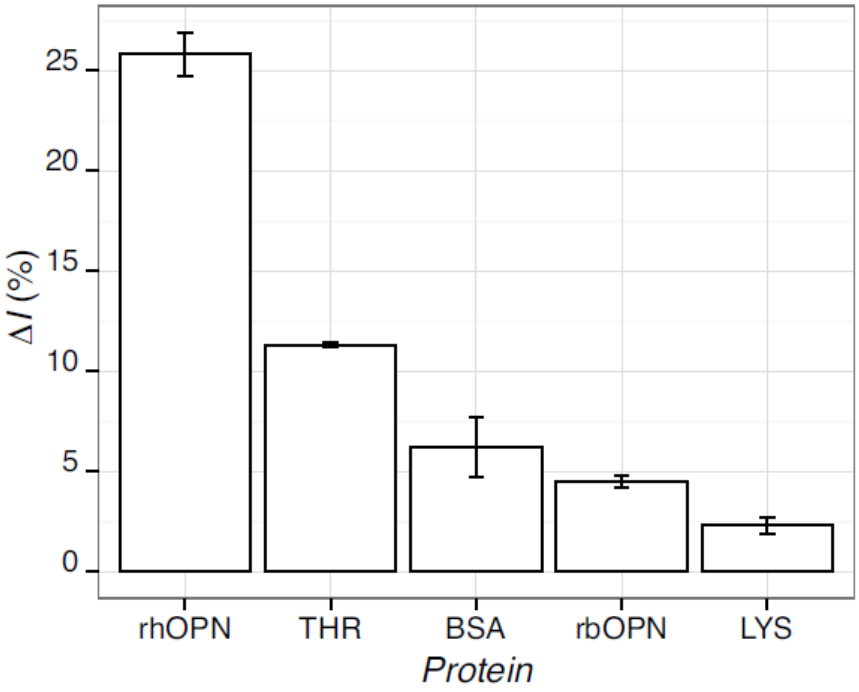

Fig. 5.7. The relative current response (*ΔI*/%) to non-specific proteins (200 nM): BSA – bovine serum albumin, LYS – lysozyme, rbOPN – bovine osteopontin and THR-thrombin and for specific-protein rhOPN – human osteopontin. Error bars correspond to the relative standard deviation of three independent experiments.

The aptasensor stability was evaluated through the detection of the electrochemical signal of three SPGEs stored at 4 °C during different time periods. When compared with the initial *ΔI*/% value, the response after 5, 10, 15 and 20 days was found to retain 94.3 %, 94.7 %, 92.1 % and 90.5 % of the original value, respectively, thus demonstrating a good stability of the aptasensor response along time. The results showed that the *ΔI*/% only decreases about 10 % of the original value after 20 days of storage in buffer at 4 °C. After 10 days, the stability of the DNA aptasensor was higher than that obtained with the previously reported RNA aptasensor (that retain 88 %) (Meirinho et al., 2015). This interesting gain in stability may be due to the fact that the RNA aptamer sequences are more susceptible to degradation by nucleases than the DNA aptamers (Prieto-Simón et al., 2010; Sassolas et al., 2009). In addition, the method herein proposed showed satisfactory intra-day repeatability. Indeed, the electrochemical signals recorded with three SPGE prepared in the same day and inoculated with 200 nM and 1540 nM rhOPN, showed relative standard deviations (RSD) of 4.7 % and 5.7 %, respectively. Furthermore, the method also showed satisfactory inter-day repeatability since, for five SPGE prepared in different days, the electrochemical signals recorded for 200 nM and

1540 nM showed a RSD of 4.2 % and 5 %, respectively. The development of sustainable and cost-effective biosensors implies their reusability. In this sense, the possible regeneration of the binding surface is of utmost importance, but often it is very difficult to achieve. To evaluate the possible regeneration of the aptasensor, considering that aptamers can be denatured several times without losing its function, tests using two regenerate reagents (NaCl and urea) (Liu et al., 2010; Ocaña et al., 2012; Radi et al., 2006) were carried out. The $\Delta I/\%$ values obtained after aptamer-protein binding (rhOPN analysis) and after incubation with the regenerate reagents were found to be statistically the same. Therefore, the regenerate solutions used were not effective in disrupting the aptamer-protein complex without degradation of the aptamer. Nevertheless, given its potential for the detection of rhOPN, it would be of great interest to further explore the possibility of regenerating it, possibly through an increase of the incubation time with the regenerate reagent or by testing other reagents more aggressive and efficient in breaking the aptamer-protein complex.

5.4. Conclusion

This chapter proposes a simple and sensitive label-free electrochemical aptasensor for the detection of human OPN using a SPGE modified with a newly isolated DNA aptamer as the bioreceptor. The developed aptasensor showed high sensitivity, specificity, stability and repeatability towards the detection of rhOPN. The aptasensor was found to be superior to other reported methods as it consists in an efficient and simple strategy to directly analyze relevant biomarkers in complex samples, thus enabling a fast and cheap method for diagnosis and therapy monitoring. The availability of two different aptamers with different binding sites for the detection of the same protein could allow the design of different aptasensors, such as sandwich format and could enable the development of multiplexed aptamer arrays, thus increasing the sensibility and specificity.

5.5. References

Ahmed, M., Kundu, G.C., 2010. Mol. Cancer 9, 101–114.

Anborgh, P.H., Mutrie, J.C., Tuck, A.B., Chambers, A.F., 2011. J. Cell Commun. Signal. 5, 111–122.

Anborgh, P.H., Wilson, S.M., Tuck, A.B., Winquist, E., Schmidt, N., Hart, R., Kon, S., Maeda, M., Uede, T., Stitt, L.W., Chambers, A.F., 2009. Clin. Chem. 55, 895–903.

Bache, M., Kappler, M., Wichmann, H., Rot, S., Hahnel, A., Greither, T., Said, H.M., Kotzsch, M., Würl, P., Taubert, H., Vordermark, D., 2010. BMC Cancer 10, 132-148.

Balamurugan, S., Obubuafo, A., Soper, S. a, Spivak, D.A., 2008. Anal. Bioanal. Chem. 390, 1009–1021.

Bang, G.S., Cho, S., Kim, B., 2005. Biosens. Bioelectron. 21, 863–870.

Beausoleil, M.S., Schulze, E.B., Goodale, D., Postenka, C.O., Allan, A.L., 2011. BMC Cancer 11, 25-37.

Bramwell, V.H.C., Doig, G.S., Tuck, A.B., Wilson, S.M., Tonkin, K.S., Perera, F., Vandenberg, T.A., Chambers, A.F., 2006. Clin. Cancer Res. 12, 3337–3343.

Bramwell, V.H.C., Tuck, A.B., Chapman, J.-A.W., Anborgh, P.H., Postenka, C.O., Al-Katib, W., Shepherd, L.E., Han, L., Wilson, C.F., Pritchard, K.I., Pollak, M.N., Chambers, A.F., 2014. Breast Cancer Res. 16, R8.

Cao, Y., Chen, D., Chen, W., Yu, J., Chen, Z., Li, G., 2014. Anal. Chim. Acta 812, 45–54.

Chen, H., Mei, Q., Jia, S., Koh, K., Wang, K., Liu, X., 2014. Analyst 139, 4476–4481.

de-los-Santos-Álvarez, N., Lobo-Castañón, M.J., Miranda-Ordieres, A.J., Tuñón-Blanco, P., 2008. TrAC 27, 437–446.

Dogan-Topal, B., Ozkan, S.A., Uslu, B., 2010. Open Chem. Biomed. Methods J. 3, 56–73.

Dua, P., Kim, S., Lee, D.-K., 2011. Methods 54, 215–225.

Ermer, J., Miller, J., 2005. Wiley: New York. Wiley-VCH GmbH and co. KGaA. Weinheim, ISBN: 3-527-31255-2.

Farabullini, F., Lucarelli, F., Palchetti, I., Marrazza, G., Mascini, M., 2007. Biosens. Bioelectron. 22, 1544–1549.

Farghaly, O. a, Hameed, R.S.A., 2014. Sci. 9, 3287–3318.

Gokulrangan, G., Unruh, J.R., Holub, D.F., Ingram, B., Johnson, C.K., Wilson, G.S., 2005. Anal. Chem. 77, 1963–1970.

Gursoy, G., Acar, Y., Alagöz, S., 2010. J. Med. Med. Sci. 1, 055–060.

He, J., Liu, Y., Fan, M., Liu, X., 2011. J. Agric. Food Chem. 59, 1582–1586.

Hianik, T., Wang, J., 2009. Electroanal. 21, 1223 – 1235.

Kanwar, J.R., Mohan, R.R., Kanwar, R.K., Roy, K., Bawa, R., 2010. Nanomedicine 5, 1435–1445.

Kim, Y.S., Niazi, J.H., Gu, M.B., 2009. Anal. Chim. Acta 634, 250–254.

Kim, Y.S., Song, M.Y., Jurng, J., Kim, B.C., 2013. Anal. Biochem. 436, 22–28.

Li, L., Zhao, H., Chen, Z., Mu, X., Guo, L., 2011. Biosens. Bioelectron. 30, 261–266.

Likui, W., Hong, W., Shuwen, Z., 2010. J. Gastrointestinal Surg. 14, 74–81.

Liu, Y., Tuleouva, N., Ramanculov, E., Revzin, A., 2010. Anal. Chem. 82, 8131–8136.

Lönne, M., Zhu, G., Stahl, F., Walter, J.-G., 2014. Adv. Biochem. Eng. Biotechnol. 140, 121–154.

Macrì, A., Versaci, A., Lupo, G., Trimarchi, G., Tomasello, C., Loddo, S., Sfuncia, G., Caminiti, R., Teti, D., Famulari, C., 2009. Tumori 95, 48–52.

Marimuthu, C., Tang, T.-H., Tominaga, J., Tan, S.S.-C., Gopinath, S.C.B., 2012. Analyst 137, 1307–1315.

Meirinho, S.G., Dias, L.G., Peres, A.M., Rodrigues, L.R., 2015. Biosens. and Bioelectron. 71, 332–341.

Mi, Z., Guo, H., Russell, M.B., Liu, Y., Sullenger, B. a, Kuo, P.C., 2009. Mol. Ther. 17, 153–161.

Mirza, M., Shaughnessy, E., Hurley, J.K., Vanpatten, K.A., Pestano, G. a, He, B., Weber, G.F., 2008. Int. J. Cancer 122, 889–897.

Ocaña, C., Pacios, M., del Valle, M., 2012. Sensors 12, 3037–3048.

Ohno, K., Nishimori, H., Yasoshima, T., Kamiguchi, K., Hata, F., Fukui, R., Okuya, K., Kimura, Y., Denno, R., Kon, S., Uede, T., Sato, N., Hirata, K., 2010. Surg. Today 40, 347–356.

Ozer, A., Pagano, J.M., Lis, J.T., 2014. Mol. Ther. Nucleic Acids 3, e183.

Palchetti, I., Mascini, M., 2012. Anal. Bioanal. Chem. 402, 3103–3114.

Potty, A.S.R., Kourentzi, K., Fang, H., Jackson, G.W., Zhang, X., Legge, G.B., Willson, R.C., 2009. Biopolymers 91, 145–156.

Prieto-Simón, B., Campàs, M., Marty, J.-L., 2010. Bioanal. Rev. 1, 141–157.

Radi, A., Lluis, J., Sa, A., Baldrich, E., Sullivan, C.K.O., 2006. J. Am. Chem. Soc. 128, 117–124.

Radi, A.-E., 2011. Int. J. Electrochem. 2011, 1–17.

Rodrigues, L.R., Lopes, N., Sousa, B., Vieira, D., Milanezi, F., 2009. TOBCJ 1, 1–9.

Rodrigues, L.R., Teixeira, J.A., Schmitt, F.L., Paulsson, M., Lindmark-Mansson, H., 2007. Cancer Epidemiol. Biomark. Prev. 16, 1087–1097.

Ruigrok, V.J.B., Levisson, M., Eppink, M.H.M., Smidt, H., Oost, J.V.A.N.D.E.R., 2011. Biochem. J. 436, 1–13.

Sase, S.P., Ganu, J. V, Nagane, N., 2012. Ind. Med. Gaz. xxx, 62–66.

Sassolas, A., Blum, L.J.J.J., Leca-Bouvier, B.D.D.D., Lyon, D., 2009. Electroanal. 21, 1237–1250.

Scatena, M., Liaw, L., Giachelli, C.M., 2007. ATVB 27, 2302–2309.

Sett, A., Das, S., Sharma, P., Bora, U., 2012. Open J. Appl. Biosens. 01, 9–19.

Song, K.-M., Lee, S., Ban, C., 2012. Sensors. 12, 612–631.

Song, S., Wang, L., Li, J., Zhao, J., Fan, C., 2008. Anal. Chem. 27, 108–117.

Stoltenburg, R., Nikolaus, N., Strehlitz, B., 2012. J. Anal. Methods Chem. Volume 2012, Article ID 415697, 1-14.

Strehlitz, B., Nikolaus, N., Stoltenburg, R., 2008. Sensors 8, 4296–4307.

Strehlitz, B., Reinemann, C., Linkorn, S., Stoltenburg, R., 2012. Bioanal. Rev. 4, 1–30.

Tombelli, S., Minunni, M., Mascini, M., 2005. Biosens. Bioelectron. 20, 2424–2434.

Tran, D.T., Janssen, K.P.F., Pollet, J., Lammertyn, E., Anné, J., Van Schepdael, A., Lammertyn, J., 2010. Molecules 15, 1127–1140.

Tuck, A.B., Chambers, A.F., Allan, A.L., 2007. J. Cellular Biochem. 868, 859–868.

Wai, P., Kuo, P., 2008. Cancer Metastasis 27, 103–118.

Wai, P.Y., Kuo, P.C., 2004. J. Surg. Res. 241, 228 –241.

Weber, G.F., Lett, G.S., Haubein, N.C., 2010. Br. J. Cancer 103, 861–869.

Weber, G.F., Lett, G.S., Haubein, N.C., 2011. Oncol. Rep. 25, 433–41.

Xie, S., Yuan, R., Chai, Y., Bai, L., Yuan, Y., Wang, Y., 2012. Talanta 98, 7–13.

Xu, Y.-Y., Zhang, Y.-Y., Lu, W.-F., Mi, Y.-J., Chen, Y.-Q., 2015. Mol. Clin. Oncol. 3, 357–362.

Ye, M., Hu, J., Peng, M., Liu, J., Liu, J., Liu, H., Zhao, X., Tan, W., 2012. Int. J. Mol. Sci. 13, 3341–3353.

Yu, T., Li, J., Liu, Q., Cheng, W., Zhang, D., Ju, H., 2012. Int. J. Electrochem. Sci. 7, 8533–8542.

Zhang, H., Guo, M., Chen, J.-H., Wang, Z., Du, X.-F., Liu, P.-X., Li, W.-H., 2014. Cell. Phys. Biochem. 33, 991–1002.

Zhao, J., Zhang, Y., Li, H., Wen, Y., Fan, X., 2011. Biosens. Bioelectron. 26, 2297–2303.

Zuker, M., 2003. Nucleic Acids Res. 31, 3406–3415.

CHAPTER 6

Electrochemical aptasensor array for multiple detection of human osteopontin

The early cancer diagnosis is crucial for patient's survival and disease monitoring. Although many efforts have been conducted, sensitive, fast and cheap methods for multiple detection of protein disease biomarkers are still to be designed and/or improved. This study describes the development of a label-free aptasensor array for the simultaneous detection of human OPN using two specific aptamers. To enable multiplexing, the RNA and DNA aptamers were immobilized in the working electrodes of the dual-screen-printed gold working electrodes (dual-SPGEs) via streptavidin-biotin interaction and using the $[Fe(CN)_6]^{3-/4-}$ as the redox probe for cyclic voltammetry (CV) measurements. CV was used to characterize the aptamers immobilization and the human OPN protein detection. The multiplexed protein assay was prepared through the immobilization of RNA/RNA aptamer, DNA/DNA aptamer and DNA/RNA aptamers in the working electrodes (WE1 and WE2) of the dual-SPGEs, respectively. The dual-SPGEs holding the same aptamer in both working electrodes exhibited a relative standard deviation (RSD %) of 8 % (RNA/RNA aptamer) and 10 % (DNA/DNA aptamer), respectively. The dual-SPGEs holding the DNA and RNA aptamer in WE1 and WE2, respectively, showed a relative current change ($\Delta I/\%$) of 20 ± 3 % and $\Delta I/\%$ of 19 ± 2 %, respectively, considering only the decrease in current signal observed for the oxidation peak. Moreover, the DNA/RNA aptasensor array was able to selectively detect rhOPN in the presence of other interfering proteins, being $\Delta I/\%$ values for rhOPN, 4 to 20 times higher compared to those recorded for thrombin, bovine serum albumin, bovine osteopontin and lysozyme. Considering these preliminary results, the

aptasensor array holding the two aptamers could be a good alternative for the specific detection of rhOPN and for cancer diagnosis overall.

6.1. Introduction

The possibility of measuring multiple proteins or to simultaneously detect the same protein at different working electrodes of a biosensor device holds a huge promise regarding the design of new and personalized approaches for the early detection and therapy of diseases, such as cancer (Rusling et al., 2010; Xiang et al., 2011; Xie and Walton, 2010). Most cancer diseases are associated with the presence of several biomarkers (molecules that exhibit an altered expression when the disease emerges). The detection and quantification of these protein biomarkers in the patient's biological fluids can provide a continuously updated record of the disease status. An early diagnosis of the disease is of utmost importance to improve the patient's survival rate and therapeutic efficacy, as well as to monitor the disease recurrence. In this sense, it is essential to develop new, simple and cost-effective methods holding a high sensitivity and reliability for the simultaneous detection of multiple protein disease biomarkers in biological fluids using a single device (Saberian-Borujeni et al., 2014). The simultaneous detection of multiple protein biomarkers using multi-electrodes arrays based on immunosensors has been reported (Chikkaveeraiah et al., 2012; Vidotti et al., 2011). Yang et al., (2014) developed a multianalyte immunosensor to simultaneously detect six biomarkers, combining multi-label and multi-spots assay for an early detection of hepatocellular carcinoma (HCC). The electrodes array used for the multi-spots assay was composed by platinum and Ag/AgCl as counter and reference electrodes, respectively, and of four carbon working electrodes. The six biomarkers were simultaneously detected with significant improved sensitivity, specificity and detection efficiency using "sandwich" immunoreactions and distinct voltammetric peaks. Zhao et al., (2014) proposed an electrochemical immunosensor array, prepared with disposable dual-screen-printed electrodes (dual-SPGE) for the simultaneous detection of α-fetoprotein (AFP) and carcinoembryonic antigen (CEA). The method used linear sweep voltammetry (LSV) and streptavidin/nanogold/carbon nanohorn as a signal tag to induce silver deposition wide linear concentrations ranges with detection limits of 0.024 pg/mL and 0.032 pg/mL for AFP and CEA, respectively. The simultaneous multiplex assay, compared with the single analyte assay, exhibits several potential advantages such as fast detection, easier experimental procedures and lower cost of the analysis, as well as the possibility to perform several replicates per assay (Bai et al., 2012; Saberian-Borujeni et al., 2014; Xiang et al., 2011). Despite these recognized advantages multiplex assays based on electrochemical aptasensors have been rarely reported for the simultaneous detection of multiple targets (Bai et al., 2012; Saberian-Borujeni et al., 2014). Indeed, the

electrochemical detection using aptasensors has only recently attracted an increased attention mainly due to their advantages, such as high sensitivity, specificity and stability, fast response, low cost and the potential for miniaturization (Hianik and Wang, 2009; Lönne et al., 2014; Mascini, 2009; Palchetti and Mascini, 2012; Prieto-Simón et al., 2010; Radi, 2011; Sassolas et al., 2009; Velasco-Garcia and Missailidis, 2009). These aptasensors have been developed and extensively used for the single detection of several protein disease biomarkers such as PDGF (Degefa and Kwak, 2008; K. Deng et al., 2013), OPN (Cao et al., 2014; Meirinho et al., 2015), VEGF (Zhao et al., 2011), MUC1 (Ma et al., 2013). However, as previously mentioned, for the diagnosis and monitoring of the disease status, often the detection of a single target analyte is not sufficient and the simultaneous detection of multiple targets is envisaged. Therefore, new designs of electrochemical aptasensors for the simultaneous detection of multiple targets are required (Xiang et al., 2011). Some strategies have been reported towards this end using for example, a dual-functional aptamer (Min et al., 2010; Xie and Walton, 2010), an aptamer-complementary DNA that hybridizes with two aptamers (Zhao et al., 2011), or nanomaterials (Bai et al., 2012; Du and Li, 2010; Erdem et al., 2009; Qian et al., 2010). In the last years, the use of electrodes arrays to develop these electrochemical aptasensor devices has been gaining popularity. Song et al., (2014) described an electrochemical aptasensor array for multiplexed detection of PDGF-BB and thrombin proteins using “in situ” DNA hybridization-inducing AgNPs for signal amplification. The aptasensor array was fabricated using a SPE array chip containing four subarrays with four independent carbon working electrodes (WE1, WE2, WE3 and WE4) and one counter electrode. The specific aptamers for PDGF-BB, THR, and a mixture of both were immobilized onto the surface of WE1, WE2 and WE3, respectively after electrodeposition of AuNPs. In the WE4, an non-specific ssDNA (negative control) was immobilized. The aptasensor array proposed allowed multi-detection with good selectivities, showing both PDGF-BB and THR aptamer-modified electrodes only stripping responses towards their respective proteins and no cross-reaction between the two aptamers towards non-cognate proteins was observed. Liu et al., (2012) described an electrochemical aptasensor for the detection of interferon gamma (IFN-γ) and tumor necrosis factor alpha (TNF-α) using micropatterned aptamer-modified gold electrodes. The two aptamers were conjugated with MB redox label and immobilized via thiol-gold chemistry on several gold electrode pairs micro-fabricated on glass and packaged with a non-fouling PEG hydrogel. The developed aptasensor showed detection limits of 0.06 nM for IFN-γ and 0.58 nM for TNF-α. Additionally, it was found to be applicable for the detection of those proteins in activated T cells and monocytes cell line. Recently, Liu et al., (2015) reported an electrochemical aptasensor for the specific detection of

multiple cytokines (IFN-γ and TNF-α) using an electrodes array with a set of four miniature working electrodes. The aptasensor contained IFN-γ and TNF-α aptamers conjugated with the redox reporter molecule anthraquinone (AQ) and MB, respectively, which were immobilized onto the gold working electrodes by chemisorption. The aptasensor showed high specificity and sensitivity, similarly to that of the single analyte aptasensor for each biomarker. In the construction of multi-aptasensors arrays, the high affinity, selectivity and specificity of the aptamers against their targets could be affected by the experimental conditions such as pH, temperature and ionic changes. Therefore, it is important that all the aptamers used in these arrays perform adequately at the same operational conditions (e.g. pH, temperature). Besides, the differences in the length of the aptamers sequences can constitute a problem in the fabrication of the aptasensors array (Saberian-Borujeni et al., 2014). Nevertheless, in comparison with conventional analytical methods, the biosensors fabricated with electrodes arrays are extremely useful and advantageous as they are able to distinguish multiple analytes/targets in a single sample, low amounts of samples and reagents are necessary, they present a high miniaturization potential and sample throughput can be achieved (Saberian-Borujeni et al., 2014; Touhami, 2015).

6.2. Material and Methods

6.2.1. Materials and reagents

Recombinant human osteopontin (rhOPN, 65 kDa) and recombinant bovine osteopontin (rbOPN, 60 kDa) were purchased from R&D Systems. Thrombin from human plasma (THR, 37.4 kDa), bovine serum albumin (BSA, 66 kDa), lysozyme from chicken egg white (LYS, 14.3 kDa) and streptavidin were obtained from Sigma-Aldrich. All proteins were acquired lyophilized and manipulated according to the manufacturers' specifications. Diethypyrocarbonate (DEPC), 3,3-dithiodipropionic acid (DPA), N-(3-dimethylaminopropyl)-N-ethylcarbodiimide hydrochloride (EDC), N-hydroxysuccinimide (NHS), ethanolamine (ETA) and sulfuric acid (purity of 99.999 %) were obtained from Sigma-Aldrich. Potassium hexacyanoferrate (III) ($K_3Fe(CN)_6$) and potassium hexacyanoferrate (II) ($K_4Fe(CN)_6$) were obtained from Acros Organics and potassium dihydrogen phosphate (KH_2PO_4) from Merck. Sodium chloride (NaCl), potassium chloride (KCl) and sodium hydrogen phosphate (Na_2HPO_4) were acquired from Panreac. All chemicals were of analytical grade and used as received.

6.2.1.1. Solutions

Phosphate buffer saline (PBS) solution (137 mM NaCl, 2.7 mM KCl, 8.1 mM Na_2HPO_4 and 1.47 mM KH_2PO_4) with an adjusted pH of 7.4 was used. The ferro/ferricyanide redox probe (5 mM $K_3Fe(CN)_6$ and $K_4Fe(CN)_6$ (1:1) and 10 mM KCl in 100 mL of PBS), with an adjusted pH of 7.4, was daily prepared. Stock solutions of 200 mM EDC, 100 mM NHS, as well as the stock solution of 1 mg/ml of septravidin in PBS (pH 7.4) were stored at -20 °C before use. Stock solutions of 200 nM DPA and 100 mM of ethanolamine (ETA) were stored at 4 °C. Stock solutions of each protein were prepared according to the manufacturer specifications and were stored at -20 °C. The protein working solutions were obtained by dilution of the stock solutions with PBS buffer (pH 7.4) and were stored at 4 °C until use. Deionized water (18.2 MΩ) purified by a milli-QTM system (Millipore) was used throughout the experiment for aqueous solutions preparation.

6.2.1.2. Synthetic oligonucleotides

The RNA aptamer (R3-OPN, Mi et al., (2009)) and DNA aptamer (C10K2, described in the Chapter 5) were synthesized by Integrated DNA Technologies (Belgium), their sequences were as follow: RNA aptamer (5'-Biotin- CGG CCA CAG AAU GAA AAA CCU CAU CGA UGU UGC AUA GUU G-3') and DNA aptamer (5'-Biotin-TGT GTG CGG CAC TCC AGT CTG TTA CGC CGC-3').

Stock solutions of DNA and RNA aptamers were prepared with ultra-pure water containing 1 % DEPC (v/v) to avoid the RNase interference at 100 µM. The working DNA and RNA aptamer solutions was prepared by dilution of the stock solutions using fresh PBS. Before the DNA and RNA aptamers immobilization on the gold working electrodes, the biotinylated aptamers prepared in PBS buffer (pH 7.4) were subjected to a temperature treatment (95 °C during 5 min, 4 °C for 5 min and 10 min at room temperature) in order to obtain an adequate structure flexibility of the aptamers for their interaction with streptavidin on the gold electrode surface.

6.2.1.3. Apparatus

Cyclic voltammetry (CV) signals were recorded using a Potentiostat-Galvanostat device (PG580, Uniscan Instruments). The pH was measured using a pH meter (iHANNA instruments pH 211). The dual-screen-printed gold electrodes (dual-SPGE) were purchased from DropSens (Oviedo, Spain). These dual-SPGEs include a four-electrode system configuration printed on the same strip of ceramic

substrate (3.4 x 1.0 x 0.05 cm) and were subjected to low temperature (BT) curing ink. Dual-SPGEs are composed of two ellipses of gold-BT working electrodes (WE1 and WE2, 6.3 mm^2 each) arranged in a parallel way in the ceramic strip, an Ag/AgCl reference electrode and a gold-BT counter electrode (19.8 mm^2 and 1 mm wide) as shown in **Fig. 6.1**.

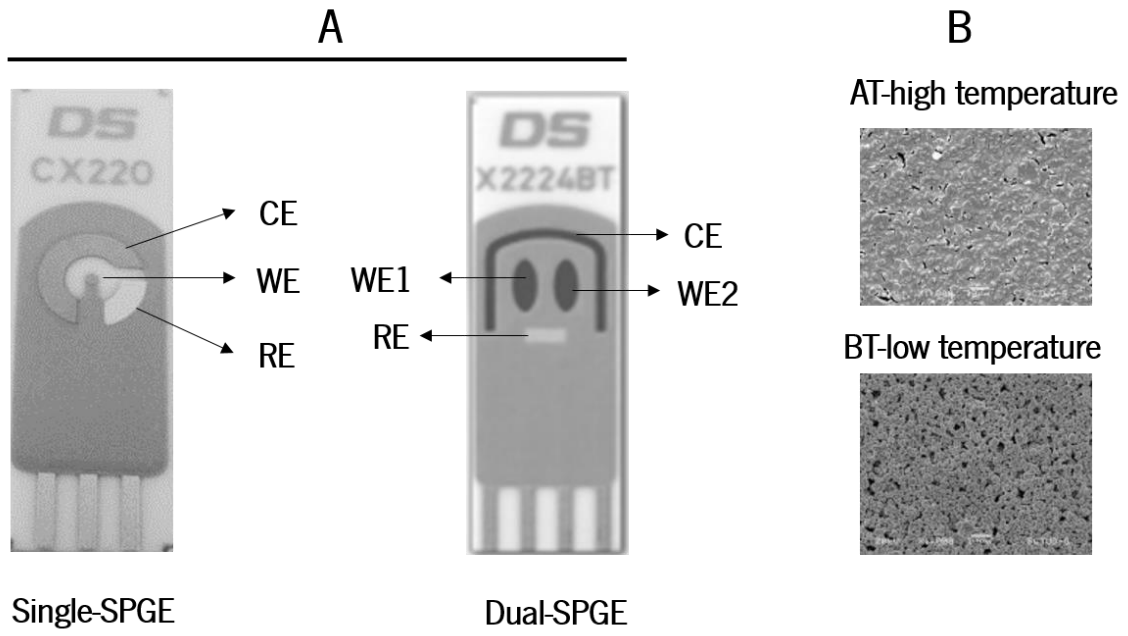

Fig. 6.1. Schematic design of the single-SPGEs and dual-SPGEs (A) and SEM images of the gold electrodes surfaces processes at high (AT) and low temperature (BT) curing inks (B). The images were provided by DropSens Inc. (Oviedo, Spain).

6.2.2. Immobilization of aptamers onto the dual-SPGEs

The aptamers immobilization was achieved through the streptavidin-biotin interaction as reported by Meirinho et al., (2015). Briefly, each dual-SPGE electrode was cleaned using three solutions (0.5 M H_2SO_4, 0.01 M KCl/0.1 M H_2SO_4 and 0.05 M H_2SO_4) under an electric potential in the range of -0.3 to 1.5 V, and at a scan rate of 100 mV/s. Afterwards, the working gold electrodes surfaces were functionalized using 200 mM DPA for 30 min at room temperature, washed with ethanol and by treatment with 100 mM EDC and 1 mM of NHS (1:1 v/v, 60 min at room temperature) for self-assembled monolayer formation and to convert the terminal carboxyl groups into an active NHS ester, respectively. Next, the functionalized gold working surfaces were incubated with 1 mg/ml of

streptavidin solution overnight at 4 °C and were then exposed to 100 mM ETA during 20 min at room temperature to block any remaining activated carboxyl groups. Finally, 4 nM of biotinylated aptamers were immobilized onto the gold working electrodes by streptavidin-biotin interaction (40 min at room temperature) and the surface was rinsed thoroughly with PBS buffer (pH 7.4) to remove the free aptamers.

The aptasensor array was evaluated for the detection of rhOPN and non-specific proteins (BSA, THR, LYS and rbOPN). For the detection of rhOPN, two approaches were used. First, three dual-SPGE functionalized with RNA aptamer (WE1/WE2) and three functionalized with DNA aptamer (WE1/WE2) were used. These were incubated with 10 µL of rhOPN at 200 nM on each working electrode for 60 min at room temperature. Second, seven dual-SPGE functionalized with DNA aptamer (WE1) and RNA aptamer (WE2) were used. The incubation conditions were the same as the ones used in the first approach. To remove the non-specifically bound protein, the electrodes surfaces were washed with PBS buffer. For all CV measurements, 100 µL of $[Fe(CN)_6]^{3-/4-}$solution (redox probe) was applied on the electrochemical reaction area of the dual-SPGE electrode. Additionally, the second approach was also used to evaluate the aptasensor array response to non-specific proteins. Interfering proteins (THR, BSA, rbOPN and LYS) were all at a concentration of 200 nM and were tested under the same experimental conditions as rhOPN.

6.2.3. Cyclic voltammetry measurement

All dual-SPGEs used were characterized and evaluated by CV in the presence of $[Fe(CN)_6]^{3-/4-}$ at room temperature. The CV measurements were performed under a potential range of -0.5 to 0.8 V and at a scan rate of 50 mV/s. The decrease in the peak current intensities was expressed as relative current change (ΔI %). The ΔI % was calculated considering the current values of the cyclic voltammogram oxidation peak recorded after aptamer immobilization and protein incubation by using the equation (6.1):

$$\Delta I\,\% = (I_0 - I_1)/I_0 \times 100 \qquad (6.1)$$

where ΔI is the relative current change (%); I_0 and I_1 represents the current before and after the sample incubation, respectively.

6.3. Results and Discussion

6.3.1. Characterization of the dual-SPGE

The aim of this study was to develop an electrochemical aptasensor array for the simultaneous detection of rhOPN. The optimal concentration of aptamers to be immobilized onto the gold working electrodes (WE1/WE2), as well as the best incubation time for the aptamer-rhOPN interaction were established previously during the development of the RNA (Chapter 4) and DNA (Chapter 5) aptasensors for the detection rhOPN using a single-SPGE (Meirinho et al., 2015). The optimal aptamer concentration and incubation time were 4 nM and 60 min, respectively. CV is a simple, rapid and sensitivity technique, which gives overall information regarding the reversibility of the oxidation and reduction mechanisms that occur at the electrode surface (Farghaly and Hameed, 2014; Olowu et al., 2011). During the preparation of the aptasensor array, CV was used to monitor all changes introduced on the working surfaces. As an example, **Fig. 6.2** illustrates the voltammograms obtained by CV for the aptasensors comprising a single-SPGE and a dual-SPGE, using $[Fe(CN)_6]^{3-/4-}$ as the redox probe solution, the bare Au electrode and after three experimental steps, namely, surface cleaning with different H_2SO_4 solutions, aptamers' immobilization and aptamer-rhOPN binding. In the RNA aptasensor (**Fig.6.2.A1**) and DNA aptasensor (**Fig. 6.2.A2**) using a single-SPGE, a characteristic quasi-reversible electrochemical cyclic voltammogram of the $[Fe(CN)_6]^{3-/4-}$ redox probe solution at the bare Au electrode was observed. The current response decreased slightly after the cleaning step, which may be due to obtaining a homogeneous surface. The aptasensor array showed a similar behavior compared to the RNA and DNA aptasensors previously described, except for the cyclic voltammograms of the bare Au electrode and cleaning step (**Fig. 6.2.B1 and B2**). The voltammograms obtained for the dual-SPGEs before the cleaning step, clearly showed that the current response was practically nil for both working electrodes (WE1 (**Fig. 6.2.B1**) and WE2 (**Fig. 6.2.B2**)). The almost absence of current response could be attributed to the fact that for these electrodes a low temperature (BT) curing ink process was used, thus leading to a more irregular surface (**Fig. 6.1.B**) compared to that obtained with the high temperature (AT) curing ink process used during the production of the single-SPGE electrodes (**Fig. 6.1.B**). After the cleaning step, a typical cyclic voltammogram was obtained for the dual-SPGEs, showing that this step led to an activated and smooth surface of the Au electrode.

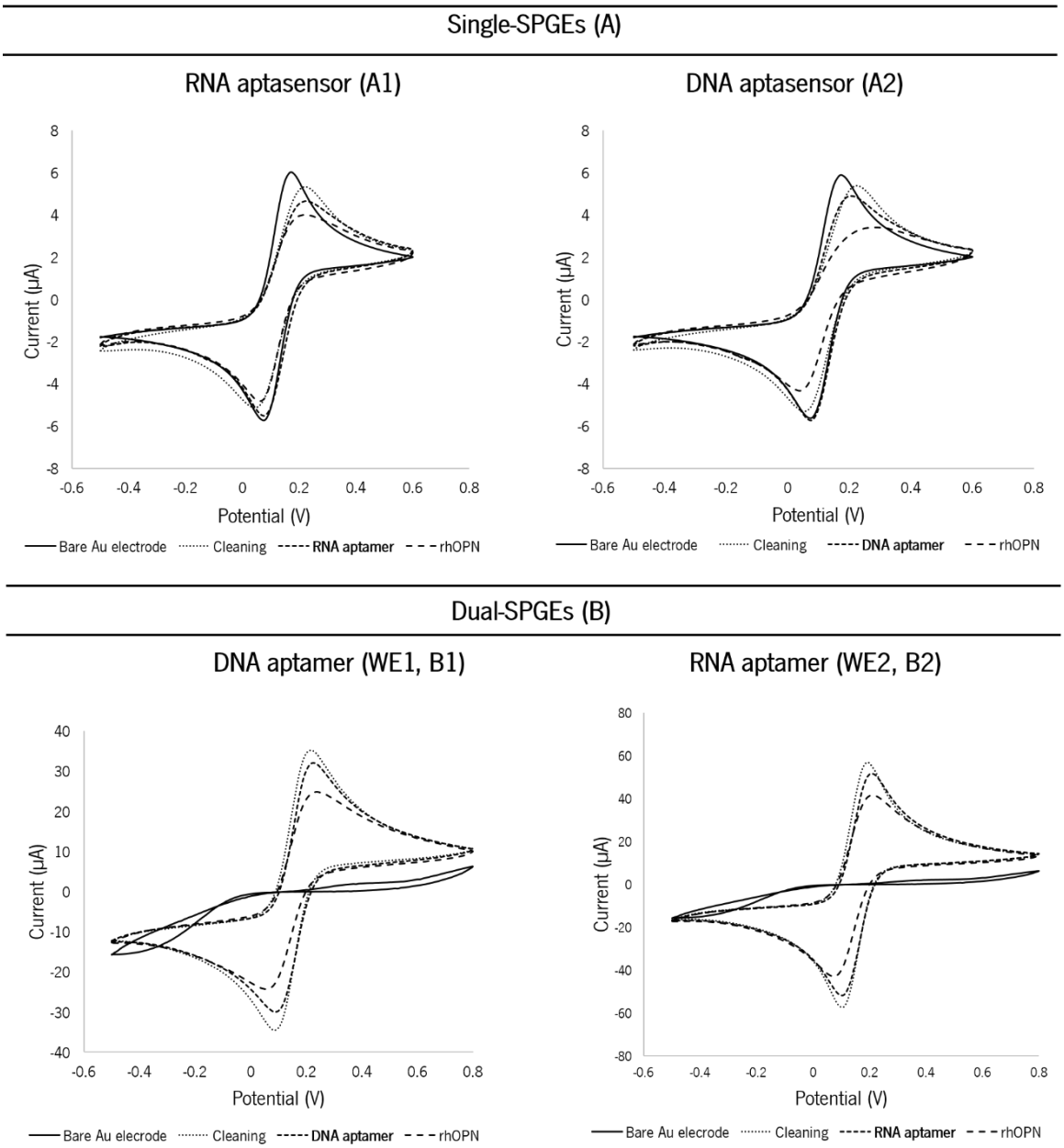

Fig. 6.2. Cyclic voltammograms of the bare Au electrode, surface cleaning step, aptamers' immobilization and aptamer-protein binding for RNA aptasensor (A1) and DNA aptasensor (A2) using single-SPGEs; and for DNA aptamer (WE1,B1) and RNA aptamer (WE2, B2) using a dual-SPGEs, in the solution of 5 mM $[Fe(CN)_6]^{-3/-4}$.

However, in the dual-SPGEs, successive cleaning cycles were necessary compared with the single-SPGEs, possibly due the different surface properties arising from the two different curing ink processes applied (low- and high-temperatures). The step corresponding to the RNA and DNA aptamers immobilization onto the gold working surface showed lower peak current intensities compared to the bare gold electrode (single-SPGEs) and cleaning step (dual-SPGEs). This probably

occurs due to the negative charges of the aptamers backbone phosphate group and $[Fe(CN)_6]^{3-/4-}$ redox probe and the electrostatic repulsive interaction that is expected to block the electron transfer (Bang et al., 2005). These results suggest that both aptamers were successfully assembled onto the gold working surface. After incubation of the rhOPN, a significant change of the voltammograms could be observed possibly due to the change of the aptamer conformation upon protein binding. The specific recognition of RNA and DNA aptamers led to the formation of the aptamer-rhOPN complexes and a consequent decrease of the peak current intensities, which is an evidence of the inhibition of electron transfer between the redox solution and the electrode surface. The aptasensor array, as well as the RNA aptasensor and DNA aptasensor developed with single-SPGE presented a negative readout signal upon protein binding to aptamer, i.e. exhibit a signal-off sensing mechanism.

6.3.2. Evaluation of the aptasensor array

The "signal-off" aptasensor array was designed for the simultaneous detection of rhOPN using two approaches as previously described. In the first approach, three dual-SPGE electrodes holding DNA or RNA aptamers in both working gold electrodes were prepared in different days and tested with 200 nM rhOPN standard solution. The current response obtained from the DNA/DNA and RNA/RNA aptasensors arrays showed a relative standard deviation (RSD %) of 10 % and the 8 %, respectively. These values are slightly higher than those previously determined for the single-SPGE holding the RNA or DNA aptamers (RSD of 5.7 % or 4.2 %, respectively) but even so are quite satisfactory and of the same order of those reported in the literature for multiplex measurements (between 5.5 % and 8.2 %) (Civit et al., 2012; Liang et al., 2014). Taking into account these satisfactory results it can be stated that the dual-SPGE array may be a sensitive sensing platform for multiple immobilization of the same aptamer (DNA/DNA or RNA/RNA). Nevertheless, since the performance of the dual-aptasensor was evaluated for the experimental conditions optimized for the single-aptasensor, a better performance may be foreseen if the best experimental conditions (incubation time and temperature, as well as aptamer concentration) were also studied for the dual-aptasensor, as mentioned in the literature (Chen et al., 2014). Indeed, the optimal aptamer concentration for the dual-aptasensor is expected to be different from that used (set equal to 4 nM based on the optimization process carried out for both the single-aptasensors) taking into account that the surface area of the working electrode of the dual-SPGEs (6.3 mm^2 each one) is much greater than the surface area of the single-SPGEs (0.5 mm^2).

In the second approach, four different dual-SPGEs combining the two aptamers (both DNA and RNA immobilized in WE1 and WE2) were prepared and a ΔI (%) of 20 ± 3 (DNA aptamer-rhOPN, **Fig. 6.2.B1**) and 19 ± 2 (RNA aptamer-rhOPN, **Fig. 6.2.B2**) was obtained. The decrease in the current in both working gold electrodes was quite similar and of the same order of magnitude as those obtained with the single-SPGEs (ΔI (%) of 14 ± 1 for the RNA aptasensor, **Fig. 6.2.A1**; and 26 ± 1 for DNA aptasensor, **Fig. 6.2.A2**). The dual-SPGEs exhibited a good response towards rhOPN, despite the used experimental conditions but with lower sensitivity compared to the single-DNA aptasensor. These results suggest that all the aptamer was immobilized onto the surface. Thus, an increase in the aptamer concentration, considering the surface area of the dual-electrodes, would possibly increase the sensitivity and repeatability of the dual-aptasensor array.

The response of the dual-aptasensor array, with both DNA and RNA aptamers immobilized, for non-specific proteins was also evaluated (**Fig. 6.3**). The relative current response (ΔI %) for the non-specific proteins tested was found to be negligible as compared to the binding response obtained for rhOPN. These preliminary results showed that dual-SPGEs are less prone to cross-reactivity from non-specific proteins than single-SPGEs, except for the rbOPN protein. However, this does not represent a problem, since being this protein from animal origin it is not expected to be present in a real context, i.e. whenever using human biological samples. Also, these results clearly demonstrated that the dual-aptasensor array may represent an interesting alternative to detect rhOPN in biological samples such as blood, plasma or serum.

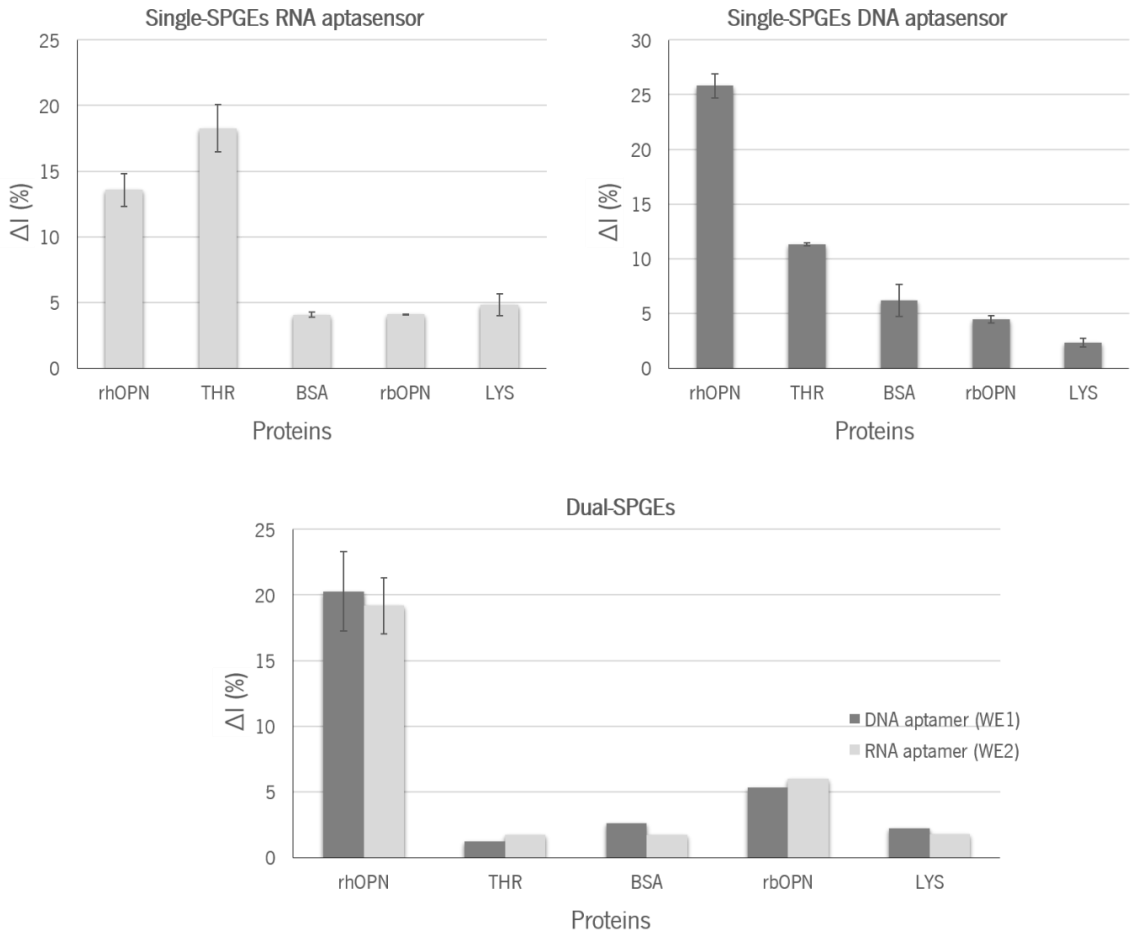

Fig. 6.3. Current relative change (ΔI / %) to rhOPN and non-specific proteins (200 nM); THR-Thrombin, BSA – bovine serum albumin, rbOPN – bovine osteopontin and LYS – lysozyme using the single-SPGE and dual-SPGE. Error bars indicate the relative standard deviation of independent experiments.

6.4. Conclusions

In the current study, we have designed and evaluated a label-free signal-off aptasensor array using a dual-SPGE for the simultaneous detection of human OPN. The preliminary results herein report showed a good response of the aptasensor array for the detection of human OPN. However, the dual-SPGE have a different surface composition and a greater area of working electrodes than the single-SPGEs (12.6 times), thus several parameters need to be further optimized, such as incubation time and temperature for the immobilization of each aptamer onto dual-SPGE, as well as the concentration of aptamer to be immobilized onto dual-SPGEs. These experimental conditions play an important role in the development of multiplexed sensing platforms (aptasensors arrays). Although these are

only preliminary results, the use of this dual-SPGEs electrode could be a good alternative for the specific detection of rhOPN and consequently be used with real biological samples for cancer diagnosis.

6.5. References

Bai, L., Yuan, R., Chai, Y., Zhuo, Y., Yuan, Y., Wang, Y., 2012. Biomaterials 33, 1090–1096.

Bang, G.S., Cho, S., Kim, B., 2005. Biosens. Bioelectron. 21, 863–870.

Cao, Y., Chen, D., Chen, W., Yu, J., Chen, Z., Li, G., 2014. Anal. Chim. Acta 812, 45–54.

Chikkaveeraiah, B. V, Bhirde, A.A., Morgan, N.Y., Eden, H.S., Chen, X., 2012. ACS Nano 6, 6546–6561.

Civit, L., Fragoso, A., Hölters, S., Dürst, M., O'Sullivan, C.K., 2012. Anal. Chim. Acta 715, 93–98.

Degefa, T.H., Kwak, J., 2008. Anal. Chim. Acta 613, 163–168.

Deng, K., Xiang, Y., Zhang, L., Chen, Q., Fu, W., 2013. Anal. Chim. Acta 759, 61–65.

Du, Y., Li, B., 2010. Bioanal. Rev. 1, 187–208.

Erdem, A., Karadeniz, H., Mayer, G., Famulok, M., Caliskan, A., 2009. Electroanal. 21, 1278–1284.

Farghaly, O. a, Hameed, R.S.A., 2014. Int. J. Electrochem. Sci. 9, 3287–3318.

Hianik, T., Wang, J., 2009. Electroanal. 21, 1223 – 1235.

Liang, R.-P., Tian, X.-C., Qiu, P., Qiu, J.-D., 2014. Anal. Chem. 85, 9256–9263.

Liu, Y., Kwa, T., Revzin, A., 2012. Biomaterials 33, 7347–55.

Liu, Y., Matharu, Z., Rahimian, A., Revzin, A., 2015. Biosens. Bioelectron. 64, 43–50.

Lönne, M., Zhu, G., Stahl, F., Walter, J.-G., 2014. Adv. Biochem. Eng. Biotechnol. 140, 121–154.

Ma, F., Ho, C., Cheng, A.K.H., Yu, H.Z., 2013. Electrochim. Acta 110, 139–145.

Mascini, M., 2009. Aptamers in Bioanalysis. A JOHN WILEY & SONS, INC.

Meirinho, S.G., Dias, L.G., Peres, A.M., Rodrigues, L.R., 2015. Biosens. Bioelectron. 71, 332 – 341.

Mi, Z., Guo, H., Russell, M.B., Liu, Y., Sullenger, B. a, Kuo, P.C., 2009. Mol. Ther. 17, 153–161.

Min, K., Song, K.-M., Cho, M., Chun, Y.-S., Shim, Y.-B., Ku, J.K., Ban, C., 2010. Chem. Comm. 46, 5566.

Olowu, R.A., Ndangili, P.M., Baleg, A.A., Ikpo, C.O., Njomo, N., Baker, P., Iwuoha, E., 2011. Int. J. Electrochem. Sci. 6, 1686–1708.

Palchetti, I., Mascini, M., 2012. Anal. Bioanal. Chem. 402, 3103–3114.

Prieto-Simón, B., Campàs, M., Marty, J.-L., 2010. Bioanal. Rev. 1, 141–157.

Qian, X., Xiang, Y., Zhang, H., Chen, Y., Chai, Y., Yuan, R., 2010. A Chem. Eur. J. 16, 14261–14265.

Radi, A.-E., 2011. Int. J. Electrochem. 2011, 1–17.

Rusling, J.F., Kumar, C. V., Gutkind, J.S., Patel, V., 2010. Analyst 135, 2496-xxx.

Saberian-Borujeni, M., Johari-Ahar, M., Hamzeiy, H., Barar, J., Omidi, Y., 2014. Bioimpacts 4, 205–215.

Sassolas, A., Blum, L.J.J.J., Leca-Bouvier, B.D.D.D., Lyon, D., 2009. Electrochemical Aptasensors. Electroanal. 21, 1237–1250.

Song, W., Li, H., Liang, H., Qiang, W., Xu, D., 2014. Anal. Chemistry 86, 2775–2783.

Touhami, A., 2015. Nanomedicine 374–400.

Velasco-Garcia, M.N., Missailidis, S., 2009. Gene Ther. Mol. Biol. 13, 1–9.

Vidotti, M., Carvalhal, R.F., Mendes, R.K., Ferreira, D.C.M., Kubota, L.T., 2011. J. Braz. Chem. Soc. 22, 3–20.

Xiang, Y., Qian, X., Jiang, B., Chai, Y., Yuan, R., 2011. Chem. Comm. 47, 4733.

Xie, S., Walton, S.P., 2010.. Biosen. Bioelectron. 25, 2663–2668.

Yang, Z.-H., Zhuo, Y., Chai, Y.-Q., Yuan, R., 2014. Sci. Rep. 4, 4747-xxx.

Zhao, C., Wu, J., Ju, H., Yan, F., 2014. Anal. Chim. Acta 847, 37–43.

Zhao, S., Yang, W., Lai, R.Y., 2011. Biosens. Bioelectron. 26, 2442–2447.

CHAPTER 7

General Conclusions and Recommendations for Future Work

This chapter draws the main conclusions of this thesis. Also, some general recommendations for further research in this field are presented. Detailed conclusions and suggestions are given in each chapter.

This page was intentionally left blank

7.1. General Conclusions

The aim of this thesis was to design novel aptamer-based mono/multi-sensor devices for the detection and quantification of human OPN, envisaging the development of new strategies for the early detection and diagnosis of breast cancer.

Electrochemical aptasensor devices have been widely explored for the detection of various proteins disease biomarkers, mainly due to their interesting features including high sensitivity, simple and low cost preparation, rapid response and reusability. In this thesis, a screen-printed gold electrode (SPGE) with a gold working electrode (0.8 mm of diameter), a gold counter electrode and a silver-pseudo electrode, was used to design a new electrochemical aptasensor. The use of SPGE allows miniaturizing the biosensors and reducing the amount of reagents and solutions required.

Additionally, whenever developing an aptasensor, the detection of the target (e.g. human OPN) depends on the complex formation between the target molecule and its specific aptamer (bioreceptor). Herein, an electrochemical RNA aptasensor for the detection of human OPN was successfully developed using a RNA aptamer (called, OPN-R3) previously isolated through SELEX methodology by other researchers. Aptamers have been generally reported as suitable bioreceptors due to their high thermal stability, easy chemical production, and possibility to be modified with chemical groups that are useful for functionalization of the electrode surfaces. These aptamers can bind their targets with high affinity and specificity due to their specific three-dimensional structures.

The formation of the complex between the RNA aptamer and the proteins (human OPN and thrombin (a possible interfering protein)) was evaluated by means of *Kd* estimation using fluorescence assays, considering that the formation of the complex is an equilibrium process (1:1). The RNA aptamer exhibited a high affinity-binding for human OPN, showing low dissociation constants (1.6 nM and 8.5 nM for 30 min and 4 hours, respectively). However, it also exhibited a high affinity-binding for thrombin, showing a *Kd* of 1.3 nM after 4 hours of incubation. This result suggested that the RNA aptamer could have a binding site for THR.

The performance of an aptasensor can be affected by several parameters. Experimental conditions, such as incubation time and temperature used during the immobilization of the aptamer, the concentration of the aptamer to be immobilized onto the SPGE, as well as the aptamer-protein incubation time were optimized. Every step towards the immobilization of the aptamer onto the gold

electrode surface was evaluated and controlled using CV and SWV. The sensitivity, specificity, stability and reproducibility of the proposed aptasensor were investigated using CV.

The novel label-free, signal-off voltammetric RNA aptasensor designed for the detection of human OPN, using an aptamer as bioreceptor element and $[Fe(CN)_6]^{-3/-4}$ as redox probe, was found to exhibit a satisfactory performance, reproducibility and stability. However, despite this simple and sensitive method has many desirable features, few limitations should be further studied, such as the specificity of the aptasensor through the use of a different aptamer or the increase of the RNA aptamer stability to nucleases degradation by introducing some modifications, further allowing its use in real biological samples analysis.

Based on these promising results, another electrochemical aptasensor was developed using a DNA aptamer with high affinity and selectivity towards human OPN, selected by SELEX methodology. Following this procedure, 19 aptamer sequences with the expected affinity were isolated.

All these aptamer sequences were examined regarding their homology, lowest Gibbs energy and ability to form stable secondary structures considering the aptamer full-sequence (70 nucleotides (nt)) or the random region (30 nt). All aptamer sequences exhibited a variable region with 30 nt and a common trinucleotide sequence (TGT), except for C10K9, C10K3 and C10K5. Using the 30 nt region for the analysis, the sequences C10K2, C10K7 and C10K15 were found to exhibit the lower ΔG values and a stable secondary structure. From this analysis, the DNA aptamer C10K2 was selected. This aptamer showed 80 % of homology with the clones C10K1 and C10K10, lowest ΔG value with 70 nt (-4.89 Kcal/mol) and 30 nt (-4.21 Kcal/mol) and the same stable stem-loop secondary structure with trinucleotide sequence with 70 nt, 30 nt and 35 nt.

The selected DNA aptamer (C10K2) was characterized regarding its binding affinity towards its target (human OPN), as well as its specificity over other proteins (THR, BSA, rbOPN). The DNA aptamer showed high affinity and specificity for human OPN (*Kd* of 2.5 nM and 1.1 nM for 30 min and 4 hours, respectively).

Similarly to the RNA-aptasensor, the experimental conditions (aptamer concentration and aptamer-target incubation time) were also optimized. CV and SWV techniques were again used to evaluate each immobilization step of the aptamer onto the gold electrode surface. The aptasensor performance was assessed by CV. The label-free, signal-off electrochemical DNA aptasensor showed high sensitivity, stability, specificity and repeatability towards the detection of human OPN. Despite

its interesting performance, the results clearly demonstrate that the designed aptasensor is for a single-use application. Therefore, further studies on the possible regeneration of the aptasensor should be carried out. Nevertheless, this newly designed aptasensor is still very promising for a broad potential application in clinic assays and protein analysis.

In conclusion, the two electrochemical aptasensors herein developed can be an efficient and simple strategy for the detection of relevant biomarkers, for the diagnosis and therapy monitoring, as well as a promising alternative to directly analyze complex samples such as biological fluids.

Additionally, a label-free signal-off aptasensor array using a dual-SPGE for the simultaneous detection of human OPN was designed and evaluated using the experimental conditions optimized for the development of the RNA and DNA aptasensors. This multi-biosenssor showed a good response and selectivity for human OPN, thus representing also an encouraging approach to be further explored for cancer diagnosis.

7.2. Recommendations for Future Work

This thesis led to the development of a new method for the detection of human OPN, through the design of new electrochemical aptasensors. Notwithstanding, despite the relevant and interesting results herein gathered, additional research is still needed. Some suggestions to be considered in future work are described below.

- ✓ The DNA sequences obtained by SELEX that presented low Gibbs energy and predicted stable secondary structures should be characterized using fluorescence assays and/or other methods described in the literature including surface plasmon resonance and affinity capillary electrophoresis. Regarding the DNA aptamer sequences C10K15, C10K7 and C10K18, it may be worth exploring their application in the development of other DNA aptasensors (or aptasensor arrays) for the detection of human OPN.

- ✓ Evaluation of the possibility to increase the aptasensors sensitivity through the use of nanomaterials, such as gold nanoparticles. The AuNPs are often employed to modify the

electrodes surfaces, due to their properties such as chemical stability, high biocompatibility, large specific surface area and high electro-transfer ability.

- ✓ Assessment of the selectivity of the two electrochemical aptasensors herein developed against other proteins present in biological fluids, such as serum and plasma (e.g. human serum albumin (HSA) and human immunoglobulin G (hIgG)). The selectivity of the aptasensor plays an important role in diagnostic applications. Thus, the biosensor or diagnostic method must be robust against the interference from the most abundant proteins present in complex biological matrixes.

- ✓ Investigation on new methods to regenerate electrochemical aptasensors. The regeneration of an aptasensor consists in breaking the complex formed between the aptamer and the target, given the ability of aptamers to undergo multiple denaturation/regeneration cycles. This characteristic allowed the development of reusable aptasensors able to detect proteins multiple times. Although the regeneration of aptamers-functionalized sensor surfaces is often easy to perform, it can be very difficult to achieve. Several strategies have been reported, such as the use of temperature, concentrated salt solutions, acidic or basic solutions, chaotropic reagents (e.g. urea or guanidinium hydrochloride), surfactants (e.g. SDS), chelating agents (e.g. EDTA) or a combination of two or more of the abovementioned regenerating agents. In this thesis, two unsuccessful solutions (2M NaCl and 7 M urea for 2 min at room temperature) were tested for the regeneration of both developed aptasensors.

- ✓ Evaluation of the human OPN detection by both RNA and DNA aptasensors in biological fluids (e.g. plasma and blood).

- ✓ Optimization of the aptasensor array for the simultaneous measurement of human OPN and/or different proteins using different aptamers immobilized onto an electrode array. For the design of an aptasensor array to detect human OPN, some experimental conditions must be optimized, namely the incubation temperature and time used for the immobilization of each aptamer, as well as each aptamer concentration to be immobilized onto the electrode surface. Finally, the aptasensor must be characterized regarding its sensitivity, specificity,

reproducibility, stability and reusability, along with its potential use with real biological samples.

This page was intentionally left blank

APPENDIX

This page was intentionally left blank

Appendix A1: Secondary structures of DNA aptamers isolated with the lowest ΔG value in the analysis with 70 nt.

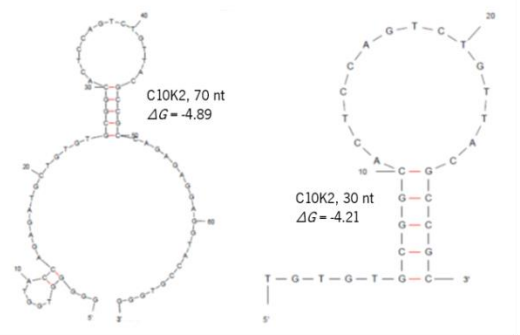

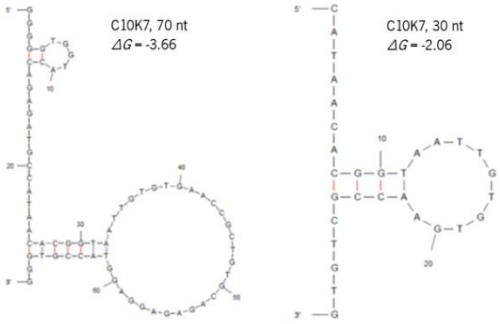

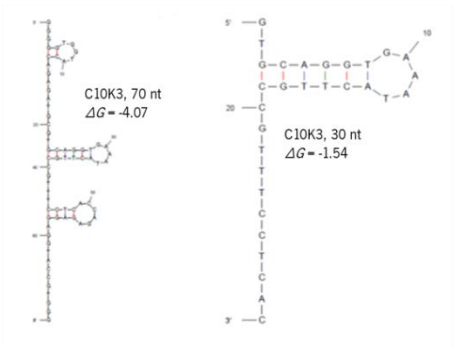

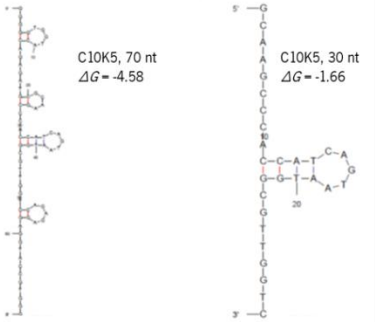

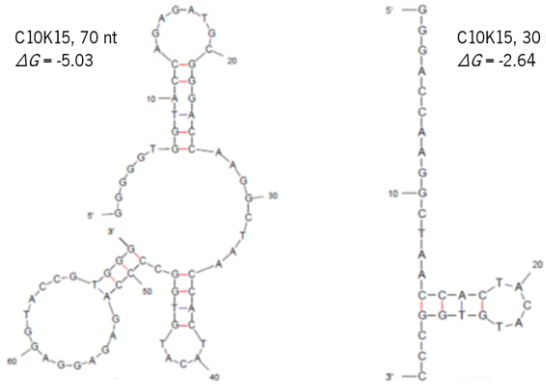

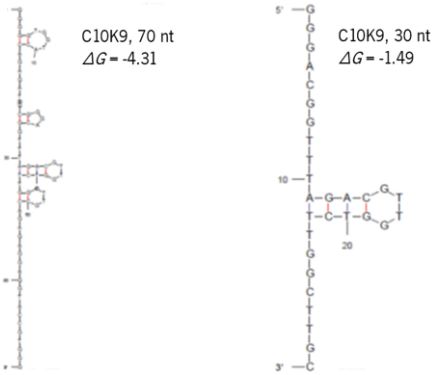

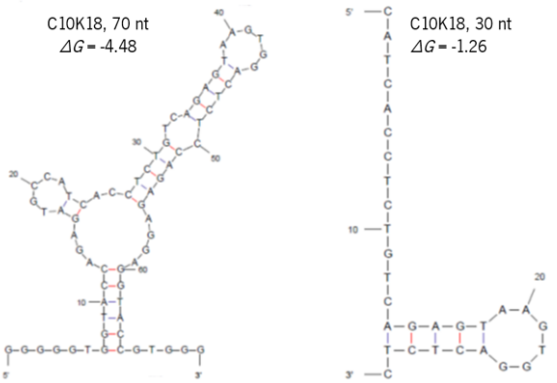

Appendix A2: Secondary structures of DNA aptamers with the lowest ΔG value in the analysis with 30 nt and adding parts of the conserved regions.